

LEVEL III

Aug 1981 (12) FR-81-10071

AD A105626

(6) HgCdTe FABRICATION USING DIRECTED ENERGY TECHNIQUES

(10) Anton Co./Greenwald
Robert G./Wolfson

ROBERT WOLFSON
(617) 275-6000 EXT. 211
ANTON GREENWALD
(617) 275-6000 EXT. 227

DTIC ELECTE
OCT 16 1981
S D E

(9) AUGUST 1981
Final Report

(12) 97

(14) AUG 81

THIS RESEARCH WAS SPONSORED BY THE DEFENSE ADVANCED RESEARCH PROJECTS AGENCY UNDER ARPA ORDER NO. 3800 CONTRACT NO. MDA 903-79-C-0434 MONITORED BY: MR. SVEN ROOSILD, DARPA/MSO 1400 WILSON BLVD., ARLINGTON, VA 22209

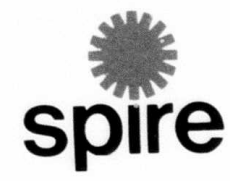
(15) MDA 903-79-C-0434
DARPA Order - 3800

EFFECTIVE DATE: 16 AUGUST 1979
EXPIRATION DATE: 30 JUNE 1981

Approved for Public Release: distribution unlimited.

DTIC FILE COPY

81 10 16



393483

JOB

The views and conclusions contained in this document are those of the author and should not be interpreted as necessarily representing the official policies, either expressed or implied, of the Defense Advanced Research Projects Agency or the United States Government.

Unclassified

SECURITY CLASSIFICATION OF THIS PAGE (When Data Entered)

REPORT DOCUMENTATION PAGE		READ INSTRUCTIONS BEFORE COMPLETING FORM
1. REPORT NUMBER FR-81-10071	2. GOVT ACCESSION NO. AD-A205626	3. RECIPIENT'S CATALOG NUMBER
4. TITLE (and Subtitle) RESEARCH ON HgCdTe FABRICATION USING DIRECTED ENERGY TECHNIQUES	5. TYPE OF REPORT & PERIOD COVERED Final Technical Report	
	6. PERFORMING ORG. REPORT NUMBER FR-81-10071	
7. AUTHOR(s) A.C. Greenwald and T. Wong	8. CONTRACT OR GRANT NUMBER(s) MDA 903-79-C-0434	
9. PERFORMING ORGANIZATION NAME AND ADDRESS SPIRE CORPORATION Patriots Park Bedford, MA 01730	10. PROGRAM ELEMENT, PROJECT, TASK AREA & WORK UNIT NUMBERS	
11. CONTROLLING OFFICE NAME AND ADDRESS Advanced Research Projects Agency 1400 Wilson Boulevard, Arlington, VA 22209	12. REPORT DATE August 1981	
	13. NUMBER OF PAGES	
14. MONITORING AGENCY NAME & ADDRESS (if different from Controlling Office)	15. SECURITY CLASS. (of this report) Unclassified	
	15a. DECLASSIFICATION/DOWNGRADING SCHEDULE	
16. DISTRIBUTION STATEMENT (of this Report) Approved for public release; distribution unlimited.		
17. DISTRIBUTION STATEMENT (of the abstract entered in Block 20, if different from Report)		
18. SUPPLEMENTARY NOTES mercury cadmium telluride. cadmium telluride		
19. KEY WORDS (Continue on reverse side if necessary and identify by block number) HgCdTe Mercury Cadmium Telluride CdTe Cadmium Telluride Pulsed Electron Beam Processing		EDICT (Evaporation and Diffusion at Constant Temperature) Pulse Processing Hot Wall Epitaxy Heteroepitaxy Thin Films
20. ABSTRACT (Continue on reverse side if necessary and identify by block number) The goal of this research is to produce large-area, thin-film, single crystal HgCdTe material for infrared detectors. The successful approach is to (1) evaporate CdTe in an enclosed furnace on insulating crystalline substrates (hot wall epitaxy), (2) melt a thin surficial layer by pulsed electron beam irradiation to improve morphology, and (3) convert to HgCdTe by evaporation and diffusion at constant temperature. (continued overleaf)		

Unclassified

SECURITY CLASSIFICATION OF THIS PAGE(When Data Entered)

20. The final result is a single crystal film of Hg $(1-x)$ Cd $_x$ Te, 30 microns thick and 0.5 inch square, with a compositional variation of x less than ± 0.0007 . Films of up to 20 microns thick, 1 inch o.d., single crystal (but twinned) CdTe were produced by the first process. These faceted films were smoothed without change of surface stoichiometry or structure by the second process. Evaporation of HgTe at less 0.5 atm Hg overpressure onto the CdTe film produced the final result on mica or quartz substrates. Electron mobility at 77°K was as high as 1.5×10^5 cm²/V-s in the final samples.

Unclassified

SECURITY CLASSIFICATION OF THIS PAGE(When Data Entered)

DISTRIBUTION

Director
Defense Advanced Research Projects Agency
Arlington, VA 22209

Attn: Program Management (2)
Attn: Dr. Richard A. Reynolds (1)
Attn: Mr. Sven Roosilid (1)

Defense Documentation Center (12)
Cameron Station
Alexandria, VA 22314

Spire Corporation Distribution

A. Greenwald (1)
R. Little (1)
R. Wolfson (1)
Files Original + (6)

NERC Distribution

T. Wong (1)
J. Miles (1)
Files (1)

Accession For	
NTIS GRA&I	X
DTIC TAB	
Unannounced	
Justification	
By _____	
Distribution/	
Availability Codes	
Dist	Avail and/or Special
A	

FOREWARD

The work reported in this document was performed in part at Spire Corporation, Bedford, Massachusetts, and in part at New England Research Center, Inc., Sudbury, Massachusetts, under contract MDA 903-79-C-0434, DARPA order number 3800. The contract monitor is Mr. Sven Roosild.

The program manager at Spire was Dr. Robert Wolfson. The principal investigator at Spire was Dr. Anton Greenwald, who was in charge of pulsed electron beam processing and ion implantation studies. The program manager at NERC was Dr. Theordore Wong. The principal investigator at NERC was Dr. John Miles, who was in charge of the epitaxial deposition and vapor exchange processes.

Work performed at Spire is described in Section 2. The report of the main subcontractor, NERC, is included in Section 3.

SUMMARY

The goal of this successful research program was to produce large-area, single-crystal HgCdTe material suitable for infrared detectors. The key approach was (1) to evaporate CdTe films onto insulating substrates for epitaxial crystal growth; (2) to heat the film with a pulsed, directed energy beam to reduce defect concentration and improve surface morphology; and (3) to convert the material to HgCdTe by vapor-exchange with HgTe. Alternate approaches investigated included graphoepitaxy of CdTe on patterned, amorphous substrates and the conversion of thin CdTe films to HgCdTe by ion implantation and/or directed energy processing techniques.

Single crystal films of $\text{Hg}_{(1-x)}\text{Cd}_x\text{Te}$ up to 30 microns thick were fabricated on 1.2 x 1.2 cm mica substrates. Excellent compositional uniformity was achieved, with the variation in x being 0.2 ± 0.0007 . The electron mobility in this material was as high as $1.5 \times 10^5 \text{ cm}^2/\text{V-s}$ at 77°K . Good reproducibility has been demonstrated with the result that HgCdTe films can be grown with predictable thickness and composition.

The surface morphology of the CdTe films as deposited, step (1) above, were faceted. It has been shown, as noted in step (2) above, that pulsed electron beam processing can melt and polish this surface without degradation of crystal structure or compositional uniformity. The final surface was suitable for making devices.

The initial objectives of this research were achieved.

TABLE OF CONTENTS

<u>Section</u>		<u>Page</u>
1	INTRODUCTION	1-1
	1.1 Purpose - Long-Term Objective	1-1
	1.2 Technical Considerations.	1-1
	1.3 General Method.	1-1
	1.4 Technical Results and Conclusions	1-2
2	TECHNICAL INFORMATION - REPORT OF MAIN CONTRACTOR - SPIRE CORPORATION	2-1
	2.1 Directed Energy Processing Assessment	2-1
	2.1.1 Objectives.	2-1
	2.1.2 Physical Modeling	2-1
	2.1.3 Equipment	2-8
	2.1.4 Pulse Processing Results.	2-11
	2.1.5 Evaluation of Pulse-processing Effects	2-17
	2.2 Pulsed Electron Beam Processing of CdTe Films	2-19
	2.2.1 Objective	2-19
	2.2.2 Heteroepitaxy and Surface Polishing	2-19
	2.2.3 Graphoepitaxy	2-24
	2.3 Modification of CdTe by Ion Implantation.	2-27
	2.3.1 Objective	2-27
	2.3.2 Ion-Implantation Experimental Results	2-27
	2.3.3 Analysis of High-Dose Implantation of Hg into CdTe	2-30
	2.3.4 Evaporation and Pulse Diffusion Results	2-32
3	TECHNICAL INFORMATION - REPORT OF SUBCONTRACTOR - NEW ENGLAND RESEARCH CORPORATION	3-1
	3.1 Deposition of Single Crystal CdTe Films	3-1
	3.1.1 Objective	3-1
	3.1.2 HWE Process Description	3-1
	3.1.3 Description of Apparatus	3-3
	3.1.4 Heteroepitaxial Growth of CdTe on Mica	3-5
	3.1.5 Characterization of CdTe Films on Mica	3-7
	3.1.6 Films Deposited on Other Substrates	3-14
	3.2 Vapor Exchange of CdTe to Form HgCdTe	3-20
	3.2.1 Objective	3-20
	3.2.2 Edict Process Description	3-20
	3.2.3 EDICT Ampoules and Furnace	3-22
	3.2.4 EDICT Experiments	3-22
	3.2.5 Characterization of HgCdTe Films	3-25

REFERENCES

LIST OF FIGURES

<u>Figure</u>		<u>Page</u>
2-1	Electron energy spectrum of beam used to process CdTe	2-4
2-2	Energy deposition profile into CdTe by 20 keV average electron energy beam.	2-6
2-3	Thermal history of CdTe surface pulse heated by electron beam with spectrum shown in Figure 2-2, at 0.9 J/cm^2	2-7
2-4	Schematic of SPI-PULSE TM 6000 pulsed electron beam processor	2-9
2-5	Heated sample stage for pulsed electron beam apparatus	2-10
2-6	Cryogenic cooled sample stage for pulsed electron beam apparatus	2-12
2-7	Depth profile of Cd and Te by Auger spectroscopy and argon ion sputtering for unprocessed and pulse-processed CdTe crystal at 0.5 J/cm^2	2-15
2-8	Photomicrographs of pulse-processed CdTe crystals examined for damage threshold.	2-16
2-9	Depth profile of Hg, Cd, and Te in pulse-processed $\text{Hg}_{0.8}\text{Cd}_{0.2}\text{Te}$ at 0.6 J/cm^2	2-18
2-10	CdTe films on mica, pulsed electron beam treated in 5mm x 5mm regions.	2-21
2-11	HWE deposited CdTe film before and after pulsed electron beam irradiation, showing in SEM microphotograph surface polishing by melting.	2-23
2-12	Schematic of graphoepitaxy process.	2-25
2-13	SEM micrographs of results of graphoepitaxy experiment	2-26
2-14	SIMS depth profiles of Cd and Hg in ion implanted CdTe	2-29
2-15	Concentration x of $\text{Hg}_{1-x}\text{Cd}_x\text{Te}$ as a function of sputtering yield for Hg^+ implanted into CdTe	2-33
3-1	The Vacuum System for Hot Wall Epitaxy deposition of CdTe Films and initial furnace	3-4
3-2	Redesigned hot wall furnace with enclosed source (at NERC) for evaporation of CdTe	3-6
3-3	Time-temperature cycles of the source and substrate	3-8
3-4	Source and substrate temperature necessary to give single crystal CdTe films on mica	3-9

LIST OF FIGURES (concluded)

<u>Figure</u>		<u>Page</u>
3-5	SEM photomicrograph showing CdTe nuclei	3-11
3-6	CdTe film deposited on mica	3-13
3-7	Back reflection Laue pattern from CdTe film on muscovite mica	3-15
3-8	Schematic of vapor exchange apparatus (at NERC)	3-23
3-9	A heat pipe is placed inside the EDICT furnace to ensure growth in thermodynamic equilibrium	3-24
3-10	Fourier transform reflectance spectroscopy measurements taken on a HgCdTe/mica sample and a bare mica substrate	3-28
3-11	Compositional uniformity of 0.2190 ± 0.00067 across a 1.2×1.2 cm area measured with the Fourier Transform Spectrometer which has a precision limit for resolving x of ± 0.00050	3-30
3-12	Laue x-ray pattern of a single crystal CdTe film on mica	3-31
3-13	Laue x-ray pattern taken on a bulk CdTe wafer	3-32

SECTION 1 INTRODUCTION

1.1 PURPOSE - LONG-TERM OBJECTIVE

The overall purpose of this program is to grow large size single crystal HgCdTe suitable for use in large scale detector arrays. For this purpose, the material must have the following properties:

- Uniformity of composition ($X \leq .003$)
- Dimension of 1" or greater
- Near intrinsic purity
- Freedom from residual stress and surface defects
- Large scale production capability

1.2 TECHNICAL CONSIDERATIONS

There are two main problems which prevent present melt growth methods from satisfying all the above criteria simultaneously. The first of these problems is the high vapor pressure of mercury associated with the pseudobinary phase for molten $\text{Hg}_{(1-x)}\text{Cd}_x\text{Te}$. This problem places limits on the dimension of the ampoule in which the crystals may be grown. The second major problem is the wide separation of the liquidus and solidus in the pseudobinary phase diagram which makes it very difficult to obtain a uniform composition across a large specimen.

The methods used in the program overcome these two problems without introducing any other insuperable problems as indicated in the next section.

1.3 GENERAL METHOD

The method used in this program attains the desired end of large area, uniform single crystal HgCdTe films in two steps. The first step is to grow heteroepitaxially large single-crystal films of CdTe on foreign substrates by the Hot Wall Epitaxial (HWE) technique. The second step is transformation from single crystal CdTe film to single crystal HgCdTe film by a process of vapor growth and solid state diffusion known as EDICT (Evaporation and Diffusion at Constant Temperature).

This two-step method has a number of advantages over other methods of growing large area HgCdTe single-crystal specimens. First, the film thickness is determined by the deposition of the CdTe in the first step, whereas the critical HgCd ratio is

determined by the second step. This allows the critical parameters to be separately optimized. Secondly, since all processes take place at relatively low temperatures, the excessive mercury pressure that plagues most high-temperature melt-growth processes is not a problem. In fact, this method takes advantage of the volatility of components and grows from the vapor phase. Scaling up of the specimen dimensions is rather straightforward relative to other melt-growth methods which are all limited by the 1/2" ampoule dimension as a result of high mercury pressures. Thirdly, segregation problems which limit uniformity of composition in melt-grown HgCdTe do not exist in this method because melting is not required here. Furthermore, since HgCdTe is grown directly in a thin CdTe film, no compositional gradient occurs. Thus, exceptionally uniform composition should result both across and normal to the film surface. Finally, both the Hot Wall Heteroepitaxy and the EDICT process are vapor-growth methods where the emphasis is put on the growth of epitaxial layers under conditions as near as possible to thermodynamic equilibrium, resulting in thin films of bulk quality and crystalline perfection.

An additional step is necessary for processing the CdTe film after HWE deposition. The growth morphology of the as-deposited film is faceted, with surface relief greater than one micron. The surface features remain essentially unchanged after EDICT conversion to HgCdTe. Polishing a thin film is difficult and costly. However, rapid melt/quenching by irradiation with a pulsed electron beam produces a superior surface finish. As the surface cools, epitaxial crystal growth prevents degradation of structure. The surface is typically at a high temperature for only one microsecond, and this minimizes outdiffusion of cadmium. The process is fast, noncontaminating, inexpensive, and amenable to large-scale manufacture.

1.4 TECHNICAL RESULTS AND CONCLUSIONS

Results on this program have confirmed the feasibility of combining the HWE and EDICT methods to grow large single-crystal HgCdTe films. The major accomplishments to date are listed below:

- Heteroepitaxial single-crystal CdTe films 2.5 cm in diameter have been grown by the HWE technique.
- Single-crystal HgCdTe films have been produced by means of a subsequent EDICT treatment of these CdTe films.

- Excellent compositional uniformity has been achieved in $\text{Hg}_{(1-x)}\text{Cd}_x\text{Te}$ films with compositional variation in X of less than ± 0.00067 over a nominal area of 1.2 cm x 1.2 cm as determined by spectral cutoffs at 77°K.
- Electron mobility as high as $1.5 \times 10^5 \text{ cm}^2/\text{V-s}$ at 77°K has been obtained which indicates epitaxial film quality as good as bulk material.
- Good reproducibility has been demonstrated in the HWE and EDICT processes. As a result, single-crystal HgCdTe films can be grown with predictable thickness and composition.

Additional effort on this program in seeking an alternative to the EDICT process showed that:

- The composition of CdTe cannot be modified by ion implantation to contain a substantial fraction of mercury due to very high sputtering coefficients.
- Pulsed diffusion of evaporated Hg layers into CdTe substrates or films is feasible.

SECTION 2
TECHNICAL INFORMATION
REPORT OF MAIN CONTRACTOR - SPIRE CORPORATION

2.1 DIRECTED ENERGY PROCESSING ASSESSMENT

2.1.1 Objectives

The objective of this task was to assess the directed energy processing of CdTe and HgCdTe to establish a starting point for the development of process parameters. Directed energy processing was proposed as a technique to:

- Anneal Hg ion-implantation damage in CdTe.
- Effect liquid phase heteroepitaxial growth of thin film CdTe.
- Polish the surface of very thin films of CdTe consistent with the vapor phase deposition of the compound semiconductor.

A thermomechanical model of pulsed processing was developed to estimate parameters required for each application. Using the numerical results for guidance, pulse processing experiments were performed to establish the limiting parameters of the useful processing regime, in particular, the maximum fluence above which unacceptable sample damage occurred. Amorphous CdTe, single-crystal CdTe, and polycrystalline HgCdTe were irradiated by a pulsed electron beam and examined for structure, stoichiometry, and uniformity to determine if there were any deleterious effects.

2.1.2 Physical Modeling

The sample was a thin film, 2-20 microns thick, of a ternary compound semiconductor in the system CdTe - HgTe. It was considered desirable to melt the entire film, but not the substrate, in a time so short that insignificant amounts of the volatile component would be lost. The surface could not be allowed to reach the vaporization temperature. Under similar conditions, epitaxial and heteroepitaxial crystal growth of elemental semiconductor films was observed.^(1,2)

These conditions dictated the choice of the directed energy source. Optical absorptivity in CdTe or HgTe for wavelengths shorter than 10 microns is very high. Pulsed heating of too thin a surface layer by a laser would lead to vaporization and damage prior to depositing sufficient energy to melt the film. Continuous heating by a CW laser or electron beam requires too much time, and allows the escape of volatile components from unencapsulated materials.⁽³⁾ Only pulsed electron beams were deemed capable of processing this material.

The thermal diffusivity of CdTe at room temperature is approximately 0.34 cm²/sec. For a pulsed energy source with a shallow deposition profile and a pulse width of 100 ns, the initial temperature profile after heating has the form of an error function with a characteristic distance of $\text{SQRT}(Dt) = 2$ microns. This implies a large thermal gradient across the film. Heating for a longer time is not desirable. To reduce the thermal gradient, the energy from the electron beam must be deposited deeply. The choice of electron beam spectra to be used in experiments was based upon the calculations detailed in Appendix A.

Energy transport phenomena induced by pulsed electron beams are described by a numerical model comprising four calculations. The first calculation derives the electron energy spectrum from measured diode voltage and current data. Four different beam types, evolved from distinct changes in the apparatus geometry (Section 2.1.3), were evaluated. The electron beams can be differentiated most succinctly on the basis of average particle energy.

TABLE 2-1. AVAILABLE PULSED ELECTRON BEAM PARAMETERS

TYPE	AVERAGE ELECTRON ENERGY (keV)
1	< 15
2	~ 20
3	~ 35
4	< 50

Other variations in these beams, such as average angle of incidence upon the sample, were noted where the experimental effect is significant.

The second calculation of the numerical model uses the derived electron energy spectrum (Figure 2-1) to estimate the deposition profile in the material. This second calculation gives dose (energy/gm per energy/cm²) as a function of depth below the specimen surface. The several specimen-beam combinations treated are listed in Table 2-2. The profile related to the largest number of actual experiments is shown in Figure 2-2, the other profiles are given in Appendix A. Note that several samples comprise a pure mercury layer over CdTe, and were a model of high dose implants (Section 2.3.3) or pulse diffusion of evaporated layers (2.3.4).

The third calculation uses the deposition profile and the beam fluence (average energy/unit area) to estimate the temperature profile as a function of time. To a zeroth order approximation, if the pulse width of the electron beam were infinitesimal, the temperature profile immediately following the pulse could be derived by multiplying the ordinate axis in Figure 2-2 by the fluence, and dividing by the average specific heat. The dose required to reach melt temperature for a fluence of 1 J/cm² is indicated in Figure 2-2 based upon this crude approximation. The accurate solution to the thermal diffusion equation requires knowledge of the change in thermal conductivity and specific heat as a function of temperature,⁽⁴⁾ which are not well known for CdTe between 300°K and melt. Using the best data available,⁽⁵⁾ the results of a numerical model for a fluence of 0.9 J/cm² and the deposition profile shown in Figure 2-2, are presented in Figure 2-3 showing the temperature versus depth at different times after the electron beam pulse. Note that the material (CdTe) reaches melt temperature to a depth of 2 microns, while the surface did not climb above the melt temperature (limited by heat of fusion). The surface cools rapidly, to below the melt temperature in about 2 microseconds.

On the basis of the preceding calculations, attention was directed towards beam types 1 and 2, and fluences that are considered moderate for material-processing applications (≤ 1 J/cm²). The fourth calculation, which was not performed because of insufficient data, would have estimated the effect of hydrodynamic shock upon the material. Results of the numerical model for the CdTe-HgTe system are summarized below.

- The deposition profile for beam type 1 falls sharply and monotonically from the surface, with correspondingly abrupt temperature profiles. This beam is capable of melting the material to a depth on the order of 0.5 microns.

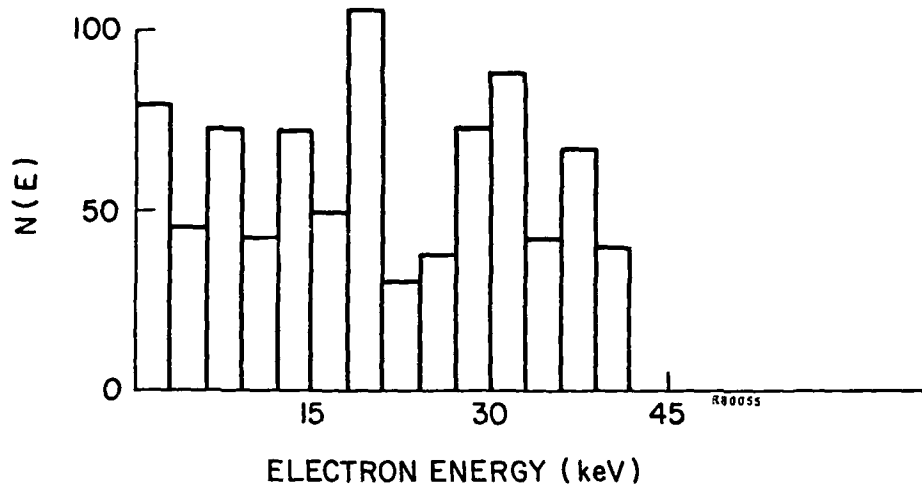


Figure 2-1. Electron energy spectrum of beam used to process CdTe.

Table 2-2. Electron-Deposition Calculations

Specimen	Beam Type*	Angle of Incidence
0.05 μm Hg over 19.95 μm CdTe	1	0°
0.10 μm Hg over 19.90 μm CdTe	1	0°
0.50 μm Hg over 19.50 μm CdTe	1	0°
4.24 μm Hg over 27.93 μm CdTe	1	0°
6.55 μm Hg over 21.44 μm CdTe	1	0°
7.20 μm Hg over 12.80 μm CdTe	1	0°
0.05 μm Hg over 19.95 μm CdTe	4	0°
0.10 μm Hg over 19.90 μm CdTe	4	0°
0.50 μm Hg over 19.50 μm CdTe	4	0°
4.24 μm Hg over 27.93 μm CdTe	4	0°
6.55 μm Hg over 21.44 μm CdTe	4	0°
7.20 μm Hg over 12.80 μm CdTe	4	0°
Hg _{0.8} Cd _{0.2} Te	3	0°
Hg _{0.8} Cd _{0.2} Te	3	60°
CdTe	3	0°
CdTe	3	60°
CdTe	1	0°
CdTe	1	60°
CdTe	2	0°
CdTe	2	45°
CdTe	2	60°

*See Table 2-1.

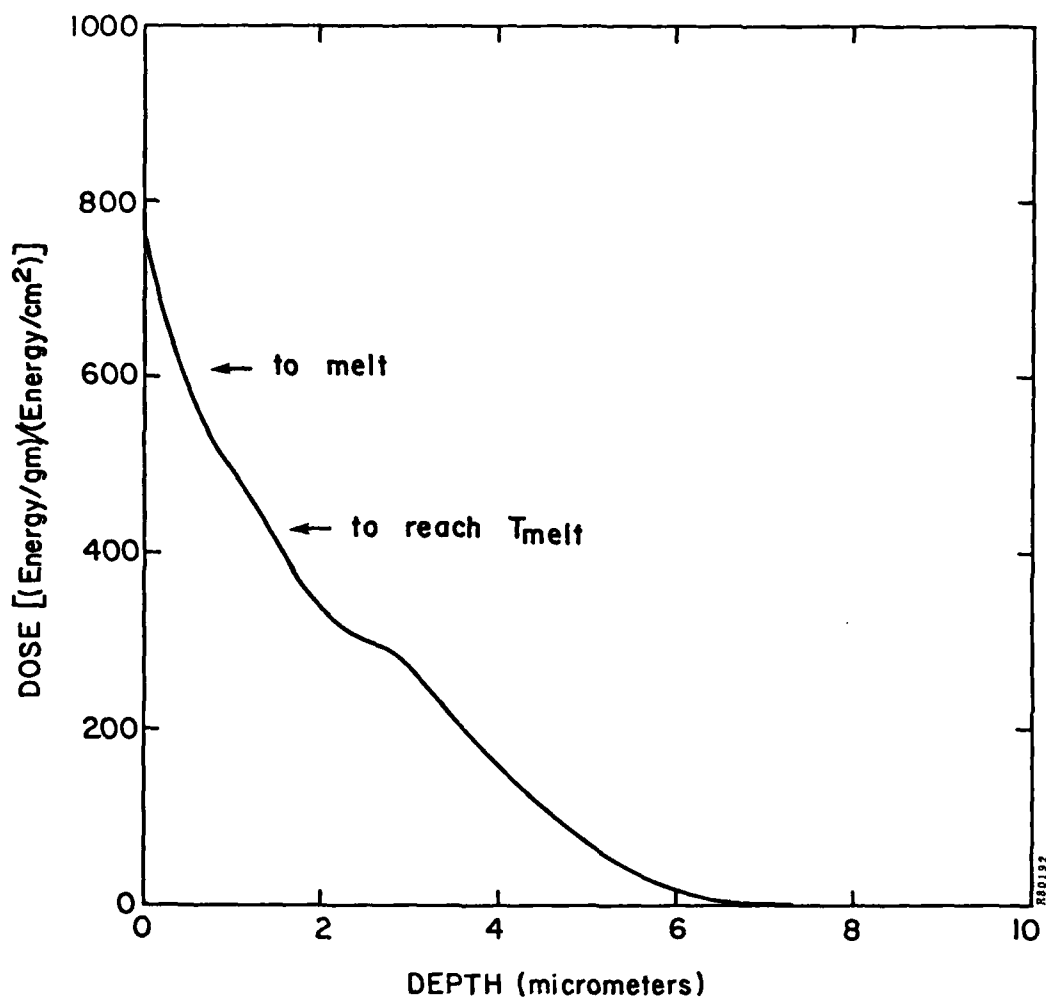


Figure 2-2. Energy deposition profile into CdTe by 20 keV average electron energy beam. (Note that dose, energy/g, is normalized to a unit fluence, energy/cm²).

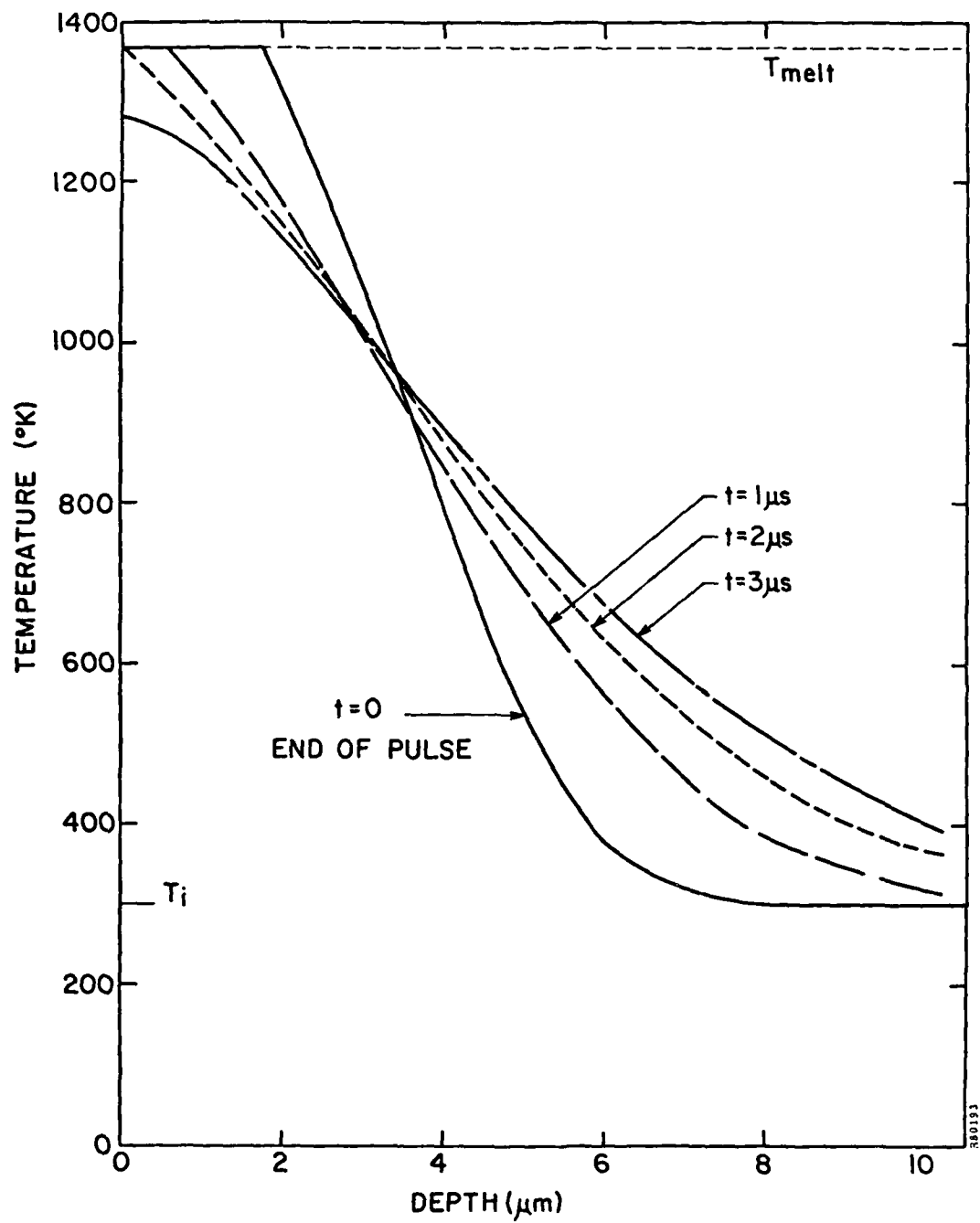


Figure 2-3. Thermal history of CdTe surface pulse heated by electron beam with spectrum shown in Figure 2-2, AT 0.9 J/cm^2 .

- The second beam (type 2) yields a deposition profile with its maximum a few tenths of a micron below the specimen surface, and with a broad peak. This beam, like type 1, produces surficial melting but with considerably less steep temperature profiles. The reduction in thermal gradient should reduce the chance for slip.⁽⁶⁾
- Beams type 3 and 4 deposit their peak energy at depths that are too great for melting thin surficial layers; indeed, their deposition profiles are characterized by maxima several microns below the surface (see Appendix A).

The type 2 electron beam, with a mean particle energy of about 20 keV, was selected for further process development. As shown by the deposition and temperature profiles in Figures 2-2 and 2-3, it offered the capability of melting thin surface layers with good depth control, which is essential for maintaining uniform composition. Moreover, the subsurface deposition peak appeared to cause little overheating of the molten surface and would promote stoichiometry. These several observations were corroborated and extended by the pulse-processing experiments described in Section 2.1.4.

2.1.3 Equipment

The pulsed electron beam equipment used for these experiments has been previously described.⁽⁷⁾ It is shown schematically in Figure 2-4. Briefly, it consists of a high voltage, d.c. charged transmission line which is rapidly switched into a diode load. The pulse width is fixed by the electrical characteristics of the discharge circuit. The electron energy is varied by changing the impedance of the field emission diode, and the current density is changed by altering the focusing of the beam. The electron beam diameter can be varied between 0.5 to 10 cm. The heating of the sample surface is controlled by altering the total energy per unit area delivered (the fluence). The fluence, quoted in joules/cm², is included in the description of each experiment.

The cooling rate of the sample surface is controlled, in part, by the initial temperature of the substrate. To test this effect, two pieces of apparatus were used for heating (or cooling) the sample above (below) ambient temperature. The heated sample stage is shown in Figure 2-5. Temperatures between 20 to 400°C can be achieved and monitored. Thermal isolation is achieved with minimal electrical resistance and inductance. The infrared heat source is external to the vacuum chamber. Measured radiation cooling rate is approximately one degree Celsius per second.

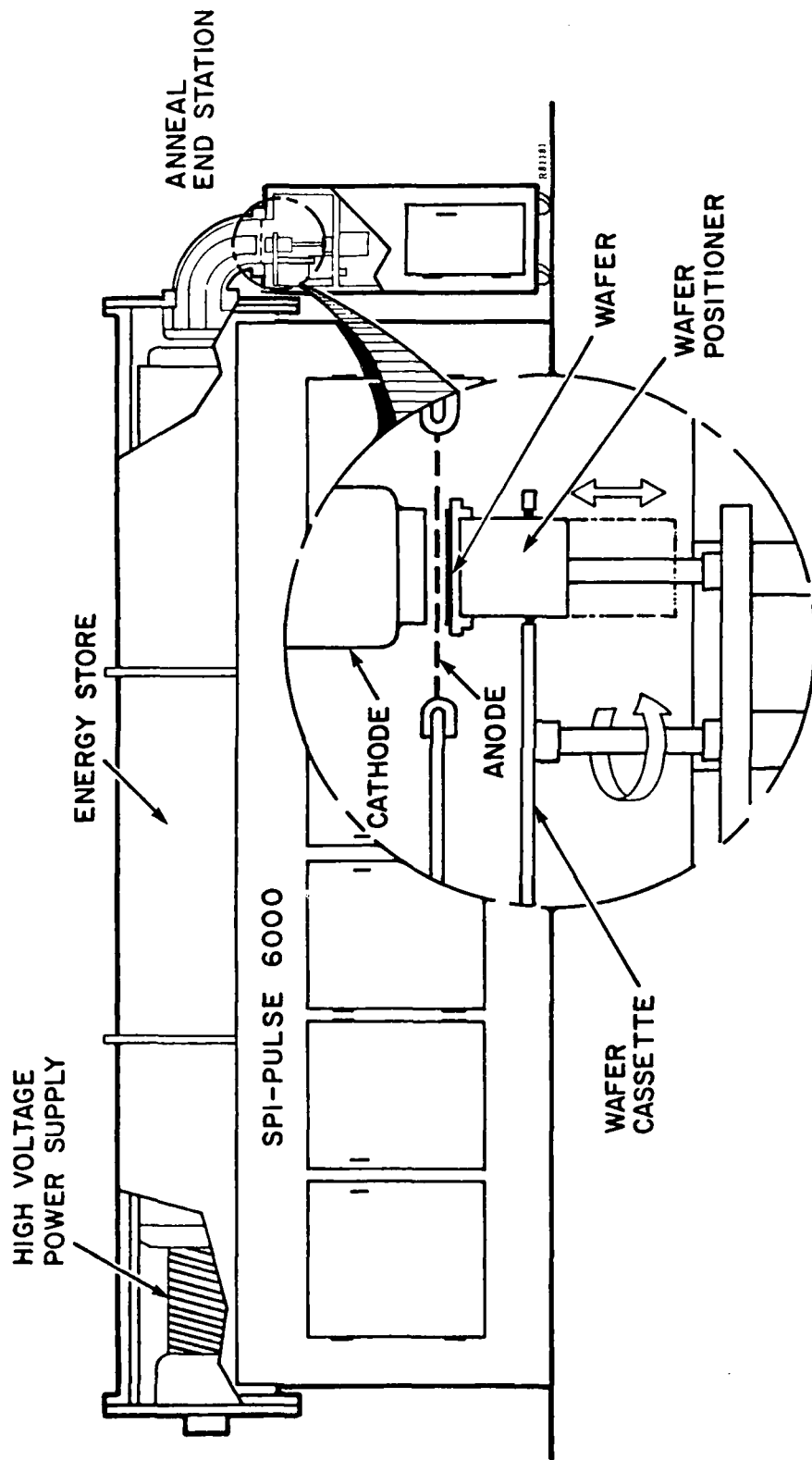
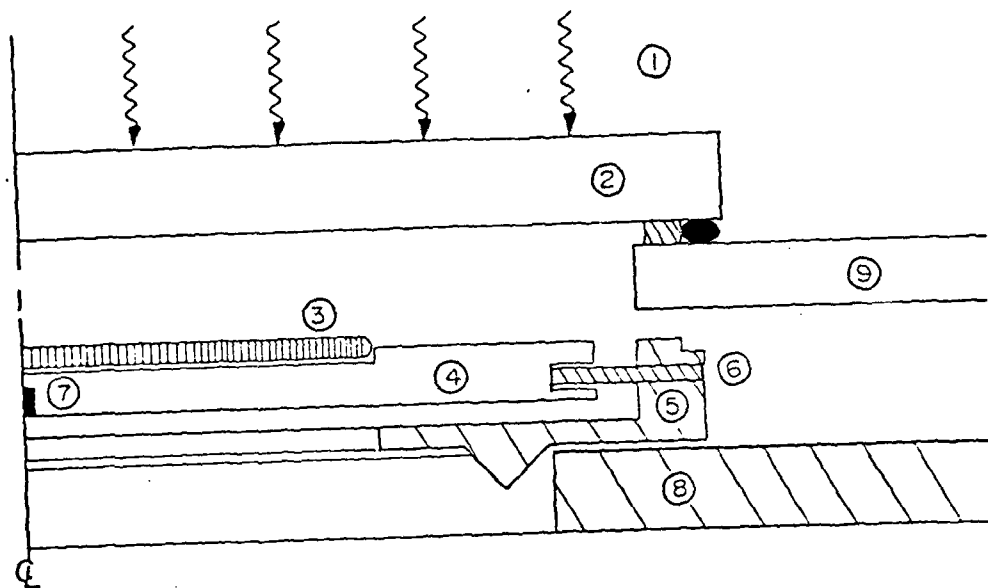


Figure 2-4. Schematic of SPI-PULSE™ 6000 pulsed electron beam processor.



1. Radiant heat source, outside of vacuum chamber.
2. Glass port, air cooled.
3. Two-inch sample with CdTe film.
4. Carbon disk.
5. Aluminum disk (normal holder assembly).
6. Set-screw thermal isolation (8).
7. Thermocouple (wires not shown).
8. Carousel for transport to diode.
9. Vacuum chamber top.

Figure 2-5. Heated sample stage for pulsed electron beam apparatus.

Samples were mounted on a cryostat, as shown in Figure 2-6, for cooling during pulsing down to 77°K. Lower temperatures are possible by special arrangement but were not used. This apparatus was used for pulsed diffusion experiments (Section 2.3.4) where Hg was evaporated onto the surface of a CdTe sample, cooled to liquid nitrogen temperatures in vacuum, and pulse heated. When the samples were warmed up to room temperature, Hg was found to be stably bound to the surface. Note that there is no appreciable change in average sample temperature as a result of the pulse process which heats only a few microns of material.

2.1.4 Pulse Processing Results

Three experiments were performed on bulk material to assess directed energy processing using electron beam type 2 (see Table 2-1) at an average angle of incidence of 45°.

- The first experiment defined the useful processing regime. The threshold values of beam fluence for melting and for damaging single-crystal CdTe were determined.
- The second experiment confirmed that the electron beam parameters indicated above were suitable for pulse-processing CdTe.
- The third experiment extended the demonstration of useful pulse-processing to $\text{Hg}_{0.2}\text{Cd}_{0.8}\text{Te}$.

Specimens of CdTe were wafers cut from a single crystal which had been rejected for optical use because of growth twins, but which were otherwise judged to be of the highest quality. The wafers were nominally 2 inches in diameter and 0.120 inch (3 mm) thick, polished on one side and lapped on the back. The area of the large twins was between 1 and 10 cm². All processing was performed on the polished surface. The sole specimen of HgCdTe was approximately 10 mm² in area and 1 mm thick, cut from a solid-state-recrystallized (SSR) wafer about 0.5 inch across. The composition of this sample, provided by NERC, was $\text{Hg}_{0.8}\text{Cd}_{0.2}\text{Te}$. Specimens were cleaned in successive baths of Alconox, de-ionized water, trichloroethylene, and methanol prior to use.

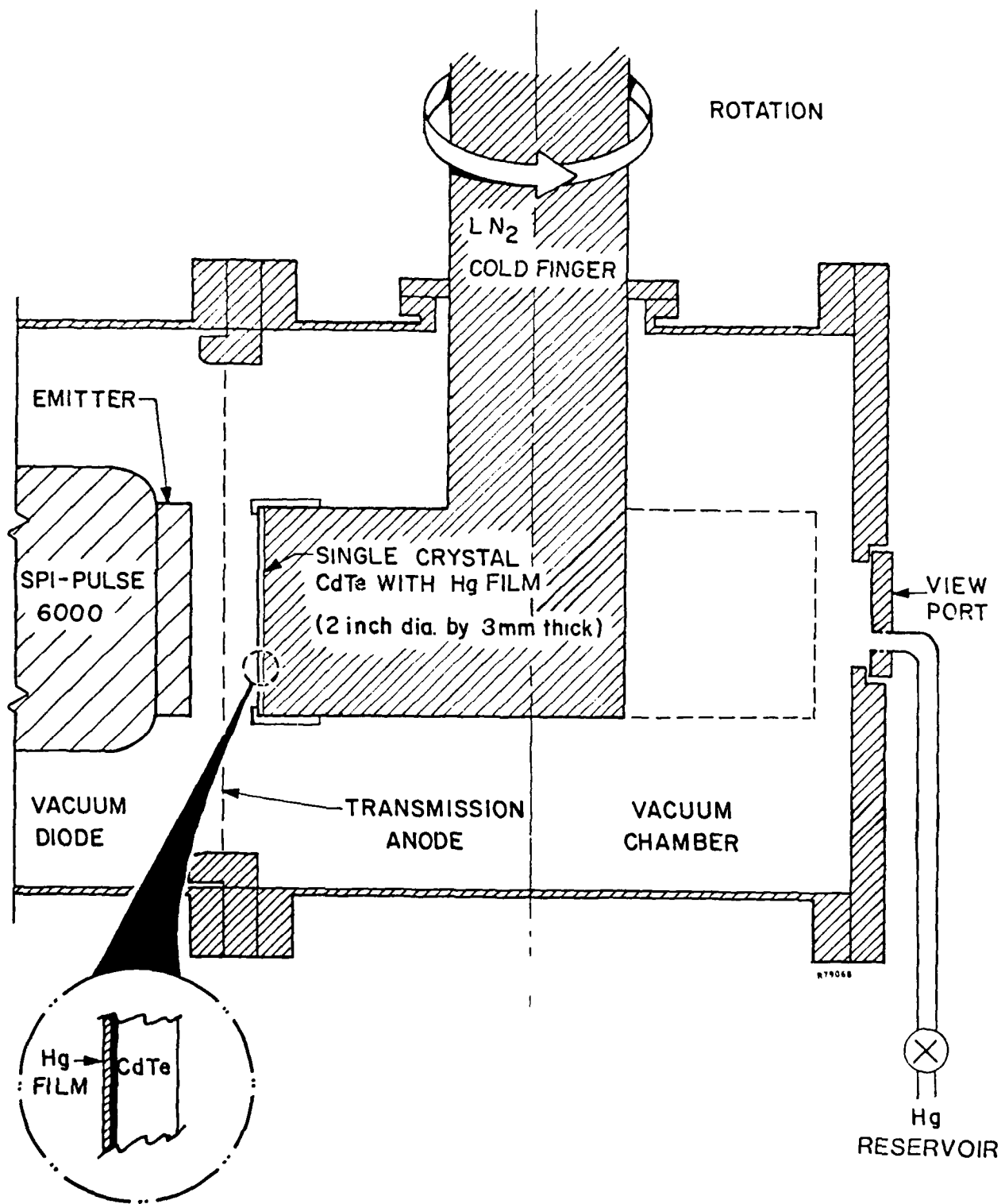


Figure 2-6. Cryogenic cooled sample stage for pulsed electron beam apparatus.

Definition of Useful Processing Regime

The first series of experiments determined the minimum fluence required to melt the surface of single-crystal CdTe, and the maximum fluence that can be sustained by the material without damage to the bulk. Since the calculations presented in Figure 2-3 indicated that the lower threshold is less than 0.8 J/cm^2 , the determination started at a fluence of 0.25 J/cm^2 and moved up in increments of approximately the same magnitude. Structural changes induced by irradiation were detected by examining the polished surface under the optical microscope.

The experimental results are given in Table 2-3. they indicate that single-crystal CdTe can be pulse-processed, i.e., surficially melted, without appreciable damage to the bulk, using a fluence of about 0.50 J/cm^2 .

TABLE 2-3 Pulse Processing of Single-Crystal CdTe;
Beam Type 2 at 45°

Fluence J/cm^2	Surface Appearance After Irradiation	Interpretation
0.25	no change	—
0.50	color change	surface melting; corroborated by SEM, EDAX, Auger spectroscopy
0.81	irregular discoloration; random pitting; a few slip lines	minor plastic flow
1.02	numerous slip lines	large-scale plastic flow
1.25	numerous slip lines	large-scale plastic flow

The wafer irradiated at 0.50 J/cm^2 (wafer T-8) was subsequently cleaved into smaller samples for substantiation of melting and for examination of stoichiometry. Scanning electron microscopy⁽⁸⁾ revealed clear evidence of surface melting; in situ energy dispersive analysis of x-rays (EDAX) showed some loss of cadmium. Table 2-4 shows the calculated elemental composition.

TABLE 2-4. Edax Analysis (15 kV Beam) of CdTe Before and After Pulse-Processing at 0.50 J/cm²

Element and Precision	Atomic Percent Calculated from X-Ray Spectrum			
	Cd	2Σ	Te	2Σ
Before Pulse-Processing	49.2	1.2	50.8	1.7
After Pulse-Processing	45.7	1.0	54.3	1.4

Since a deviation from stoichiometry was observed, a second sample from this same specimen was submitted for Auger spectroscopy⁽⁹⁾ with depth profiling by argon ion sputtering. The results, presented as Figure 2-7, confirmed that the pulse-induced melting changes the composition of the surface. In the unpulsed CdTe, surface contamination, principally carbon and oxygen, reduces the signals of the two main constituents, but the identical behavior of their traces indicates constant composition (at 50:50 atomic percent) with depth. In the pulse-processed crystal, on the other hand, the variance between the two signals indicates a drop in cadmium concentration at the surface. The depth of the affected layer is definitely less than 50 nm and possibly less than 10 nm; a more exact determination was precluded by the incompletely known dependence of the sputtering rate upon the composition.

The specimens used to locate the threshold for damage were quarter-wafers cut from wafer T-10. The specimen irradiated at 0.81 J/cm² was irregularly discolored and randomly pitted (Figure 2-8a); away from the central region of the Gaussian beam distribution, where the fluence was slightly lower, both pitting and discoloration were reduced (Figure 2-8b). Irradiation at 1.02 J/cm² and at 1.25 J/cm² induced large-scale plastic deformation, as evidenced by the appearance of slip lines on the specimen surfaces (Figure 2-8c); the extent of the deformation seemed greater at the higher fluence.

These results indicate that the middle of the useful processing regime for this beam (type 2) corresponds approximately to 0.6 J/cm², and this fluence was tentatively chosen for further process development.

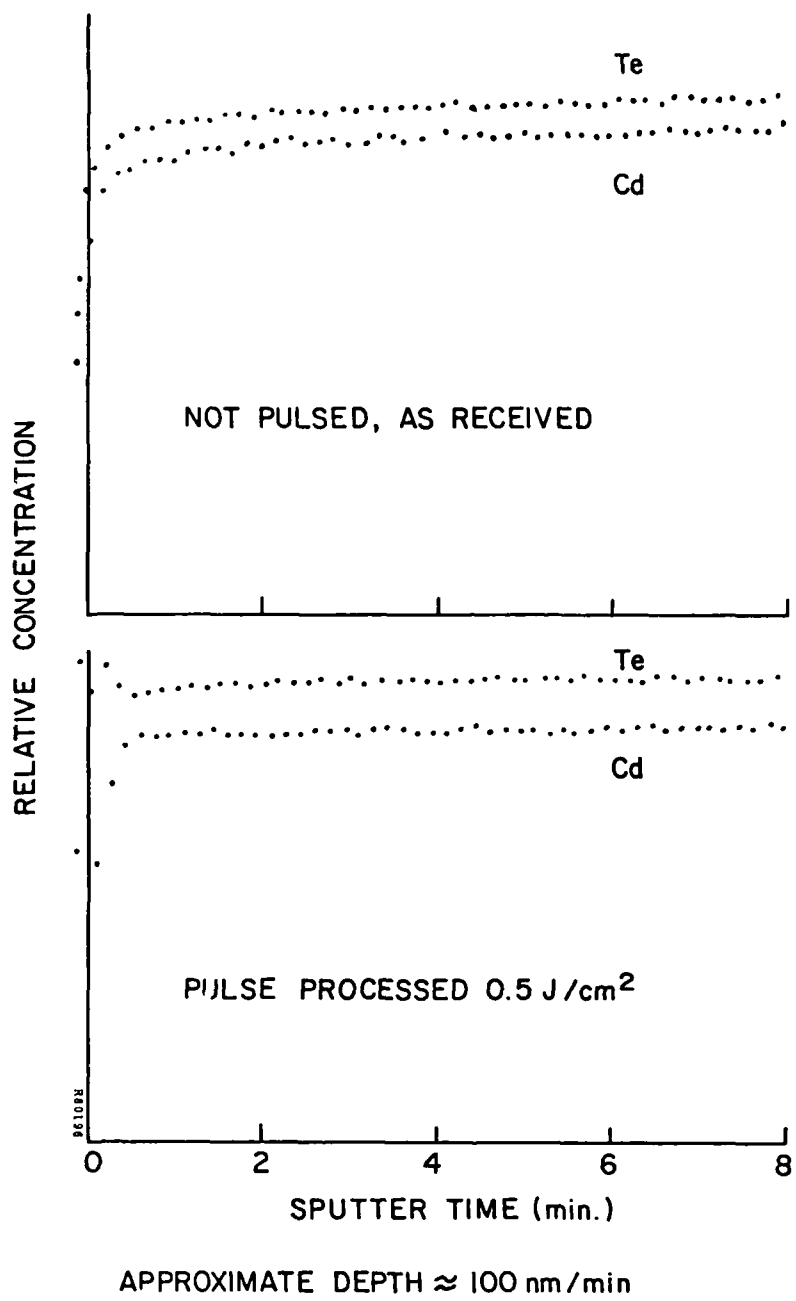
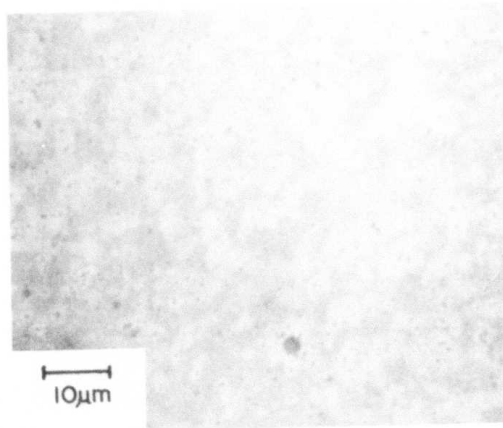
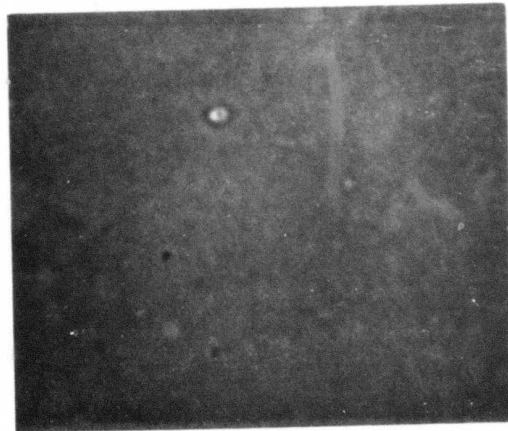


Figure 2-7. Depth profile of Cd and Te by Auger spectroscopy and argon ion sputtering for unprocessed and pulse-processed CdTe crystal at 0.5 J/cm².

(A)



(B)



(C)

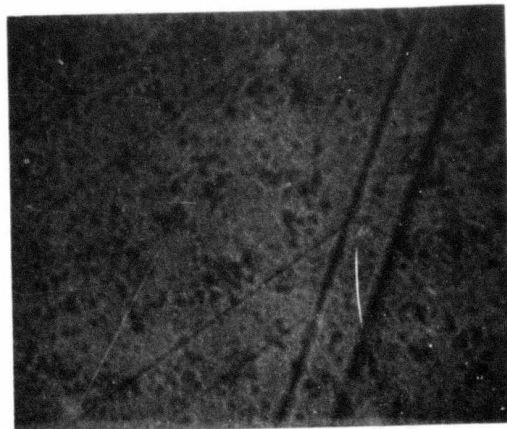


Figure 2-8. Photomicrographs (approximately 1000X) of pulse-processed CdTe crystals examined for damage threshold: (a) 0.8 J/cm^2 , (b) less than 0.8 J/cm^2 outside region of beam focus, and (c) 1.25 J/cm^2 .

Pulse-Processing of As-Implanted CdTe

The second experiment confirmed the capability of the selected beam to melt the surface of CdTe and to anneal the radiation damage left by high-dose ion implantation. A CdTe wafer (wafer T-11) was implanted with arsenic at 50 keV to a dose of 10^{16} ions per cm^2 . Arsenic was used as the implant ion in order to facilitate comparison with the literature on thermal annealing⁽¹⁰⁾; the dose was made high enough to yield an easily measured profile. The implanted wafer was cleaved into quarters, one of which was pulse-processed at the fluence of 0.6 J/cm^2 . Analysis by ion scattering spectrometry (ISS) showed that the implanted arsenic was redistributed during irradiation, thereby verifying that the surface had indeed been melted.

Pulse-Processing of $\text{Hg}_{0.8}\text{Cd}_{0.2}\text{Te}$

The third experiment demonstrated that the selected beam is also suitable for processing $\text{Hg}_{0.8}\text{Cd}_{0.2}\text{Te}$, which is the desired end-product of the present program. A specimen of polycrystalline SSR-grown material of this composition was irradiated at 0.60 J/cm^2 . No evidence of damage was found. Auger spectroscopy with ion-sputtering depth profile analysis yields curves (Figure 2-9) which are analogous to those for CdTe (Figure 2-7); namely, the concentrations of cadmium and mercury have been reduced in a thin surficial layer.

We were restricted to qualitative analysis of the Auger depth-profile data because recent results⁽¹³⁾, published after the analysis, showed that the electron beam used to generate the Auger data-signal affected composition beyond the uncertainties introduced by ion sputtering.

2.1.5 Evaluation of Pulse-processing Effects

The analytical results of physical modeling were used to establish a starting point for the development of process parameters; i.e., beam type 2 (mean electron energy ~20 keV) was identified as the best suited for producing surficial melting with minimal damage, and the angle of incidence was set at 45° . Pulse-processing experiments were then performed with this beam in order to determine proper values of fluence. (The mean electron energy and the fluence are the critical beam parameters, since processing effects are relatively insensitive to the details of the electron energy spectrum and to the pulse width.) The modest goal of these preliminary experiments was met.

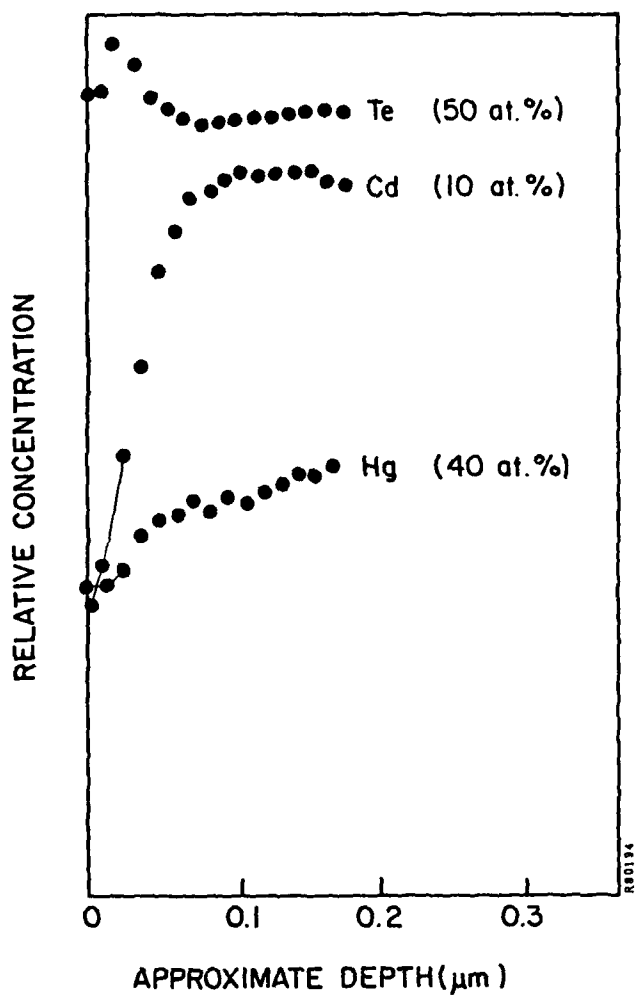


Figure 2-9. Depth profile of Hg, Cd, and Te in pulse-processed $\text{Hg}_{0.8}\text{Cd}_{0.2}\text{Te}$ at 0.6 J/cm^2 . (Note: Data by Auger spectroscopy and ion sputtering.)

A range of fluence was identified for pulse-processing CdTe, bounded on the low side by no effect and on the high side by unacceptable damage. Between these values, the material may be melted to a variable depth, with a maximum of about one to two micrometers. The material $\text{Hg}_{0.8}\text{Cd}_{0.2}\text{Te}$ appeared to behave in a similar fashion, and the same limits to pulse-processing were applied.

The experiments showed that the more volatile components, Cd and Hg, were lost from a thin surface layer believed to be less than 50 nm thick. Experience with processing GaAs has shown that good surface characteristics can be recovered by etching to remove the excess component.⁽¹¹⁾ Alternately, a cap of Si_3N_4 or similar material may be used⁽¹²⁾ to retain good surface quality. The change in surface composition was restricted and presented no problems in further experiments performed under this program.

2.2 PULSED ELECTRON BEAM PROCESSING OF CdTe FILMS

2.2.1 Objective

The objective of this task was to produce thin single-crystal CdTe films on foreign substrates with minimal defects and a smooth surface.

Optimal films deposited by evaporation upon crystalline substrates were epitaxial but with defects, such as microtwins, and a faceted surface. Directed energy processing, with which liquid-phase epitaxy (LPE) has been demonstrated for silicon⁽¹⁾, was expected to reduce the density of such defects and substantially improve surface morphology. An alternate approach, graphoepitaxy, was also tested to determine if pulsed processing could produce single-crystal films on patterned, amorphous substrates.

2.2.2 Heteroepitaxy and Surface Polishing

Heteroepitaxy obtains when the crystallographic orientation of the substrate uniquely determines the orientation of the deposited film. Thus, a single-crystal substrate induces the growth of a single-crystal layer, although the two may have totally different crystal structures, e.g., (111) silicon on (0001) sapphire. The theoretical explanation of heteroepitaxy is not complete, but its occurrence is known to be promoted by close structural matching, viz, low volume misfit and compatible symmetries across the interface plane.

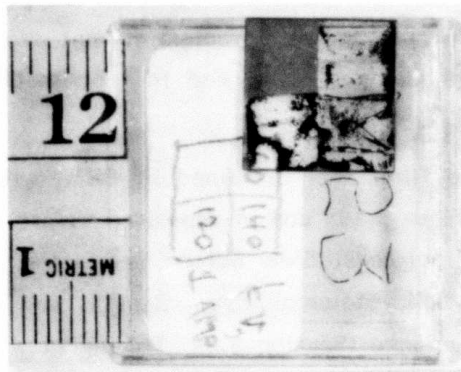
In addition, since structural control is exerted primarily by atomic interactions during film nucleation, the substrate surface must be truly clean, a condition commonly achieved by in situ vapor etching. Since etching was not part of the evaporation process described in Section 3, this may have led to some of the observed defects.

Liquid phase epitaxy by pulse processing is not as sensitive to interfacial contamination because the molten film can dissolve the impurity layer, then grow epitaxially. Compared to experiments with atomically clean surfaces, this case requires that the deposited film, when melted by pulsed processes, remain a liquid for a longer time at the interface. A greater fluence is therefore required.⁽¹⁴⁾ Impurities tend to segregate towards the surface of the film and good electrical characteristics can be recovered. The implication is that these experiments should work with thinner CdTe films at the highest fluence possible which would not damage, or melt the substrate.

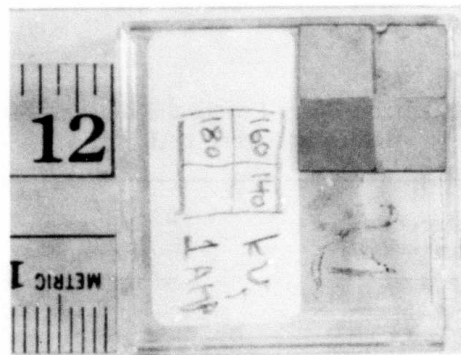
Samples were prepared (as described in Section 3) on mica, quartz, and sapphire. The CdTe films were 0.4 to over 20 microns thick. Typical results are shown in Figure 2-10 for mica; similar results were obtained for other substrates.

The CdTe films shown in Figure 2-10 were respectively (a) 0.4 μm , (b) 11 μm , and (c) 2.3 μm thick. The films in (a) and (b) were deposited before the modification to the hot wall apparatus discussed in Section 3.1.3; the film shown in (c) was deposited after the modification. To take maximum advantage of a limited number of samples, the pulse region was restricted to an area 0.5 by 0.5 cm^2 using a 0.5 mm thick carbon cask. Some interaction between the beam and the mask caused the fluence near the corners to be enhanced (visible in Figure 2-10(b)). Three different fluences were used to irradiate samples (a) and (b), but only one pulse was used on sample (c). Data are given in Table 2-5.

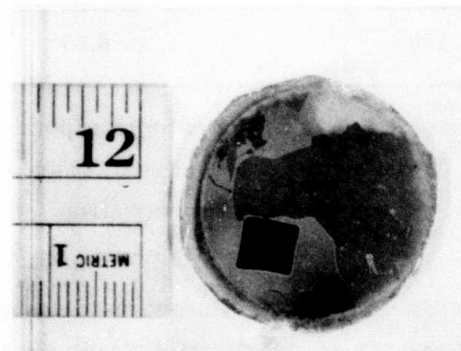
The adherence of these films to the mica substrate was poor. A tape test removed part of sample (c) in Figure 2-10 (upper right-hand corner). This is possibly the result of mismatched thermal expansion parameters between mica and CdTe. The poor adhesion, combined with definite melting of the entire film and electrostatic forces, led to the blowoff of the thinnest film (0.4 micron) pulsed on mica. The sheet resistance of the film was insufficient to carry the beam current (500 A/cm^2) without a large potential drop.



(a) 0.4 μm



(b) 11 μm



(c) 2.3 μm
(Epitaxial film)

Figure 2-10. CdTe films on mica, pulsed electron beam treated in 5mm x 5mm regions.

Hence the film blew off. This did not occur for films of practical interest, over 2 micron, as shown in (b) and (c). This blowoff problem did not occur for similar test films on sapphire. Pulsed electron beams can be used to process CdTe films on insulating substrates.

The structure of these films was examined by SEM, with EDAX, and by x-ray diffraction. Those samples (Figures 10a and b) deposited before the modification of the evaporation apparatus were polycrystalline before and after pulsing. There was no discernable change in the bulk stoichiometry. Sample (c) was not characterized completely prior to vapor exchange (Section 3.2). Pulsing at a fluence high enough to insure melting the entire depth of film improved the surface quality; it became smoother and more reflective. Thus, the area pulsed (Figure 2-10c) appears black because of specular reflection from the oblique illumination.

TABLE 2-5. Pulsed Electron Beam Processing Parameters for Samples Shown in Figure 2-10

Sample	Reference Voltage (kV)	Fluence (J/cm ²)
(a)	120	0.20
	140	0.31
	160	0.46
(b)	140	0.31
	160	0.46
	180	0.65
(c)	180	0.65

The surface melting was clear from microscopic examination (see Figure 2-11). The initial film was covered with "pyramid" structures which were absent after PEB processing. Removal of the material did not occur from weighting measurements. Melting was therefore implied.

The surface structure changed with the fluence used to irradiate the sample. At low fluence (0.2 - 0.3 J/cm²) the top of the pyramid structures melted and appeared to flow in a manner which would fill the void space. At higher fluence (0.4 J/cm²) there were still some peaks and voids visible in the surface. The smooth film shown in Figure 2-11 required 0.65 J/cm². At high fluences, films were damaged.

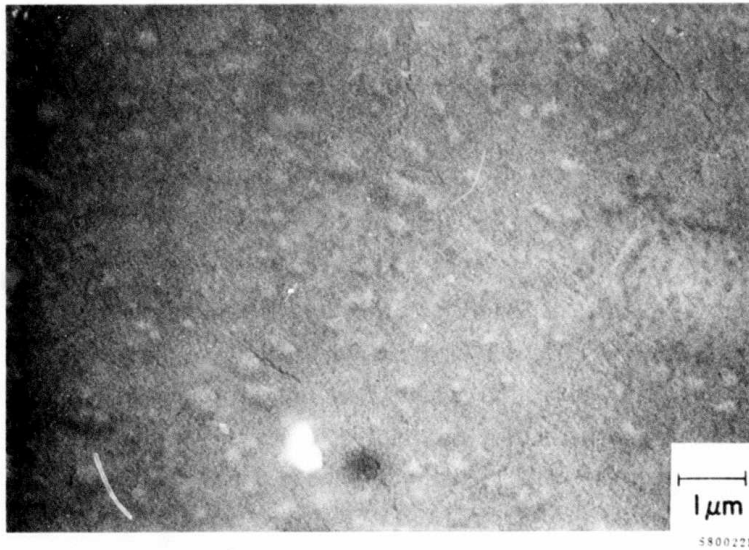
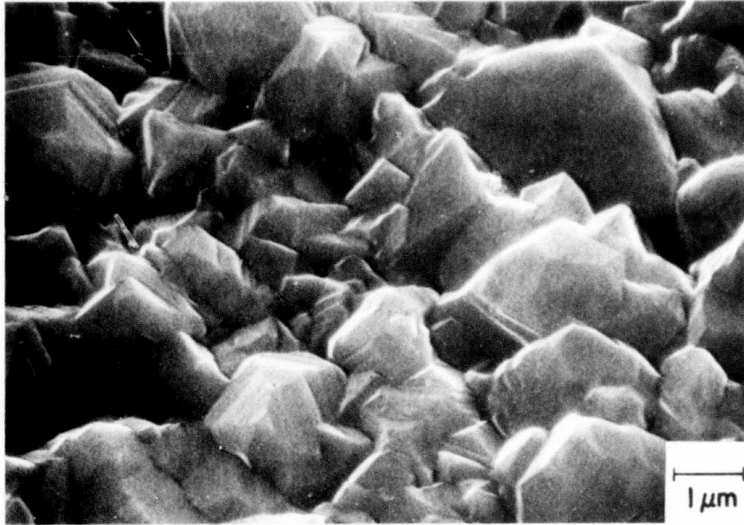


Figure 2-11. HWE deposited CdTe film before (top) and after (bottom) pulsed electron beam irradiation, showing in SEM microphotograph surface polishing by melting.

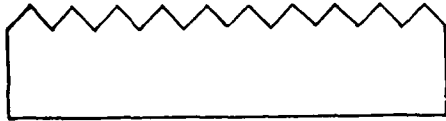
A sample (Figure 2-10c) was prepared to determine if pulsed electron beam surface melting would improve the final film after conversion to $\text{Hg}_{0.8}\text{Cd}_{0.2}\text{Te}$ by vapor exchange. Unfortunately, this sample was lost in a process malfunction.

2.2.3 Graphoepitaxy

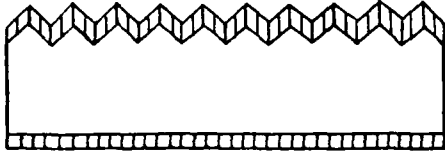
The possibility of crystal alignment of a thin film to a pattern etched into an amorphous substrate was demonstrated by H. Smith.⁽¹⁵⁾ This experiment is a variant on that process, pursued as an alternative when the initial evaporated CdTe films were not epitaxial on the crystalline substrate.

The graphoepitaxy process investigated by this research program is depicted in Figure 2-12. A (100) silicon wafer is etched anisotropically to produce a pyramid pattern with (111) faces atomically smooth and joined at exceedingly sharp corners (Figure 2-13a). This surface may be covered by a thin (~10 nm) oxide or replicated in a material to be specified later. The replication may be a positive or a reverse image. The pattern is now covered by a polycrystalline CdTe film (Figure 2-13b), sufficiently thick to fill all valleys with a smooth surface when melted. The film is pulse melted in a way that does not melt the patterned substrate. Upon rapid cooling, the film is oriented by the pattern, which corresponds exactly to a cubic structure. It is believed that the film will cool with one preferred crystal orientation induced by the patterned substrate. Furthermore, since the pattern was based on a perfect single crystal, all points in the film (which may cool at slightly different times or rates) should be in registry, and the film will become a single crystal.

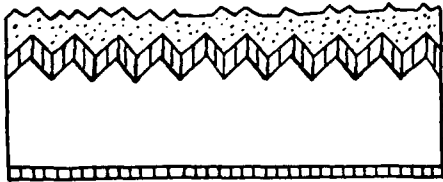
In these experiments, CdTe films were deposited directly on etched silicon, or oxidized etched silicon, only. The initial results were no different from films deposited on unetched surfaces. However, the results may not be taken as conclusive, because the deposited films had poor composition due to the faulty, initial hot wall reactor. Note, in Figure 2-13c, that the surface after pulsing is smooth due to melting.



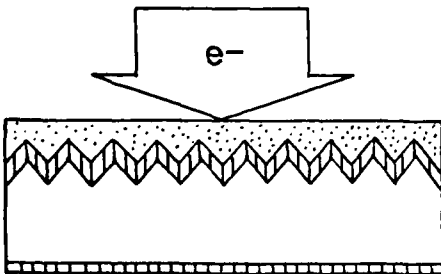
- Texture etch (100) silicon (~1 μm features)



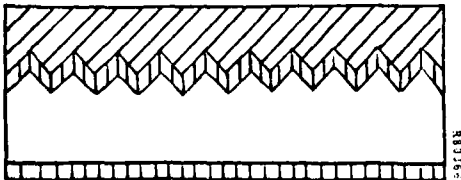
- Grow thin (~100 \AA) thermal oxide



- Deposit CdTe ($\geq 3 \mu\text{m}$)

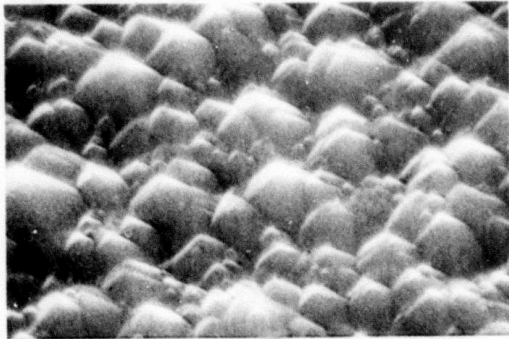


- Pulse with electron beam
- Recrystallize to single crystal film



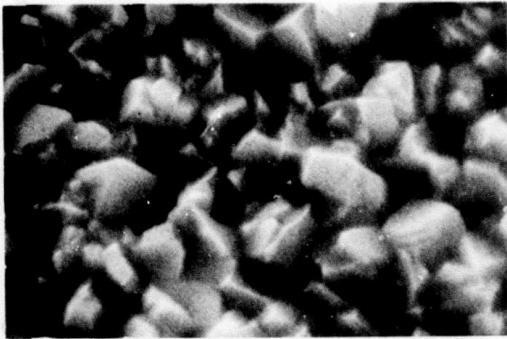
- Isothermal growth of HgTe and diffusion

Figure 2-12. Schematic of graphoepitaxy process.



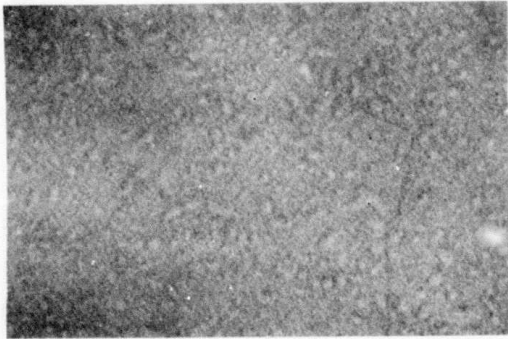
1 μ m

(a) Etched silicon substrate



1 μ m

(b) Above with 2.5 μ m CdTe film (as deposited)



1 μ m

(c) Above after pulsed electron beam heating at 0.65 J/cm²

Figure 2-13. SEM micrographs of results of graphoepitaxy experiment.

2.3 MODIFICATION OF CdTe BY ION IMPLANTATION

2.3.1 Objective

The goal of this task was to modify the composition of thin single-crystal CdTe films to form HgCdTe of specified composition. The initial approach was to implant Hg and Te and pulse anneal the film. The second approach was to evaporate Hg onto the cooled surface and pulse diffuse the layer into the substrate. Directed energy processing was chosen because of the large change in composition sought and the excellent crystal structure resulting from pulsed electron beam annealing (PEBA).⁽¹⁶⁾

2.3.2 Ion-Implantation Experimental Results

Mercury was implanted into bulk CdTe at 50 keV and at 5 keV. High total doses were used to assess the composition and film thickness which would be reached. Part of each implanted sample was pulse annealed, and pre- and post-pulse results were compared. Summarizing these results, the sputtering coefficient of Hg ions at 5 - 50 keV incident upon CdTe was so great that neither high Hg concentrations nor thick films of HgCdTe could be achieved.

The high current ion implanter at Spire Corporation was modified for these implants with the addition of an oven for solid sources and a sample holder for thick (3 mm) wafers. Purified HgCl₂ was used as a source of mercury. The implanter was initially set to admit isotopes ²⁰⁰Hg through ²⁰²Hg, to maximize the beam current (approximately 200 microamperes at 50 keV). This ion beam is scanned for 100 mm wafers, so the current density on the samples was 2 μA/cm². At 50 keV this was a power input of 0.1 W/cm², and the sample could have been heated.

The sample holder was rotated during implantation and was not actively cooled. As a worst case estimate of sample temperature (which was not monitored during implantation), radiation cooling from two sides can be assumed with an (approximate) emissivity of 0.5. At 0.1 W/cm² input this implies a sample temperature of 90°C at equilibrium. This value was considered acceptable. At 5 keV there would be a negligible temperature rise.

The implant time was 2 hours for a dose of 10¹⁷ ions/cm². This long period would allow contamination buildup as a result of residual vacuum chamber deposits on the sample being "knock-on" implanted; i.e., a Hg ion impinges upon an atom (C, H, or O) on the sample surface and "knocks" it into the CdTe. This effect was minimized through the

use of a cryopump installed on the end station of the implanter. Measurements were not made on this program for such efforts, but other work⁽¹⁷⁾ indicates that the cryopump did reduce hydrocarbon contaminants below detectable levels, whereas diffusion pumped systems degraded device performance when the implant took a long time.

Ion implanted samples were pulse annealed in the apparatus described in Section 2.1.3. The total fluence was held fixed at 0.9 J/cm^2 . Samples implanted at 50 keV to a dose of 10^{15} , 10^{16} , or 10^{17} ions/cm², and at 5 keV to 10^{16} ions/cm², were pulse annealed. Analysis compared as-implanted with post-pulse annealed samples. A comparison to thermal annealing was not attempted in view of these results.

Samples were analyzed in the order of increasing complexity and cost by EDAX, Auger spectroscopy, and SIMS (secondary ion mass spectroscopy). X-ray analysis of composition on an SEM was used as a survey technique. Mercury was not detected in any CdTe samples which were implanted at an energy of 50 keV, even at the maximum dose of 10^{17} ions/cm². At 5 keV and a dose of $10^{16} \text{ Hg}^+/\text{cm}^2$, a trace amount (about 1 percent) of mercury was detected by EDAX in the CdTe samples before pulse annealing. After annealing this element could not be detected. Presumably the surface concentration was reduced below the detection limits by diffusion during the anneal process.

Auger spectroscopy was used to analyze the high dose implanted samples. After this work it was reported⁽¹³⁾ that Auger spectroscopy was a poor technique for analysis of HgCdTe because the analyzing electron beam dissociates the material, preferentially removing the mercury from the surface. This effect could be seen when analyzing a "standard" $\text{Hg}_{0.8}\text{Cd}_{0.2}\text{Te}$ sample with Ar ion sputtering for a depth profile. The signal for Hg did not stabilize for the first 3 minutes (approximately 3000A) of sputtering. However, as the analysis failed to detect any Hg in any implanted sample, the accuracy of the technique did not affect the results. The minimum detectable Hg concentration, as determined by the "standard" sample, was about 1 atomic percent. Since we were looking for a concentration level of 40 atomic percent Hg, and found none, experiments with ion implantation were stopped.

PROCESSED DATA

CHARLES EVANS & ASSOCIATES

DEPTH PROFILE

Hg into CdTe (10:1) at 30kV

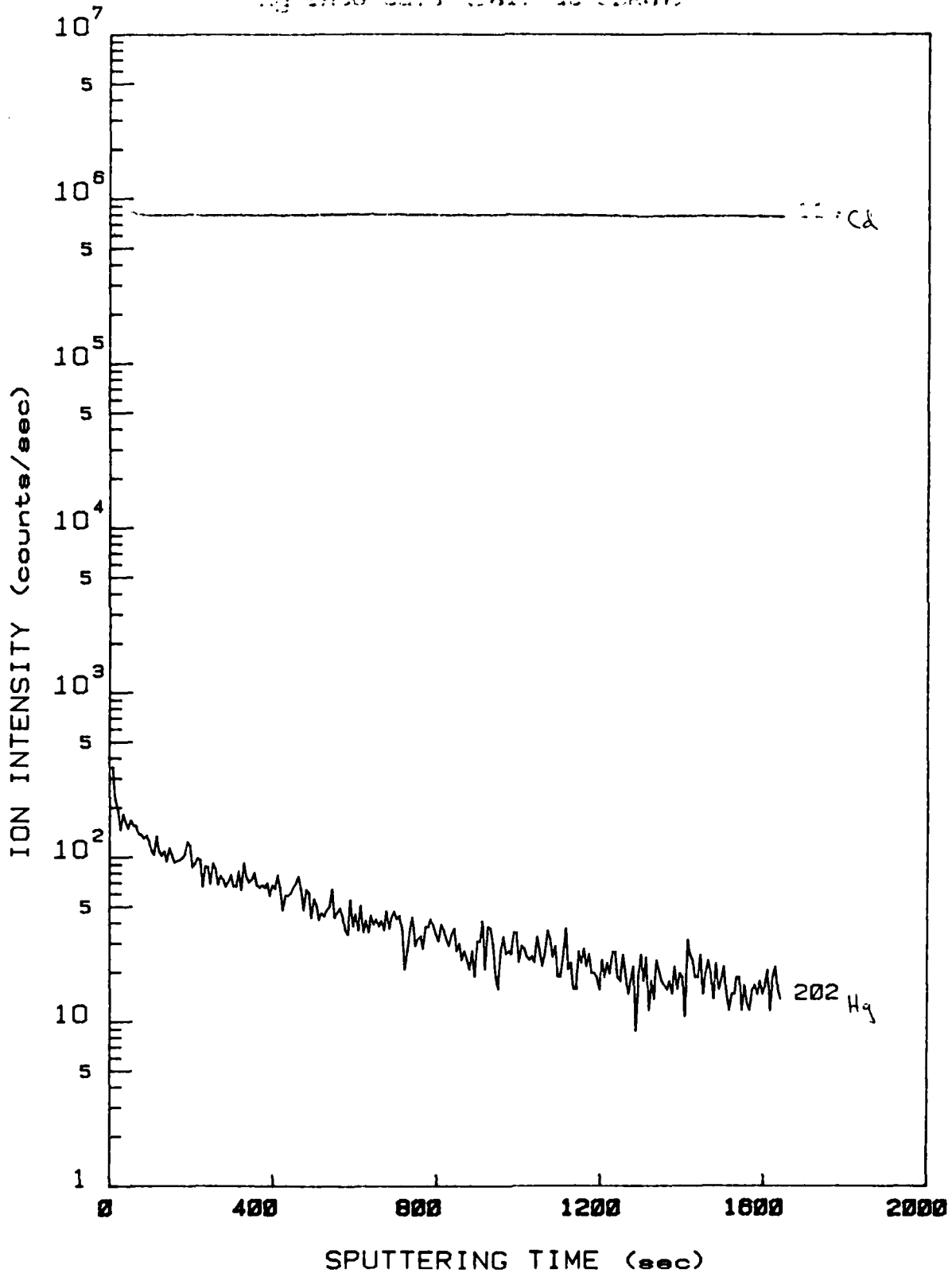
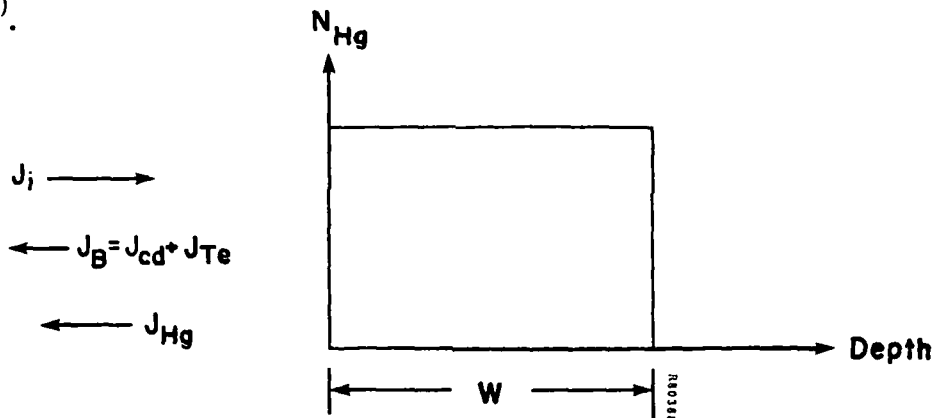


Figure 2-14. SIMS depth profiles of Cd and Hg in ion implanted CdTe.

One sample, CdTe with a 50 keV implant of 10^{17} Hg⁺/cm², was submitted for SIMS (secondary ion mass spectroscopy). The equipment used⁽¹⁸⁾ has a nominal sensitivity of 0.1 ppma. The result is shown in Figure 2-14. A rough concentration scale can be placed on the counts/sec with the (admittedly poor) assumption that the sensitivity of the detector signal to Hg and Cd is identical. The flat Cd signal is proportional to the 50 percent (atomic) constituent; the isotope ¹¹⁴Cd is 28.86 percent of the total Cd. The isotope of mercury, ²⁰²Hg, detected (mass 200 was not detected) would be 69 percent of all Hg in the sample if both isotopes 201 and 202 were implanted. The peak (surface) concentration of Hg shown in Figure 2-14 is then 100 ppm. This low value, plus the shape of the curve, imply that the implanted concentration is dominated by ion sputtering effects which are analyzed in the next section.

2.3.3 Analysis of High-Dose Implantation of Hg into CdTe

Consider the implantation of Hg into CdTe, using the treatment of Liau and Mayer⁽¹⁹⁾.



The flux of incident Hg ions J_i produces a uniform atomic mixture containing an implanted Hg concentration N_{Hg} and extending to a depth W below the surface; it also induces back-sputtered fluxes of both the implanted species J_{Hg} and the target species $J_B = J_{Cd} + J_{Te}$.

The steady-state or maximum achievable concentration of Hg is:

$$N_{Hg}/N_B = r/(S-1)$$

where the concentration of target species N_B comprises Cd and Te.

The preferential sputtering probability of the target species relative to Hg is r .

$$r = (J_B / J_{Hg})$$

The total sputtering yield is S.

$$S = (J_{Hg} + J_B) / J_i$$

Preferential Sputtering Probabilities

According to Anderson,⁽²⁰⁾ mass difference effects dominate sputtering from the target at all implant energies significantly above the threshold, with the light component preferentially sputtered; this becomes more pronounced as the mass of the projectile ion increases.

The preferential sputtering of the light component was confirmed by Liao et al.⁽²¹⁾ for the 20-80 keV energy range and by Lewis and Ho⁽²²⁾ for the low keV range. Their results suggest the following:

- For target species of different masses, the relative sputter yield is approximated by the inverse mass ratio.
- For target species of closely similar masses the relative sputter yield is approximated by the ratio of the sputter yields of the pure (atomic) components.
- The steady-state surface composition is independent of the energy of the projectile ions, whereas the thickness of the altered layer increases with increasing ion range.

Evaluation of Preferential Sputtering Probabilities of Cd and Te Relative to Hg

$$N_{Hg} / N_B = r / (s-1)$$

$$r = J_B / J_{Hg}$$

$$J_{Cd} / J_{Hg}$$

~ mass Hg/mass Cd

~ 200.59/112.40

~ 1.8

$$\begin{aligned}
 J_{\text{Te}}/J_{\text{Hg}} & \sim \text{mass Hg/mass Te} \\
 & \sim 200.59/127.60 \\
 & \sim 1.6
 \end{aligned}$$

$$\begin{aligned}
 r & \sim (J_{\text{Cd}} + J_{\text{Te}})/2J_{\text{Hg}} \sim 1.7 \\
 N_{\text{Hg}}/N_{\text{B}} & \sim 1.7/(S-1)
 \end{aligned}$$

This steady-state concentration obtains after the sputter-removal of a thickness $\sim rW$, where W can be identified with the range of the ions. This last equation is plotted in Figure 2-15. From it and Figure 2-14, the implied sputtering coefficient of 50 keV Hg^+ incident upon CdTe is over 1000.

Sputter Yield from Theory

Recent work⁽²³⁾ has estimated sputtering yields for heavy ion bombardment of metals by considering the process as evaporation from a thermal spike induced by the bombardment of a single ion. From this work, the thermal sputtering yield is given by:

$$Y = 0.0360 (\lambda a^2 F_D^2 / U^2) g$$

where $\lambda \sim 24$ and $a \sim 0.219 \text{ \AA}$ are constants, F_D is the energy deposited per unit track length of the incident ion, U is the planar surface potential, and g is a function of $U/k T_0$ where T_0 is the temperature of the spike (approximately 1 eV). The binding energy of II-VI compounds is approximately 1.4 eV, which was used as an estimate of U . The value of g was then one half.⁽²³⁾ The value of F_D at the surface was taken from tables for 50 keV gold implanted into CdTe⁽²⁴⁾ at 3.24×10^6 eV/micron. The resulting sputtering yield due to the thermal spike was approximately 1100.

The value of the sputtering yield from linear cascade theory⁽²³⁾ would be only 34, using the same approximate numbers given above. Data from this experiment, therefore, supports the thermal excitation model of sputtering.

2.3.4 Evaporation and Pulse Diffusion Results

Evaporation and pulse diffusion of thin layers have been shown to produce epitaxial crystalline layers in semiconductor materials⁽²⁵⁾. Because sputtering effects seemed to rule out ion implantation of Hg as a means of forming HgCdTe layers a few

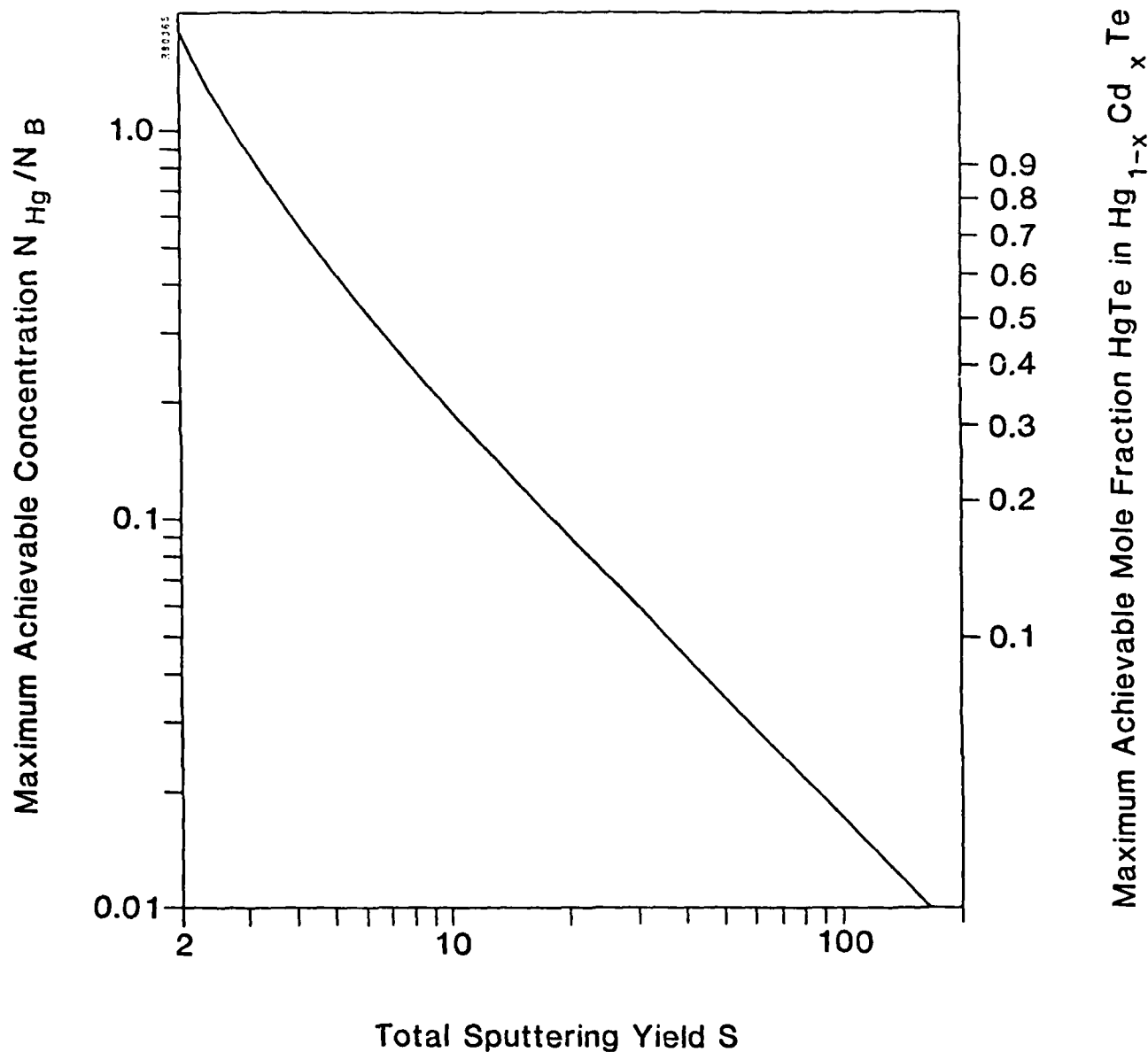


Figure 2-15. Concentration x of $\text{Hg}_{1-x}\text{Cd}_x\text{Te}$ as a function of sputtering yield for Hg^+ implanted into CdTe.

microns thick from CdTe, evaporation and pulse diffusion were tried as an alternate approach. Using the apparatus shown in Figure 2-6, two experiments were performed. Mercury vapor from a heated ($\sim 100^{\circ}\text{C}$) source was directed against a crystalline, bulk CdTe sample held at 77°K (liquid nitrogen cooled). When a visible layer accumulated, the sample was turned around and pulse heated by an electron beam (in vacuum). This experiment was repeated using a different portion of the same substrate, iterating the evaporation-pulse procedure four times. The sample was then heated to room temperature and analyzed.

The two pulsed areas had a distinct silvery appearance which did not change when warmed up to 25°C or taken out of the vacuum chamber. Analysis by an SEM showed the surface of the singly pulsed sample had a fine scale ($\leq 1\ \mu\text{m}$) texture. In the RBEI (Robinson Backscattering Electron Imaging) mode, the composition of this surface appeared nearly uniform. Auger analysis indicated that the Hg content in a region within 0.1 micron of the surface was between 1 percent and 10 percent. The sample which had been pulsed 4 times had a rough surface but also had a Hg content over 40 atomic percent. The experiment could be repeated with combined Hg and Te evaporation to achieve the correct composition.

SECTION 3
TECHNICAL INFORMATION - REPORT OF SUBCONTRACTOR
NEW ENGLAND RESEARCH CORPORATION

3.1 DEPOSITION OF SINGLE CRYSTAL CdTe FILMS

3.1.1 Objective

The objective of this task is the vapor growth of high-purity CdTe epitaxial layers on foreign substrates. The technical approach employed in achieving this goal is the Hot Wall Epitaxy (HWE) method. This method emphasizes the importance of attaining growth conditions as near as possible to thermodynamic equilibrium as well as zero vapor transport losses. Thus, heteroepitaxial CdTe films of high crystalline perfection are expected.

3.1.2 HWE Process Description

Deposition of single-crystal films of CdTe presents a number of difficulties. First, during evaporation CdTe decomposes into Cd gas and Te₂ gas (unlike the lead chalcogenides which evaporate mainly in molecular form). Second, the vapor pressures of Cd and Te₂ are different by a factor of 20. Third, CdTe is a material which can grow in either the cubic sphalerite or the hexagonal wurtzite structure, depending upon the growth conditions. These structures are similar, but differ in the ordering of their close-packed planes. Hence, the tendency of CdTe to form polymorphs and stacking faults during growth is marked.

When CdTe is deposited onto a cold substrate, the result is invariably a fine grain polycrystalline or amorphous film. This situation is not remedied by merely increasing the temperature of the substrate and a more controlled method is necessary.

In order to overcome these difficulties, the Hot Wall Epitaxy (HWE) method was developed and has been successfully used to grow epitaxial single-crystal films of many materials.⁽²⁶⁾ The system consists of a heated wall which encloses the source and the substrates in an essentially vapor-tight manner. If the entire source-hotwall-substrate system is held at the same temperature, the system would be at equilibrium and no

growth would take place. If, however, a temperature gradient is introduced, the vapor pressure of the system is limited, corresponding to that of the lowest temperature (i.e., that of the substrate). Since the source is at a higher temperature, evaporation of source material takes place and deposition of CdTe on the substrate occurs. The deposition rate depends on the temperature difference between the source and the substrate. The problem is to find a temperature difference which gives a growth rate which is fast enough to be useful and which is slow enough to give good single-crystal epitaxial films.

This method achieves the following ends:

1. It avoids the loss of the high vapor pressure components.
2. It allows growth to occur at a controlled rate close to equilibrium.

Substrate Selection

Heteroepitaxial processes require careful choice of substrates. Parameters of interest are the lattice constant, orientation, thermal expansion coefficient, and ability to achieve a truly clean surface. Epitaxial growth is not possible in the presence of contaminants, and the film will be damaged or will peel off the substrate for mismatched thermal expansion properties. The quality of the crystal structure of the final film will depend upon the match in atomic spacing and orientation.

Four substrate materials have been used for the deposition of CdTe films; namely, muscovite mica, single-crystal quartz, sapphire and silicon. The reasons for the choice of these particular materials were as follows:

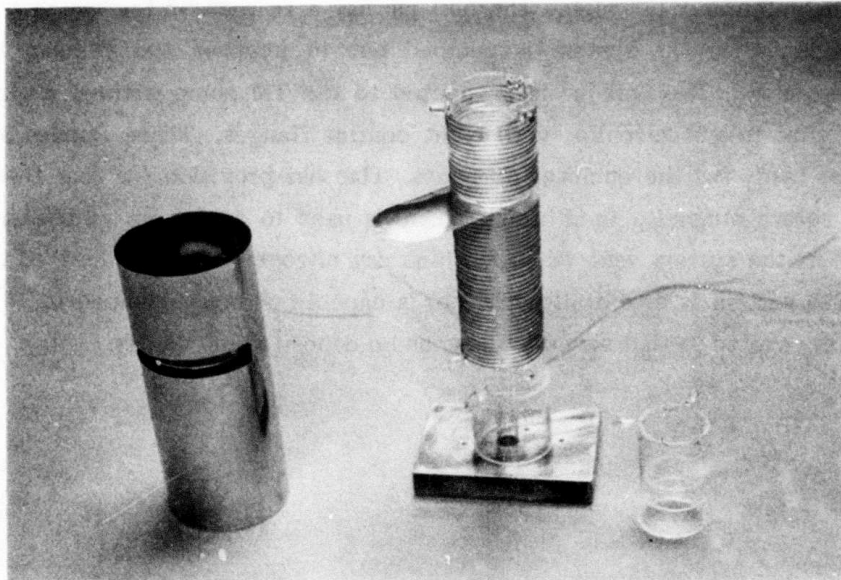
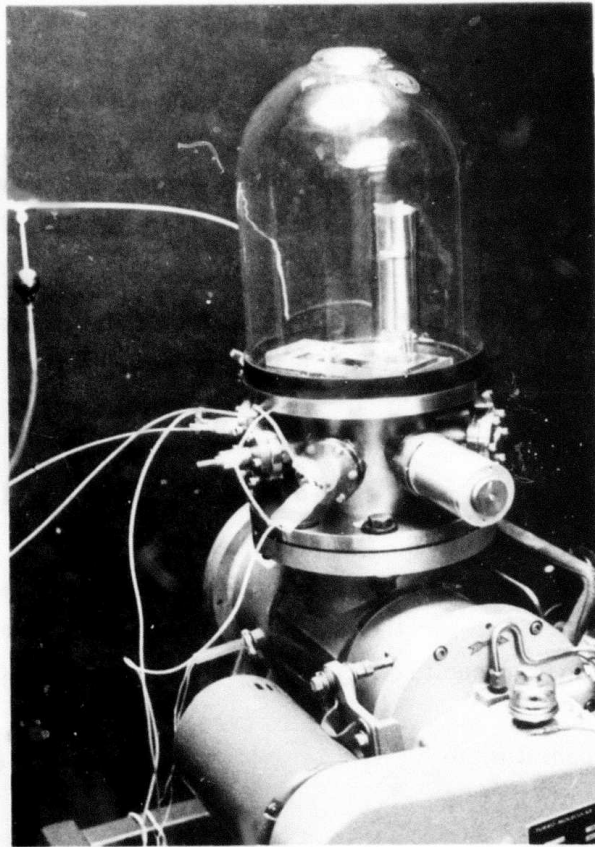
1. Mica is a readily available, cheap substrate material which has a facile cleavage plane. This allows the use of perfectly oriented substrate which is uncontaminated if carefully used. It is a cheap and easy substrate to use in quick repetitive experiments to obtain data for the optimization of deposition parameters. Its expansion coefficient normal to the cleavage plane is $8.5 \times 10^{-6}/^{\circ}\text{C}$ compared with 5.5×10^{-6} for CdTe. It may be used at temperatures up to 550°C , which is higher than the operating temperature at which the vapor transport experiments are performed. It is therefore a possible substrate for later practical use and not just a convenient substrate for calibration of the apparatus.

2. Crystalline quartz is a readily available, easily cleanable substrate. It is the crystal form of fused silica, which is known to be innocuous to HgCdTe at higher use temperatures during bulk growth. It can be obtained in oriented-polished form. It was chosen therefore as a noncontaminating substrate.
3. Sapphire is a substrate commonly used with bulk HgCdTe and has an excellent thermal expansion match. It is a clean, noncontaminating substrate and may be obtained oriented with its surface normal to the hexagonal c-axis. However, it is difficult to obtain oriented to better than 1° .
4. Silicon is cheap and easily obtainable in very pure form, oriented to the desired crystal plane. It must be protected from Te vapor at the temperature at which the vapor transport experiments are performed and hence needs a thin layer of oxide on the surface. Silicon was thus suited only for experiments in graphoepitaxy.

3.1.3 Description of Apparatus

Vacuum Systems

The vacuum system is shown in Figure 3-1. It consists of a 400 Welch Turbomolecular (TM) pump backed by a Welch mechanical pump. The bell jar is glass and is 12" in diameter and 18" high. The bell jar has a re-entrant top which is filled with liquid nitrogen when the system is pumped out to improve the vacuum by pumping condensable vapors. The bell jar is connected to the TM pump without a gate valve by means of a stainless steel collar with eight conflat flanges. Three flanges are used for high current leads for the enclosed furnaces. One has provision for four thermocouples. One has a rotary magnetic feedthrough. One is used to attach an ionization gage, and one is used as the system vent through which dry nitrogen may be admitted to break the vacuum. The system is essentially oil-free, is capable of being pumped to 10^{-8} torr, and can be rapidly cycled so that several films can be deposited in one day.



581078P

Figure 3-1. The Vacuum System for Hot Wall Epitaxy deposition of CdTe Films (top) and initial furnace (bottom).

Hot Wall Epitaxy Furnace

The Hot Wall Epitaxial furnace progressed through a number of design changes. Figure 3-2 shows the preferred modification, which produced single-crystal cadmium telluride films on mica and quartz substrates reproducibly. The source consists of a silica furnace tube on which are wound two molybdenum heaters side by side, one to heat the substrate and the other to heat the source and the entire chamber wall. The temperatures of the source and substrate are measured by means of thermocouples. The deposition chamber is contained in the furnace tube and is of the "quasi-closed" type. It consists of a silica source container, a silica baffle, a silica separating cyclinder and the substrate. These parts are held together by gravity to form a quasi-closed volume which ensures that there is minimal loss of material and that the vapor pressure of CdTe is close to the equilibrium state when the source and substrate furnaces are adjusted to their optimum temperatures.

The initial version of the quasi-closed evaporation source had a thin slot in it, so that a shutter could be inserted to prevent deposition of CdTe onto the substrate until the source and substrate temperatures had been stabilized at the desired values. It was not possible to obtain single-crystal CdTe films with this earlier evaporation source. Subsequent experiments determined that it was necessary to have the evaporation source as nearly as possible tightly closed in order to obtain epitaxial films. The reason for this is probably that CdTe decomposes incongruently to Cd and Te_2 at $500^{\circ}C$ and the vapor pressures of the component gases are different by more than a factor of 20. It is thus necessary to keep the system as close as possible to thermodynamic equilibrium, and this is done by using the system shown in Figure 3-2.

3.1.4 Heteroepitaxial Growth of CdTe on Mica

A series of calibration experiments was performed to determine the range of substrate and source temperature which give single-crystal films of CdTe. These temperatures were measured by two thermocouples placed as close as possible to the source and substrate. There is an unknown but constant difference between the measured and the actual temperature due to the fact that the thermocouples

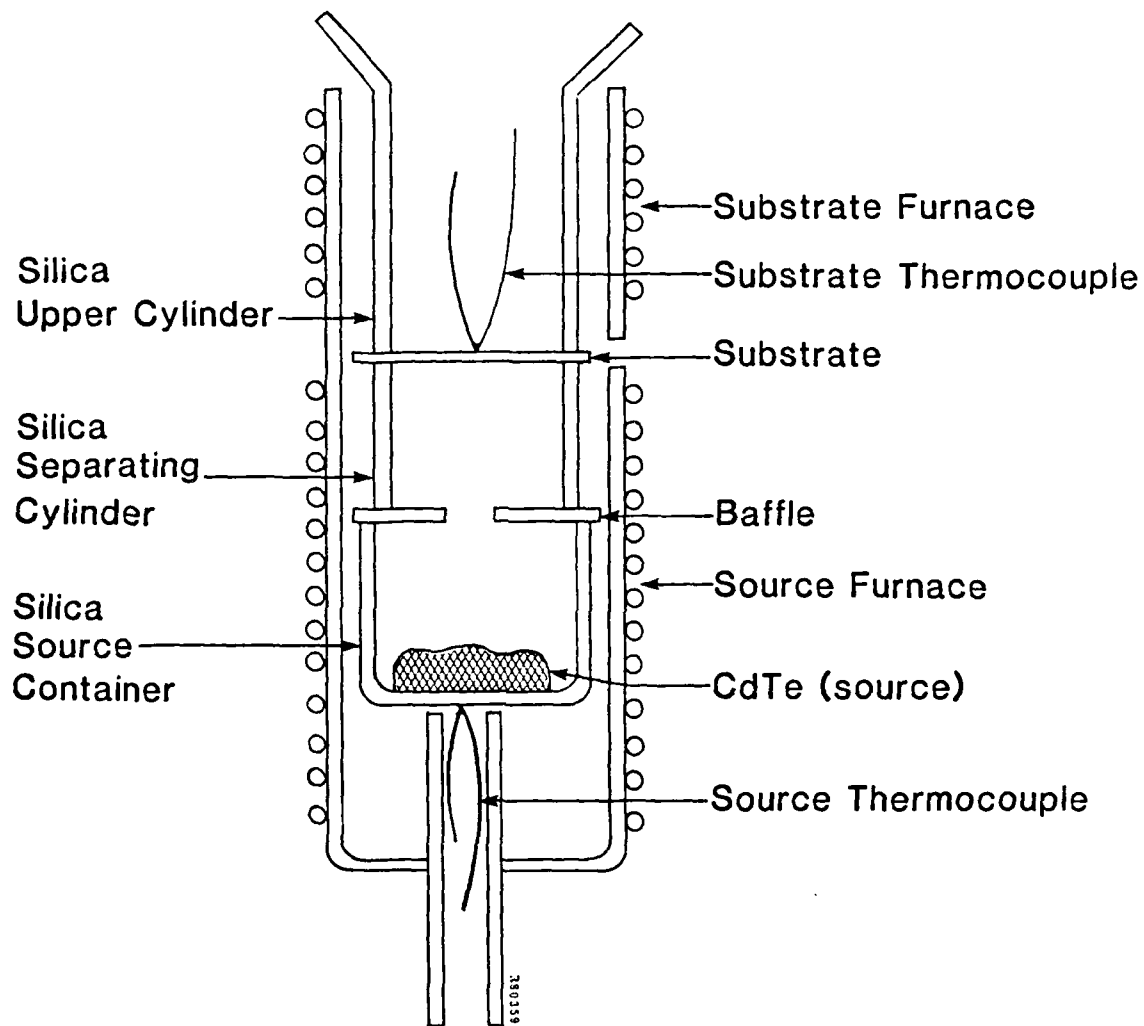


Figure 3-2. Redesigned hot wall furnace with enclosed source (at NERC) for evaporation of CdTe.

are not in physical contact with the source or the surface of the substrate that received the CdTe film. It was impractical to place them in contact with these materials without running the risk of contamination. The deviations, however, are constant from run to run.

Since the system does not allow the determination of the deposition time by means of a shutter, for the reason mentioned in Section 3.1.3, it is not possible to determine the temperature at which the film commences to nucleate on the substrate.

Table 3-1 shows the reproducibility of thickness of 16 CdTe films. Films 124 through 139 were consecutive depositions. The average film thickness was 2.18 microns with a standard deviation of 0.29 micron. This demonstrates that the Hot Wall Epitaxy apparatus has excellent film thickness control.

The film thickness is independent of the amount of CdTe source material in the boat, whether this material has been used several times, or is a fresh charge. It thus appears that the conditions of deposition are close to equilibrium, with the vapor pressure of Cd and Te_2 being determined by the lowest temperature surface inside the quasi-closed Hot Wall Chamber (i.e., the substrate surface).

The time-temperature cycle indicated in Figure 3-3 is suitable to produce single-crystal films of CdTe on mica. The envelope of suitable substrate and source temperatures to give single-crystal films of CdTe on mica is shown in Figure 3-4.

3.1.5 Characterization of CdTe Films on Mica

The crystal character of the films deposited on mica can be readily observed by an optical microscope under 400x magnification. The surface of the layer shows a structure of pyramids which are aligned over the entire area of the 2.5 cm O.D. substrate. The typical dimension of these pyramids is about 10 microns. This pattern suggests that the (111) plane of cubic CdTe is deposited parallel to the mica face.

If the deposition of the film were arrested at a very early stage, the initial nuclei of the growing film can be seen. Figure 3-5 shows a SEM picture of CdTe nuclei at a magnification of 10,000x. This figure shows that the nuclei are aligned, but that some of them are rotated by 180° with respect to the others. This twin orientation is to be expected because the surface of the mica has a sixfold symmetry whereas the (111) plane

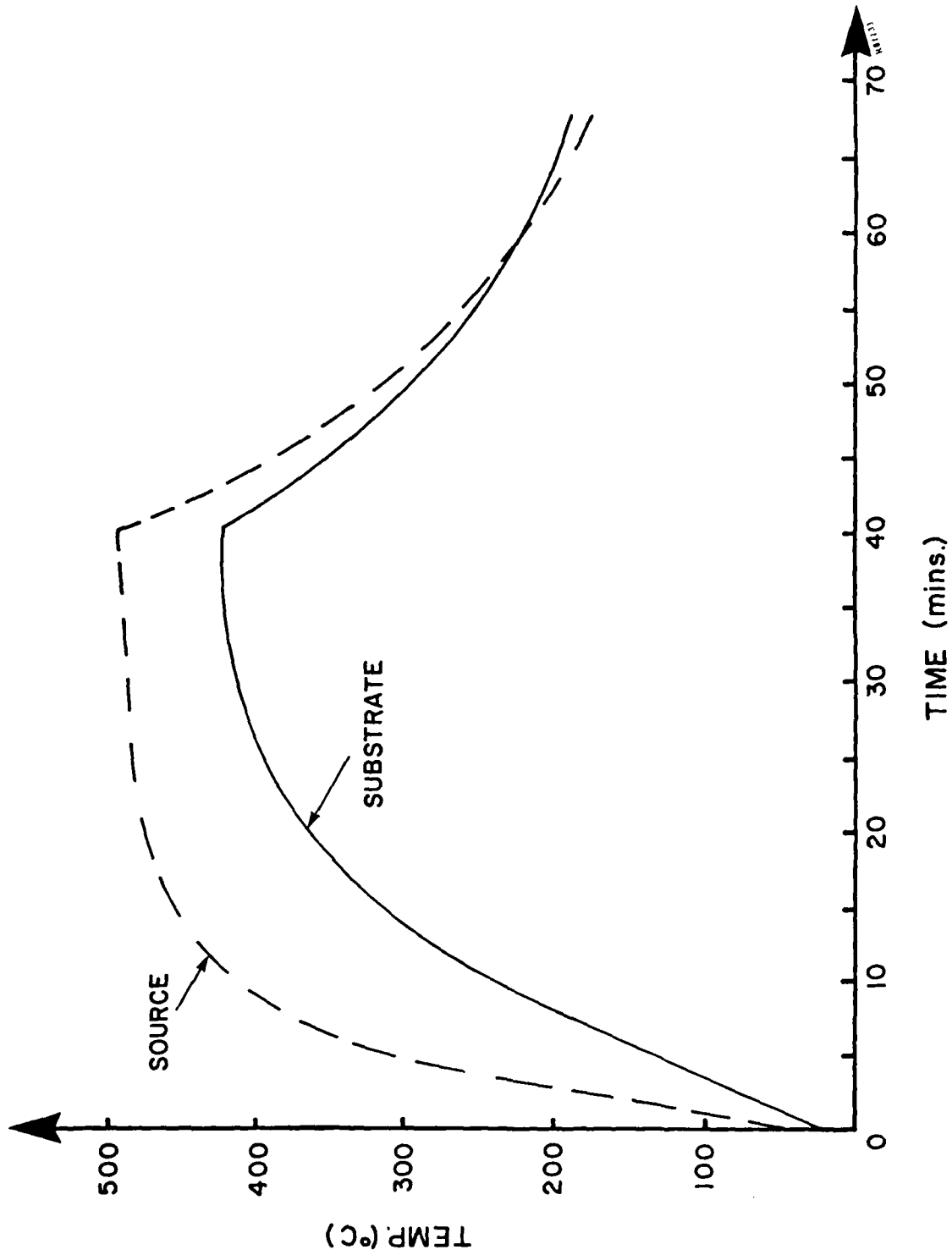


Figure 3-3. Time-temperature cycles of the source and substrate.

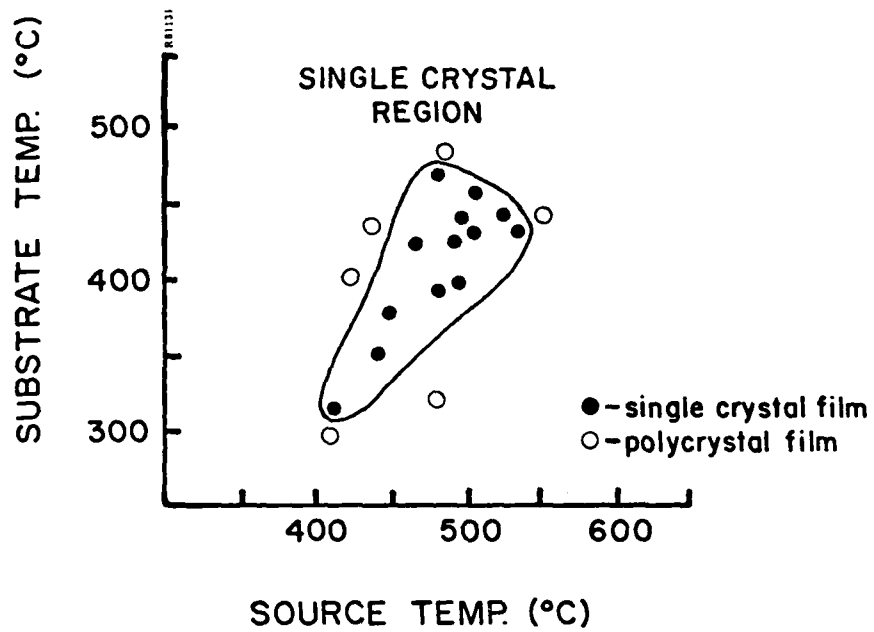


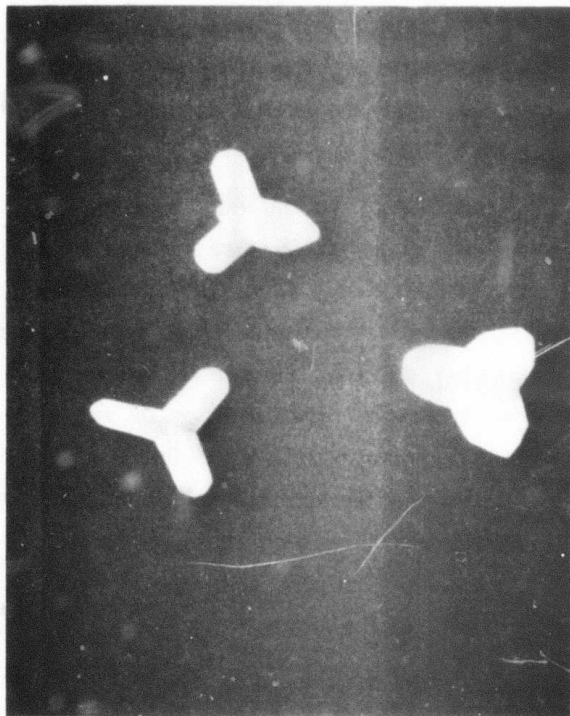
Figure 3-4. Source and substrate temperature necessary to give single crystal CdTe films on mica.

Table 3-1. Uniformity of CdTe film thickness

FILM #	SUBSTRATE	FILM THICKNESS (Microns)
124	Mica	2.02
125	Mica	2.09
126	Mica	2.43
127	Mica	3.00
128	Mica	1.80
129	Mica	1.56
130	Mica	1.99
131	Mica	1.69
132	Mica	2.27
133	Mica	2.32
134	Mica	2.04
135	Mica	2.79
136	Mica	1.94
137	Mica	2.30
138	Sapphire	1.87
139	Sapphire	2.00

Mean Thickness - 2.18 microns

Standard Deviation - 0.29 micron



R#1010P

1 μ m

Figure 3-5. SEM photomicrograph showing CdTe nuclei (10,000x magnification).

of sphalerite has a threefold symmetry. This gives a 180° twinning around the (111) axis which is very common in CdTe single crystals. Figure 3-6 is a SEM photograph of a 5 micron film of CdTe on mica and shows the typical surface of these films at a magnification of 1250x.

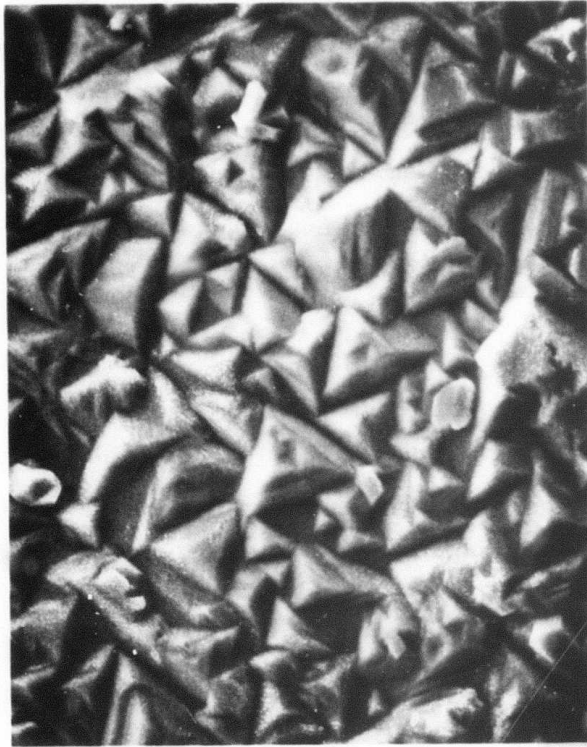
The occurrence of heteroepitaxy, which was suggested by the surface morphology of the as-grown films, was substantiated by x-ray diffraction. Back-reflection Laue patterns were obtained from three widely separated locations on a CdTe film 2.5 cm across and 17.8 microns thick on muscovite mica (specimen M81), viz., from the center and from the periphery at either end of a diameter. In addition, the pattern from the mica substrate was recorded from the opposite face of the specimen, to permit the unequivocal identification of mica contributions to the film pattern. The three CdTe patterns were identical, indicating the absence of mutual misorientation within the sensitivity of the technique. It was concluded that the region spanned by the sampled areas is a single crystal. Additional patterns from this and other CdTe/mica specimens confirmed the single-crystal nature of the films.

The macroscopic appearance of the films suggests that each is comprised of several large subgrains, (see Figure 2-10c) perhaps induced by substrate flexure during deposition. Back-reflection Laue patterns with the x-ray beam straddling apparent subgrain boundaries, failed to reveal fragmentation in all but one case, where a double pattern with a mutual misorientation less than or equal to 2° was observed.

A typical back-reflection Laue pattern from the CdTe film of specimen M81 is presented in Figure 3-7. It shows a high degree of symmetry and is readily interpreted to reveal the following orientation relationship:



i.e., the close-packed double layer of CdTe, which is polar and has trigonal symmetry, is parallel to the unique $(\text{Si}_3\text{Al})\text{O}_{10}$ hexagonal net of the mica. This is the heteroepitaxial relationship predicted on general grounds and observed previously.⁽²⁷⁾ The patterns were indexed according to cubic-system symmetry, since Debye-Scherrer analysis of as-deposited films had shown them to have the sphalerite structure of the cubic polymorph rather than the wurtzite structure of the hexagonal polymorph.



751009P

10 μ m

Figure 3-6. CdTe film (5 microns thick) deposited on mica.

Nevertheless, the CdTe patterns exhibit excess symmetry for a cubic crystal, being sixfold rather than threefold. This is interpreted as evidence that the films are twinned, a result which is to be expected because of the high degree of pseudosymmetry inherent in the sphalerite structure. As shown in Figure 3-7, the patterns are consistent with the sphalerite twinning operation: 180° rotation about the normal to (111).

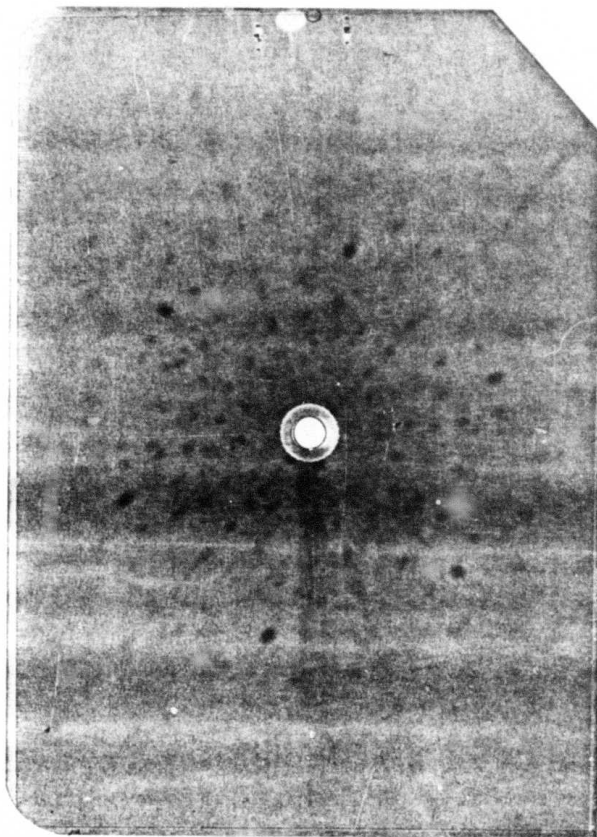
The results of the back-reflection Laue analysis were further corroborated by the diffractometer method used in the reflection geometry. The following observations were made:

- The diffraction patterns from various regions of the same CdTe/mica specimen match, indicating that the film is a single crystal.
- The diffraction peaks comprising the patterns have the relative intensities and angular positions to be expected for a CdTe single crystal of cubic symmetry.
- Rotation of the specimen in its own plane causes all diffraction peaks except (111) to pass through intensity minima (detuning), indicating that the film is a single crystal with (111) parallel to the substrate surface.

3.1.6 Films Deposited on Other Substrates

We have deposited films of CdTe onto single-crystal quartz and single-crystal sapphire, both cut perpendicular to the hexagonal c axis. Laue x-ray photographs showed that the polished face of the sapphire crystals were misaligned from the normal to the c axis by $8^\circ \pm 1^\circ$. The crystal quartz was misaligned by $1^\circ \pm 1^\circ$.

CdTe films were deposited on these substrates using the HWE method. Initially, polycrystalline films were obtained on both substrates when the deposition parameters were held the same as for the successful films on mica. X-ray patterns of these films showed many small crystals for the films on quartz and generally "powder pattern" rings for the films on sapphire. There were two possible reasons why the films did not deposit as single crystal: inadequate cleaning procedures or the misorientation of the substrate. By comparison, the mica substrates, being cleaved, were perfectly oriented and were automatically clean without any chemical treatment.



(a)

Figure 3-7. Back reflection Laue pattern from CdTe film on muscovite mica (specimen M81). (a) Pattern as recorded, negative image; molybdenum radiation, 20 kV/20 mA, 5 h exposure. (b) Important zone hyperbolae of the pattern, showing the 6-fold pseudosymmetry of the twinned crystal. (c) and (d) Components of the pattern, showing the 3-fold symmetry of the untwinned crystal in (111) orientation, with the prominent diffraction maxima indexed; the two components are related by the twinning operation: 180° rotation about the normal to (111).

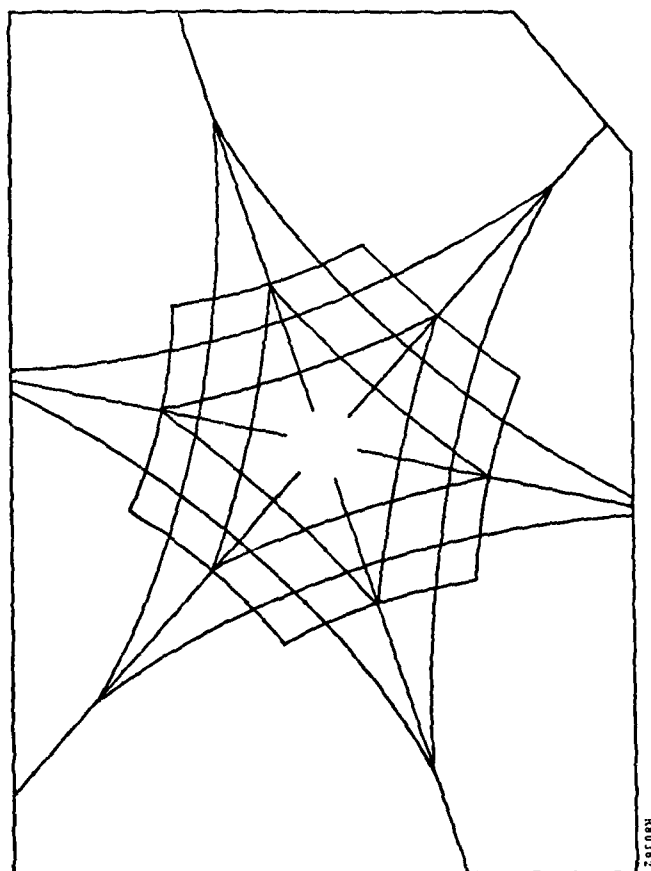
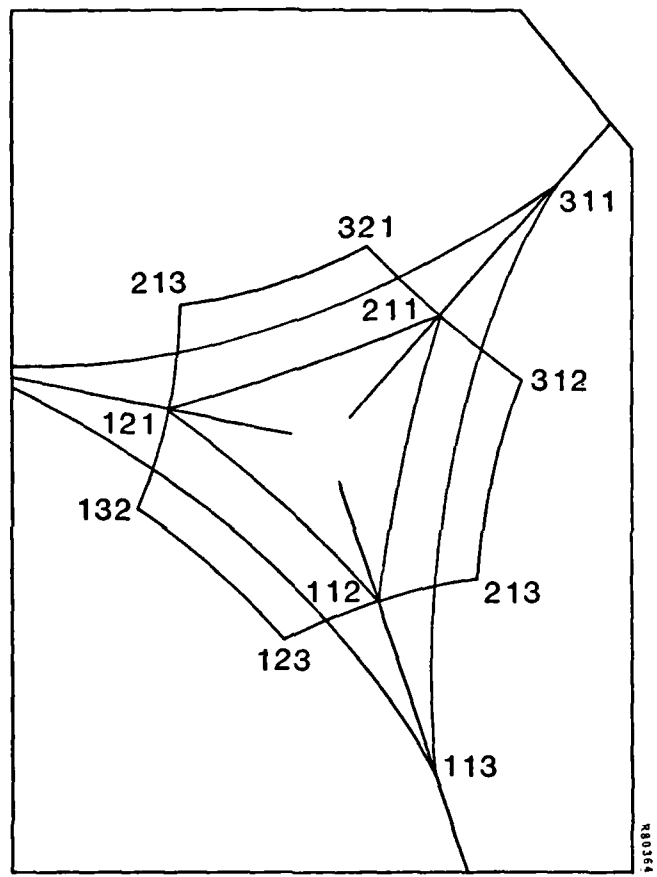


Figure 3-7. Back reflection Laue pattern from CdTe film on muscovite mica (specimen M81) (continued).



R80364

Figure 3-7. Back reflection Laue pattern from CdTe film on muscovite mica (specimen M81) (concluded).

The standard cleaning method for nonmica substrates was to use a solvent such as acetone for organic materials, followed by a deionized water treatment and then an acid cleaning, such as with aqua regia, followed by extensive rinsing in deionized water. An alternate cleaning method was attempted with crystalline quartz, which was to immerse the quartz for 20 seconds in 20% hydrofluoric acid after normal acetone treatment, to etch away 100 nm of the surface. The acid was then diluted in a running stream of deionized water until all traces of acid had gone. The substrate was taken to the vacuum system still immersed in deionized water and was taken out and blown dry by means of a nitrogen jet immediately before being placed in the vacuum system.

The result of deposition on this substrate was a single-crystal film of CdTe as determined by microscopic examination and as confirmed by x-ray technique. The adherence of the single-crystal film of CdTe to the quartz substrate was very poor, and the film fell off after an x-ray picture had been taken. It was assumed that this was the result of poor thermal expansion coefficient match. Perpendicular to the *c*-axis the thermal expansion coefficient of quartz is $13 \times 10^{-6}/^{\circ}\text{C}$, whereas that for CdTe is a $5 \times 10^{-6}/^{\circ}\text{C}$. the thermal expansion coefficient of sapphire perpendicular to the *c*-axis is $5.5 \times 10^{-6}/^{\circ}\text{C}$, and thus the match with CdTe and HgCdTe is very good. In fact, sapphire has been used as substrate material for the fabrication of HgCdTe photoconductive arrays for over a decade.

Since single-crystal CdTe was obtained on quartz as a result of removing a surface layer of the quartz substrate and keeping the substrate immersed in deionized water up to the time of deposition, it was therefore decided to try the same procedure for the sapphire substrate. However, sapphire is not soluble in HF, so a hot solution of phosphoric acid was used to remove the surface layer instead. After treatment, the sapphire substrate was wet by water, whereas before treatment with phosphoric acid, water beaded on the substrate surface. After the removal of the substrate surface, the sapphire disc was kept under deionized water until just before its use in the vacuum system. The CdTe film deposited on this substrate was polycrystalline. It thus appears that both the cleaning procedure and the exactness of the substrate orientation are of prime importance to the crystallinity of the deposited CdTe film.

CdTe films were also deposited onto silicon substrates earlier in the program, but this was before the optimized form of evaporation source had been made; thus, these films were polycrystalline. There was not sufficient time to return to deposition of CdTe films on silicon after the improvement of the deposition method.

3.2 VAPOR EXCHANGE OF CdTe TO FORM HgCdTe

3.2.1 Objective

The objective of this task is the vapor growth of uniform HgCdTe epitaxial layers from the previously deposited CdTe heteroepitaxial films. The technical approach employed is the Evaporation Diffusion at Constant Temperature (EDICT) method. This method closely resembles the Hot Wall Epitaxy (HWE) technique in that isothermal conditions for the source, ampoule wall, and substrate are emphasized and thus true thermodynamic equilibrium is assured. The only difference between the HWE and the EDICT method is that in addition to sublimation and condensation, the EDICT process utilizes a third growth mechanism, which is diffusion in the solid phase. Impinging HgTe first accumulates at the CdTe film surface and then diffuses into the CdTe layer while CdTe diffuses up to the surface until equilibrium is reached. Since the entire process, i.e., both vapor and solid phase exchange, takes place close to thermodynamic equilibrium, excellent HgCdTe epitaxial films of uniform composition and perfect crystalline quality are thus expected.

3.2.2 Edict Process Description

To change a film of CdTe into a film of HgCdTe, it is necessary to diffuse Hg and Te into it. The diffusion of the correct amount of mercury gives the correct x value, and the diffusion of the correct amount of tellurium determines the stoichiometry of the film.

As an example, to convert 1 gm of CdTe to $\text{Hg}_{(1-x)}\text{Cd}_x\text{Te}$ with an x value of 0.2, it is necessary to diffuse 5.5 grams of HgTe into it, and as a result, the volume increases by a factor of 4.15. Thus, there must be a considerable amount of atomic movement to achieve the required result.

The early work on the EDICT method was done on bulk samples at the C.N.R.S. Laboratory in Paris.⁽²⁸⁾ A slab of CdTe and a slab of HgTe would be enclosed in a sealed, evacuated quartz ampoule. After a number of days at isothermal conditions at temperatures in the range 450 to 650°C, some of the HgTe would be transferred to the CdTe slab, but no evidence of reverse transfer of CdTe to the HgTe slab would be found. Examination of the CdTe slab showed that the growth layer at the surface would have a strong gradient of x value normal to the surface, and the layer would remain essentially with $x = 1$ at the interface and $x = 0$ at the surface. This growth was found to depend upon the temperature, time of soaking, the distance apart of the slabs of material, and the pressure of mercury. This last parameter could be separately adjusted by placing excess mercury in the ampoule.

The results obtained by the bulk EDICT process were interesting but lacking in practical use because of the steep gradient in x normal to the substrate surface. This difficulty was overcome by the group at the Warsaw Technical Academy, who had the simple but brilliant idea of performing similar experiments with CdTe in thin-film form.⁽²⁷⁾ Under these conditions, the growing layer would reach the CdTe-substrate interface, and no further supply of CdTe would be available. If the supply of HgTe was also limited, the x value of the film would become uniform with depth. It was found that, if the HgTe supply was correctly calculated, all the HgTe would diffuse into the CdTe film, which would end by having the x value which had previously been calculated from the initial weights of CdTe and HgTe in the ampoule. (The excess weight of Hg in the ampoule does not affect the x value of the film, for it remains in the ampoule.) The measured x value uniformity of these films is excellent both parallel and normal to the surface.

The steps by which this process occurs are believed to be as follows:

1. As the temperature rises in the ampoule, the mercury, and tellurium pressures also rise. The vapor in the ampoule is almost all mercury, and the surface of the CdTe is covered by an equilibrium layer of mercury until the surface reaches the stoichiometry limit. At this point, no more mercury can be absorbed onto the surface.
2. The flux of Te_2 onto the growing surface is very much less than that of Hg, and the Te_2 molecules are readily captured on the Hg rich surface to cause HgTe to be formed. Note there would be no similar capturing phenomenon of Cd on the HgTe surface because that surface would already be metal saturated.

3. The final formation of the film takes place by in-diffusion of Hg and out-diffusion of Cd until all the HgTe has been used up and the film has been homogenized. At this point, there is no further driving force and the system reaches equilibrium.

3.2.3 EDICT Ampoules and Furnace

The ampoule configuration used in the vapor transport/solid exchange growth of single-crystal HgCdTe films is shown in Figure 3-8. The ampoule consisted basically of two telescoping silica tubes which are closed at one end. The I.D. of the outer tube is large enough that a 1/2" square substrate can be accommodated. The ampoules are thoroughly cleaned and then assembled with the CdTe film, a piece of HgTe and a small amount of excess Hg. The weight of HgTe is calculated so that the desired x value of HgCdTe is achieved after complete vapor transport to and diffusion into the CdTe films have occurred. The weight of Hg is chosen so that at the growth temperature, a predetermined pressure of Hg exists in the ampoule. When the free volume of the ampoule has been adjusted by sliding the inner silica tube to its correct position, the ampoule is evacuated to 10^{-6} torr on the same vacuum system that is used to deposit the CdTe films, and the two tubes are fused together as shown in Figure 3-8.

The ampoule is placed in a furnace at room temperature, and the furnace temperature is then slowly raised to the desired temperature. The temperature of the furnace is maintained uniform throughout the entire ampoule length by placing a sodium heat pipe inside the furnace as shown in figure 3-9. The entire growth process typically takes several days. If desired, the as-grown sample can be annealed at a lower temperature to adjust stoichiometry defect concentrations in the same ampoule without breaking the vacuum.

3.2.4 EDICT Experiments

A number of specimens of CdTe films on mica were subjected to vapor phase transport by the EDICT technique. The parameters of growth (i.e., EDICT time, EDICT temperature, anneal time, anneal temperature, Hg pressure, and final film thickness) together with the intended and actual x value of the final HgCdTe films are given in Table 3-2 for 14 samples.

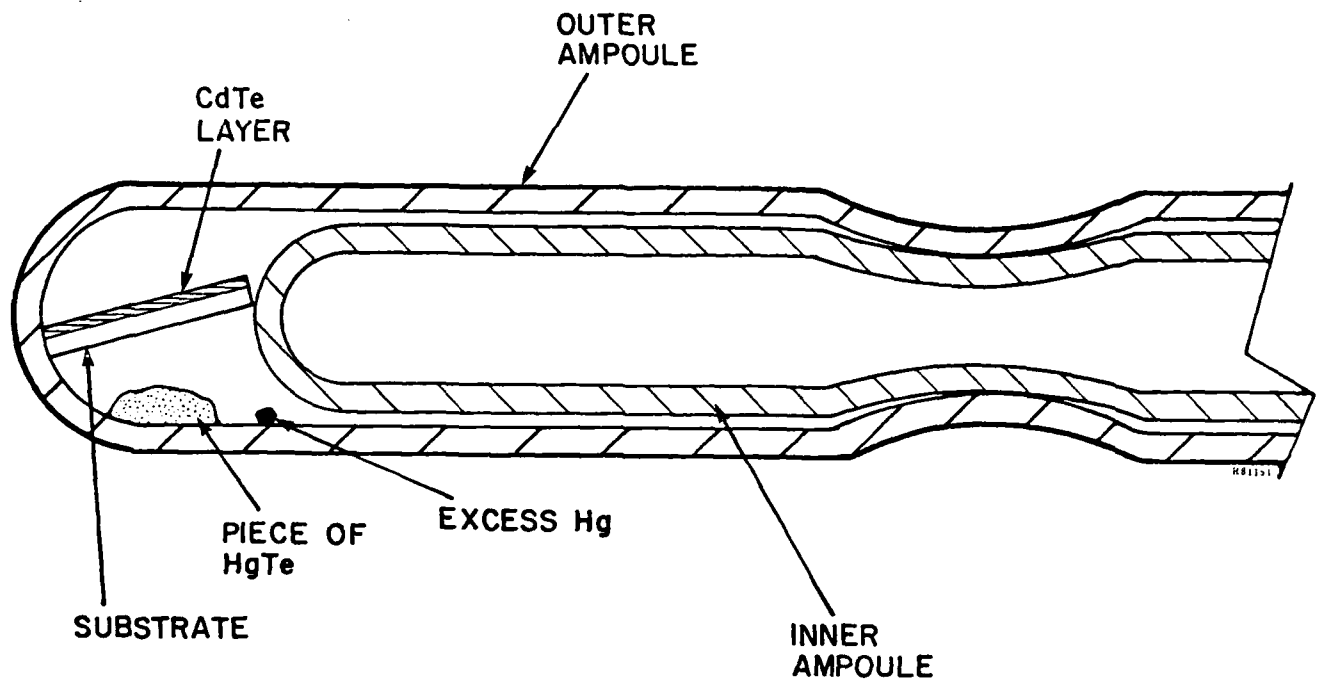


Figure 3-8. Schematic of vapor exchange apparatus (at NERC).

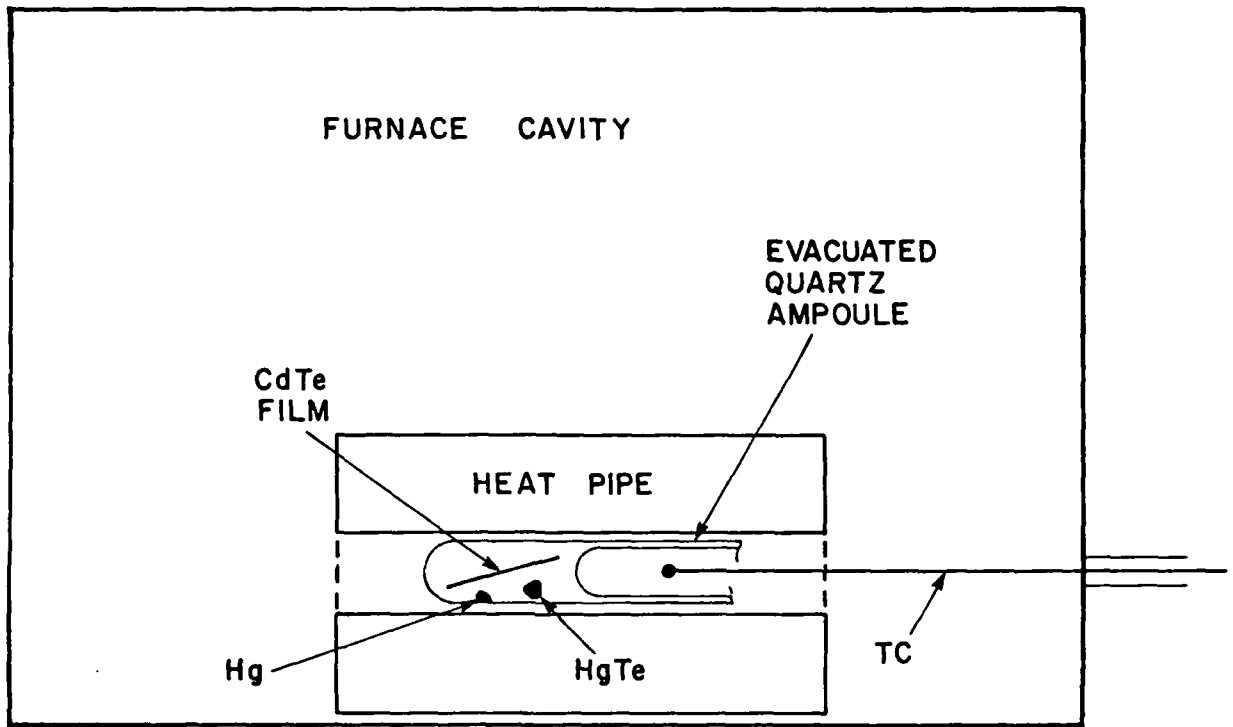


Figure 3-9. A heat pipe is placed inside the EDICT furnace to ensure growth in thermodynamic equilibrium.

The ampoules used for growth were cleaned by the standard quartz cleaning method and then the films and the additional HgTe and Hg were loaded. The films on mica were cut into 1.2 cm x 2 cm rectangles to fit inside the vapor ampoules. The weight of the films was known, so the weight of HgTe to be added was readily calculated. The weight of free Hg to be added was calculated from the free volume of the ampoule and the EDICT temperature to be used knowing the required Hg pressure for the experiment.

The ampoules were pumped to a pressure of 10^{-6} torr and then sealed off. After the EDICT and annealing treatment had been carried out, the ampoules were cooled to room temperature and opened, and the weight of the substrate and film combined was again measured so that the weight of the HgTe could be determined. The amount of HgTe transferred to the film could be calculated and the x value of the $\text{Hg}_{(1-x)}\text{Cd}_x\text{Te}$ determined.

The effect of excess Hg vapor pressure on the conversion of these films can be seen from Table 3-2. In cases where the excess Hg pressure was greater than 0.5 atmosphere, growth did not go to completion. (See samples M82, M128 and M130.) Five films for which the excess Hg pressure was 0.5 atmosphere (M107, M125, M133, M100, M127) were close to but did not achieve the intended x value, and two films for which the excess Hg pressure was 0.5 atmosphere (M99 and M135) reached the designated x value of 0.2 within experimental error. The four films for which the excess Hg pressure was less than 0.5 atmosphere (M124, M126, M106 and M132) all attained the designated value of x within experimental error, even though two of the films were treated at the lowest temperature (475°C) and for the shortest time (96h) used in the EDICT experiments. The upper limit of excess Hg pressure has thus been determined to be 0.5 atmosphere. The lower limit of excess Hg pressure has not yet been determined. In fact, good EDICT results have been achieved in bulk CdTe by using an excess of Te instead of an excess of Hg.⁽²⁹⁾ In this case, the subsequent annealing of the films to n-type would have to be performed in a separate ampoule.

3.2.5 Characterization of HgCdTe Films

Film characterization included composition and its uniformity, crystalline perfection and electrical properties. The results are presented in this section.

TABLE 3-2. Summary of 14 HgCdTe samples grown by the EDICT method.

Sample No.	EDICT Time(hr)	EDICT Temp(°C)	Anneal Time(hr)	Anneal Temp(°C)	Hg Pressure (atm.)	Final Film Thickness(μm)	Intended x Value	Achieved x Value
M82	96	500	16	300	4.8	7.7	0.2	0.085
M99	96	500	-	-	0.5	32.5	0.2	0.2
M106	96	500	-	-	0.25	30.0	0.2	0.2
M107	120	475	164	250	0.5	64.0	0.2	0.24
M124	120	475	164	250	0.25	10.6	0.2	0.2
M126	96	475	216	250	0.125	13.0	0.2	0.2
M132	96	475	216	250	0.25	12.4	0.2	0.19
M133	96	475	216	250	0.50	7.0	0.2	0.34
M128	96	525	-	-	0.75	2.3	0.2	0.085
M130	144	525	-	-	1.0	2.8	0.19	0.075
M100	120	500	-	-	0.5	11.1	0.2	0.26
M135	480	500	-	-	0.5	15.4	0.2	0.2
M127	480	500	-	-	0.5	9.3	0.2	0.33

The alloy composition of the HgCdTe layer can be determined by means of either transmittance or reflectance spectrometry. The leading edge of either the spectral transmittance or reflectance corresponds to the fundamental absorption edge of the material under study. The transmission technique, in the case of using mica as the substrate, is not applicable because mica is opaque in the infrared. As a result, reflectance measurements of HgCdTe films on mica substrates were made. One typical spectral reflectance of HgCdTe film grown on mica substrate is shown in Figure 3-10. Also in the figure is the reflectance from a bare mica substrate for reference purposes. The angle of incidence of this measurement was 45° , and the area of the film illuminated was about 1 cm^2 . The sudden change in reflectance at $8 \mu\text{m}$ is caused by the abrupt drop in absorption coefficient of the film, indicating fundamental absorption. The fact that the rise in reflectance with wavelength is rapid indicates that the film is very uniform in composition over an area of 1 cm^2 as well as normal to the surface of the layer. The fact that the reflectance change is at $8 \mu\text{m}$ at room temperature is indicative of a composition of $\text{Hg}_{(1-x)}\text{Cd}_x\text{Te}$ for which $x = 0.2$, which agrees with the value calculated by the change of weight of the film during the EDICT process.

To evaluate the compositional uniformity across the surface of the HgCdTe films, electron beam microprobe analysis was first employed. Although this technique offered excellent spatial resolution, it has a rather poor resolution in determining the mole fraction variation in HgCdTe. Our calibration study indicated that the precision of the electron beam microprobe technique was only good to ± 0.01 in alloy composition. Thus, other evaluation techniques with better sensitivity had to be used.

The most accurate technique for measuring compositional uniformity is the spectral cutoff of electro-optical devices fabricated evenly across the film surface because the spectral response of an infrared sensing device such as a photoconductor or a photovoltaic detector is a direct measurement of the bandgap of the material. For this reason, p-n junctions were formed by impurity diffusion through a mask pattern, so that a number of samples were evenly distributed across the entire HgCdTe film surface. Leads were then attached to both sides of the junction, and relative spectral responses were measured at 77°K . The composition and its uniformity can then be determined from the well-established bandgap-composition relationship. One should emphasize that the aim

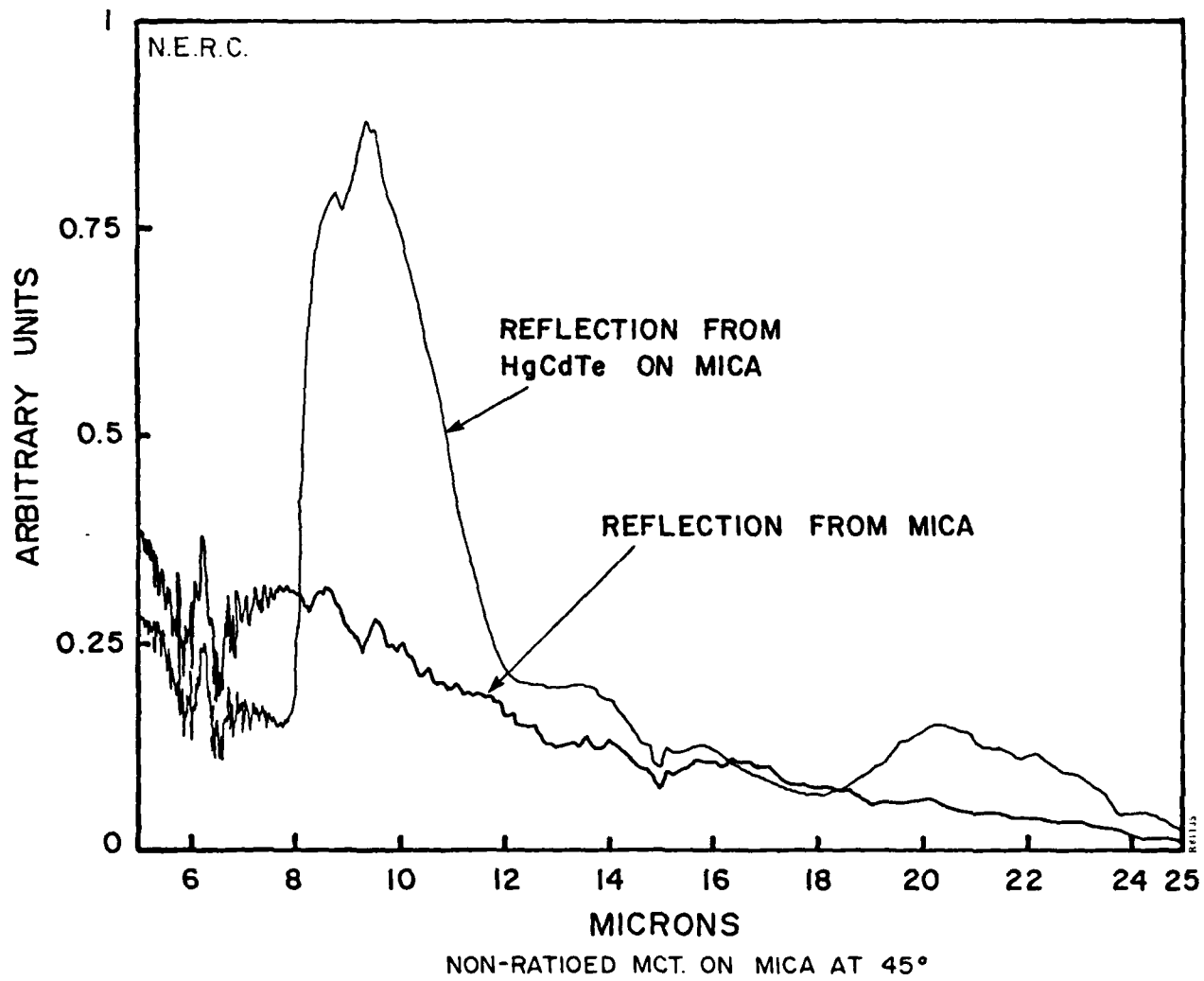


Figure 3-10. Fourier transform reflectance spectroscopy measurements taken on a HgCdTe/mica sample and a bare mica substrate.

for these test structures is to measure compositional uniformity across the surface of the films rather than to evaluate the device quality of the HgCdTe epitaxial material grown by the Hot Wall/EDICT process. The latter is beyond the scope of this program.

Figure 3-11 shows four photovoltaic test structures fabricated across a HgCdTe film of a nominal size of 1.2 x 1.2 cm. The data showed the average value and variation in cutoff wavelength to be $10 \pm 0.08 \mu\text{m}$, which corresponds to an average composition value x , with variation, of 0.2190 ± 0.00065 . The precision of the Fourier Transform Spectrometer with which these data were taken is about $0.05 \mu\text{m}$, which corresponds to 0.00050 in composition limit. Thus, most of the measured variation was due to equipment uncertainty rather than the material itself. A uniformity in composition of ± 0.00067 is one of the best ever reported in HgCdTe material grown by any method.

Crystalline perfection of the EDICT films was determined by means of back-reflection Laue diffraction. As indicated in Section 3.1.5, single-crystal CdTe films were obtained by means of Hot Wall Heteroepitaxy. The question remaining was whether the EDICT process would favorably or adversely affect the crystallinity of the final HgCdTe layer.

Figures 3-12(a) and (b) show the improvement in crystalline quality as a result of the EDICT process. The upper photograph is a Laue diffraction pattern of a CdTe film grown on mica by the Hot Wall method. The high degree of symmetry revealed in Figure 3-12(a) indicates the single-crystal nature of the CdTe film. Comparing Figure 3-12(a) to (b) which is a Laue back reflection taken from a EDICT film, one finds that the degree of symmetry improves. Specifically, most of the "background" spots clustered along symmetry lines disappear. This is an indication of improved crystalline perfection as a result of the EDICT process.

To illustrate clearly the favorable effects of the EDICT process on crystallographic defects, a bulk CdTe wafer acquired from II-VI, Inc. was studied before and after it was subjected to the EDICT process. A Laue back reflection x-ray was first taken prior to the EDICT process and the pattern was shown in Figure 3-13(a). Large dots and their irregular shape and somewhat uneven intensity indicated macroscopic crystal defects and low-angle misorientations. This CdTe wafer was then subjected to the EDICT process and a relatively thick (4 mils) HgCdTe layer was grown at the surface

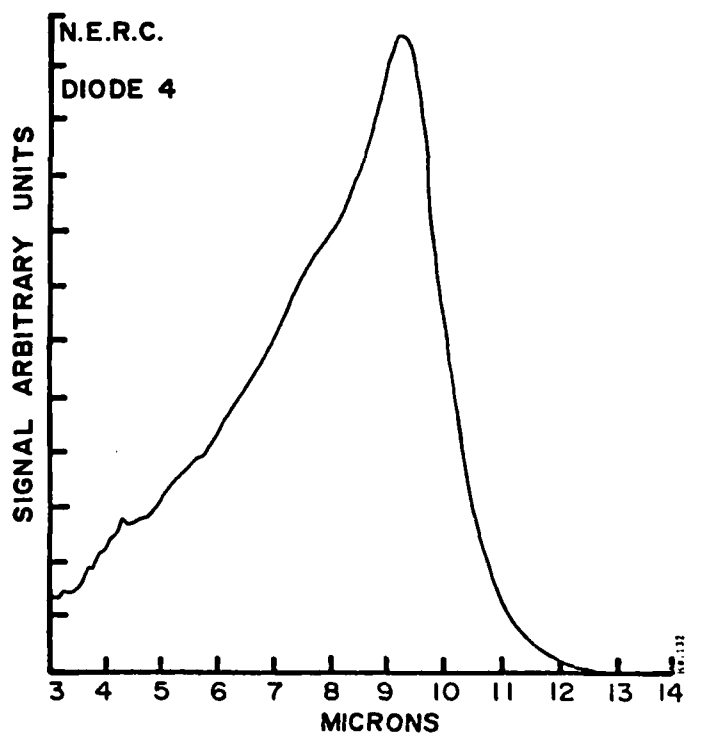
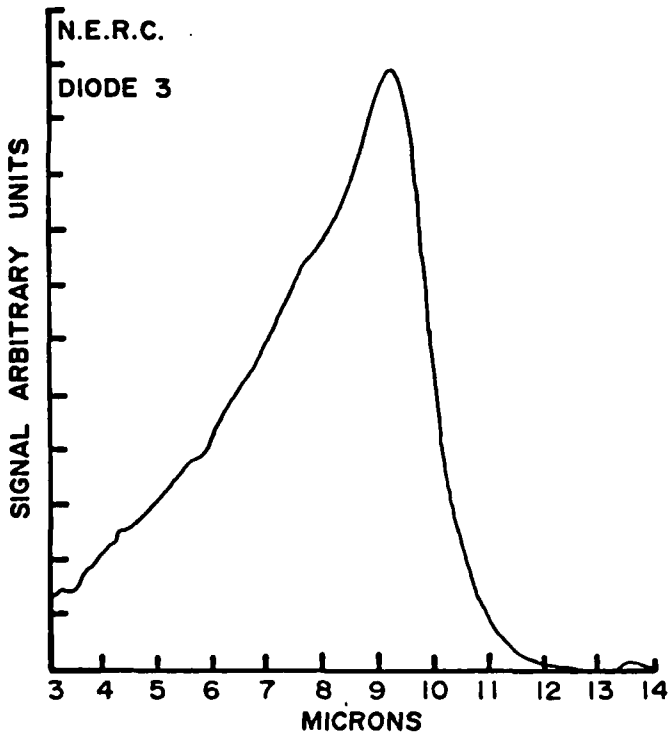
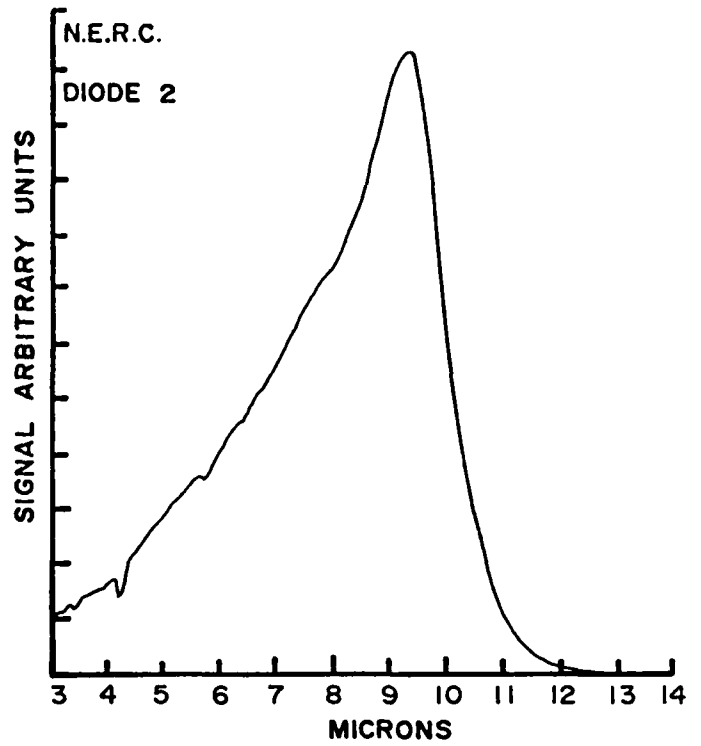
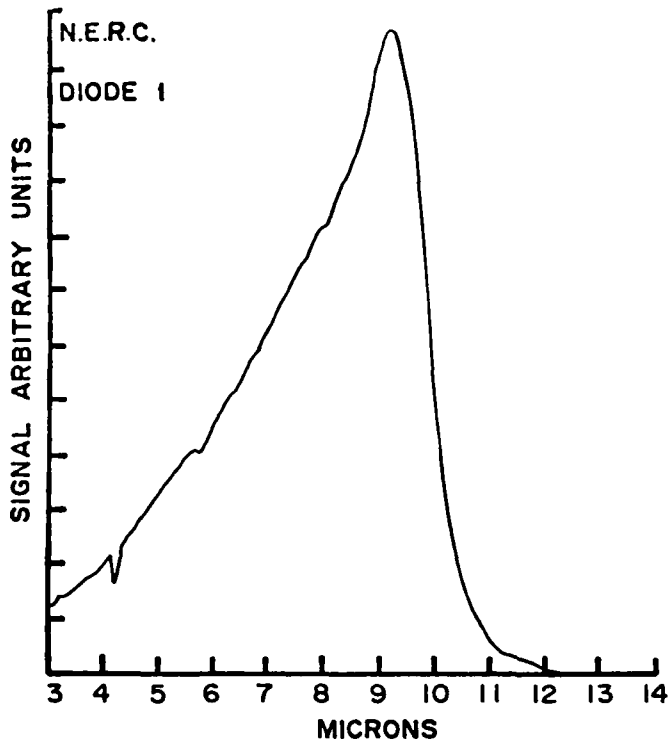


Figure 3-11. Compositional uniformity of 0.2190 ± 0.00067 across a 1.2×1.2 cm area measured with the Fourier Transform Spectrometer which has a precision limit for resolving x of ± 0.00050 .

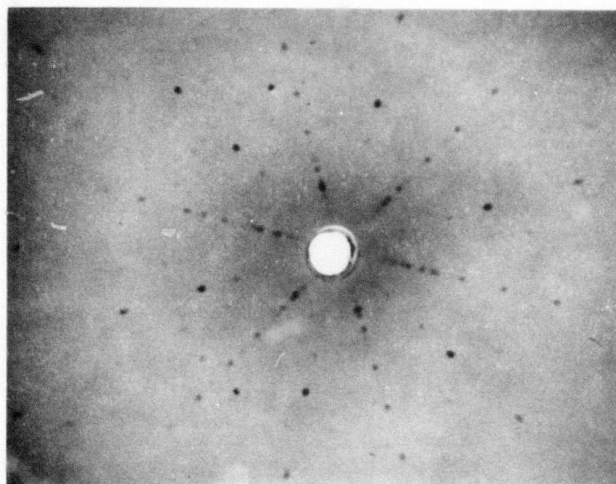


Figure 3-12(a). Laue X-ray pattern of a single crystal CdTe film on mica.

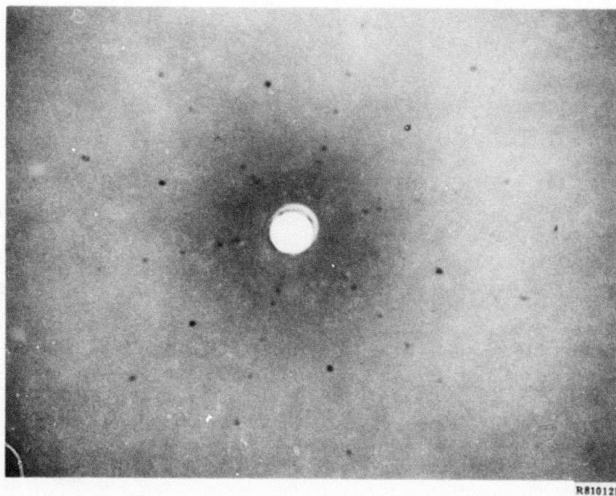


Figure 3-12(b). Laue X-ray pattern of the same sample shown above after the EDICT process showing improved crystalline quality.

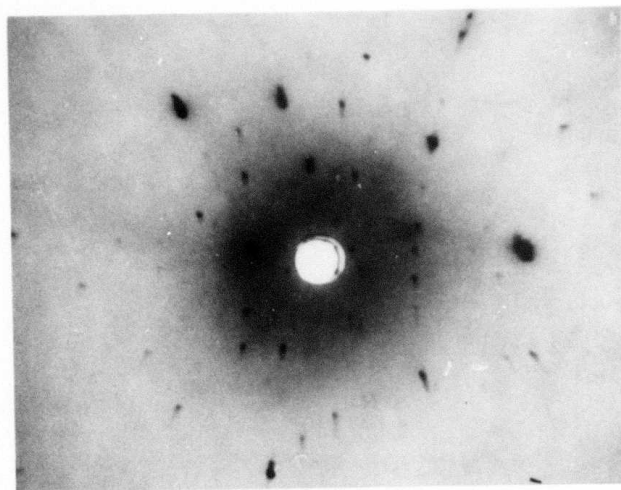


Figure 3-13(a). Laue X-ray pattern taken on a bulk CdTe wafer (1 mm thick).

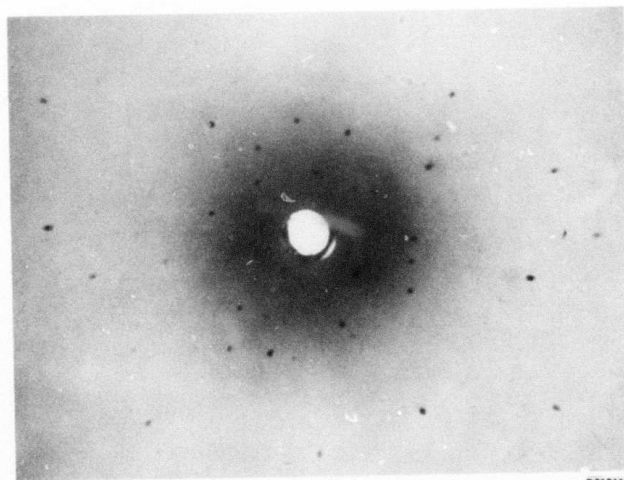


FIGURE 3-13(b). Laue X-ray pattern taken on the same sample as (a) but after the EDICT process.

with a compositional gradient normal to the surface as expected. A Laue pattern was then taken, and the result was shown in Figure 3-13(b). It was apparent from this photograph that although the diffraction pattern did not change, the size of the dots and the "substructures" inside the dots was drastically reduced. This result together with those in Figure 3-12 demonstrate that the EDICT process greatly improves crystal perfection of the final HgCdTe film.

Electrical characteristics such as mobility and carrier concentration were measured by the Van der Pauw method. The as-grown HgCdTe films were p-type. This was expected because the EDICT process took place at temperatures from 450 to 650°C. The conductivity type of these films could be altered via low temperature annealing. A number of films were annealed at 250°C for three to four days under Hg pressure. Van der Pauw samples were formed by cutting the films into squares of 3 mm size. Contacts were made by wire bonding on the extreme corners of the squares. The contacts were made as small as possible to minimize measurement error. The samples were then mounted between the pole pieces of a Varian magnet which was capable of maintaining a uniform field of 3K gauss. Hall measurements were made at room temperature and at 77°K.

The values of electron concentration in these HgCdTe films ranged from 6 to 20 x 10¹⁵ cm⁻³ while those of mobility ranged from 0.5 to 1.5 x 10⁵ cm²/V-s. The carrier concentrations were high compared to good bulk-grown HgCdTe. The electron mobilities, however, were comparable to bulk materials, considering the fact that the carrier concentrations were relatively high and impurity scattering would have lowered the mobility.

Historically, materials grown by epitaxy techniques, whether in the liquid or vapor phase, are inferior to those grown by bulk techniques in terms of electrical properties. Mobility has been one of the key parameters for the evaluation of the quality of film grown. A good mobility, meaning it is as high as that of bulk material, indicates that the epitaxial film is of high quality. The high carrier concentrations measured in the EDICT layers are believed to be caused by contamination due to handling rather than inherent in the growth processes. Impurity control will be one of the prime objectives in future development.

REFERENCES

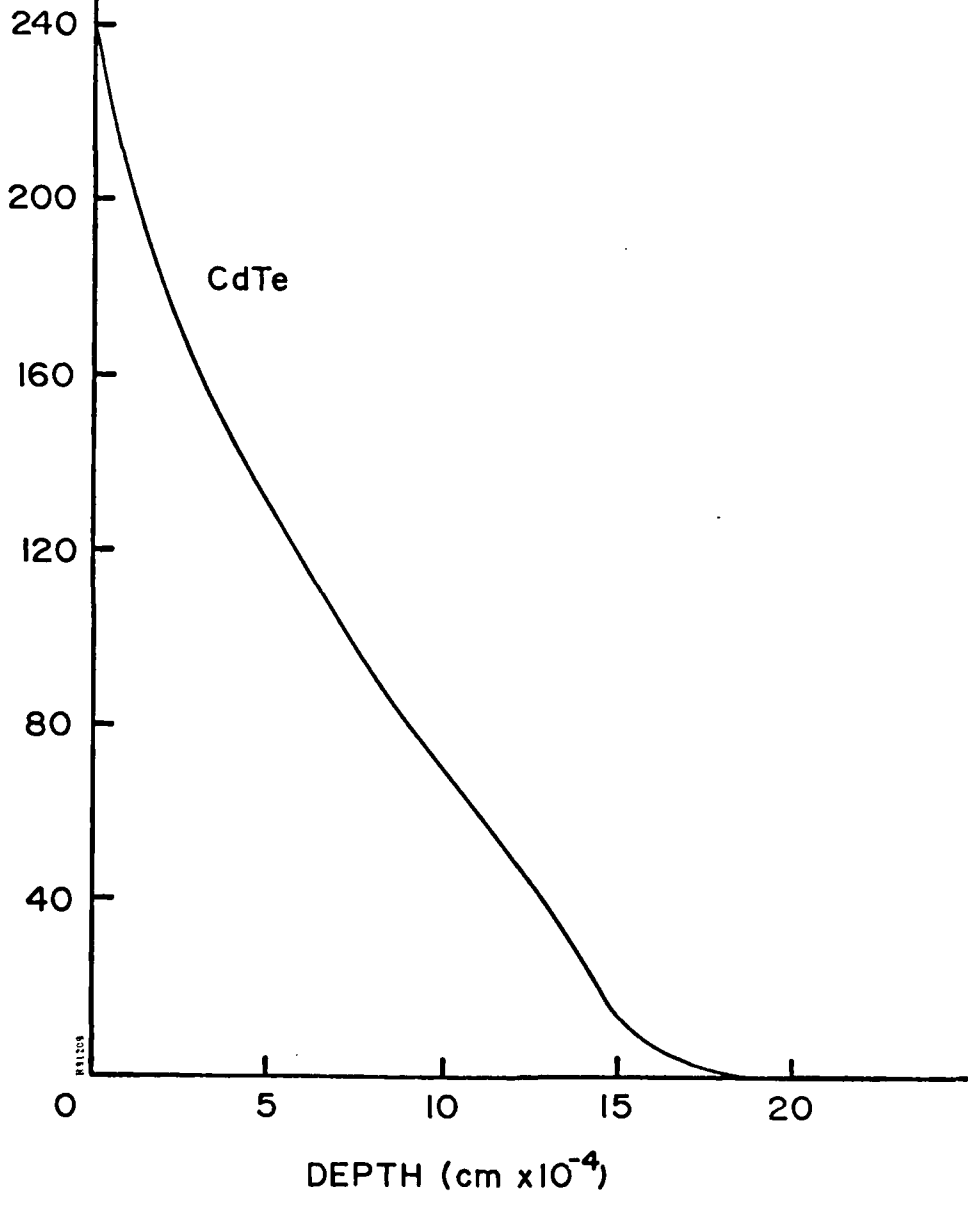
1. A.C. Greenwald and J.J. Comer, in Laser and Electron-Beam Processing of Materials, ed. C.W. White and P.S. Peercy (Cadademic Press, NY, 1980), p. 575.
2. S.S. Lau, W.F. Tseng, M.A. Nicolet, J.W. Mayer, J.A. Minnucci, and A.R. Kirkpatrick, Appl. Phys. Lett. 33, 235 (1978).
3. Y.I. Nissim and J.A. Gibbons, in Laser and Electron-Beam Solid Interactions and Materials Processing, ed. J.F. Gibbons, L.D. Hess, and T.W. Sigmon, (North Holland, NY, 1981), p 275.
4. R.O. Bell, Appl. Phys. 19, 313 (1979).
5. Whitsett and Nelson, Phys. Rev. B 5, 3125 (1972) (for thermal conductivity) and Rusakov, Ya, Vekilov, and Kadysherich, Sov. Phys. Solid State 12, 2618 (1972).
6. N.C. Schoen, J. Appl. Phys. 51, 4747 (1980).
7. A.C. Greenwald, R.G. Little, and J.A. Minnucci, IEEE Trans. Nucl. Sci. NS-26(1), 1683 (Feb. 1979).
8. Eastern Analytical Laboratories, Inc., Burlington, MA.
9. Photometrics, Inc., Woburn, MA.
10. M. Chu, R.H. Bube, and J.F. Gibbons, J. Electrochem. Soc. 127, 483 (1980).
11. R.L. Mozzi, W. Fabian, and F.J. Piekarski, Appl. Phys. Lett. 35, 337 (1979).
12. T. Inada, K. Tokukaga, and S. Taka, Appl. Phys. Lett. 35, 546 (1979).
13. T.S. Sun, S.P. Buchner, and N.E. Byer, J. Vac. Sci. Technol. 17, 1067 (1980).
14. S.S. Lau, W.F. Tseny, M.A. Nicolet, J.W. Mayer, R.C. Eckardt, and R.J. Wagner, Appl. Phys. Lett. 33, 130 (1978).
15. H.I. Smith and D.C. Flanders, Appl. Phys. Lett. 32, 349 (1978).
16. A.C. Greenwald, A.R. Kirkpatrick, R.G. Little, and J.A. Minnucci, J. Appl. Phys. 50, 783 (1979).
17. Final Report on contract NAS-3-21276, NASA Lewis Research Center.
18. Charles Evans and Assoc., San Mateo, CA.
19. Z.L. Liau and J.W. Mayer, J. Vac. Sci. Technol. 15, 1629 (1978).
20. H.H. Anderson, J. Vac. Sci. Technol. 16, 770 (1979).

21. Z.L. Liaw, W.L. Brown, R. Hover, and J.M. Poate, *Appl. Phys. Lett.* 30, 626 (1977).
22. J.E. Lewis and P.S. Ho, *J. Vac. Sci. Technol.* 16, 772 (1979).
23. P. Sigmund and C. Claussen, *J. Appl. Phys.* 52, 990 (1980).
24. J.F. Gibbons, W.S. Johnson, and S.W. Mylroie, Projected Range Statistics (Halsted Press, 1975).
25. M. Maenpaa, S.S. Lau, M. Von Allmen, I. Golecki, M-A. Nicolet, and J.A. Minnucci, *Thin Solid Films* 67, 293 (1980).
26. A. Lopez-Otero, *Thin Solid Films* 49, 3 (1978).
27. Z. Nowak, J. Piotrowski, T. Piotrowski, and J. Sadowski, *Thin Solid Films* 52, 405 (1978).
28. F. Bailly et al., *J. Appl. Phys.* 46, 4244 (1975).
29. P. Becla, J. Lagowski, H.C. Gatos, and H. Ruda, *J. Electrochem. Soc.* 128, 1172 (1981).

APPENDIX A
CALCULATED ELECTRON BEAM
ENERGY DEPOSITION PROFILES
FOR CONDITIONS IN TABLE 2-2

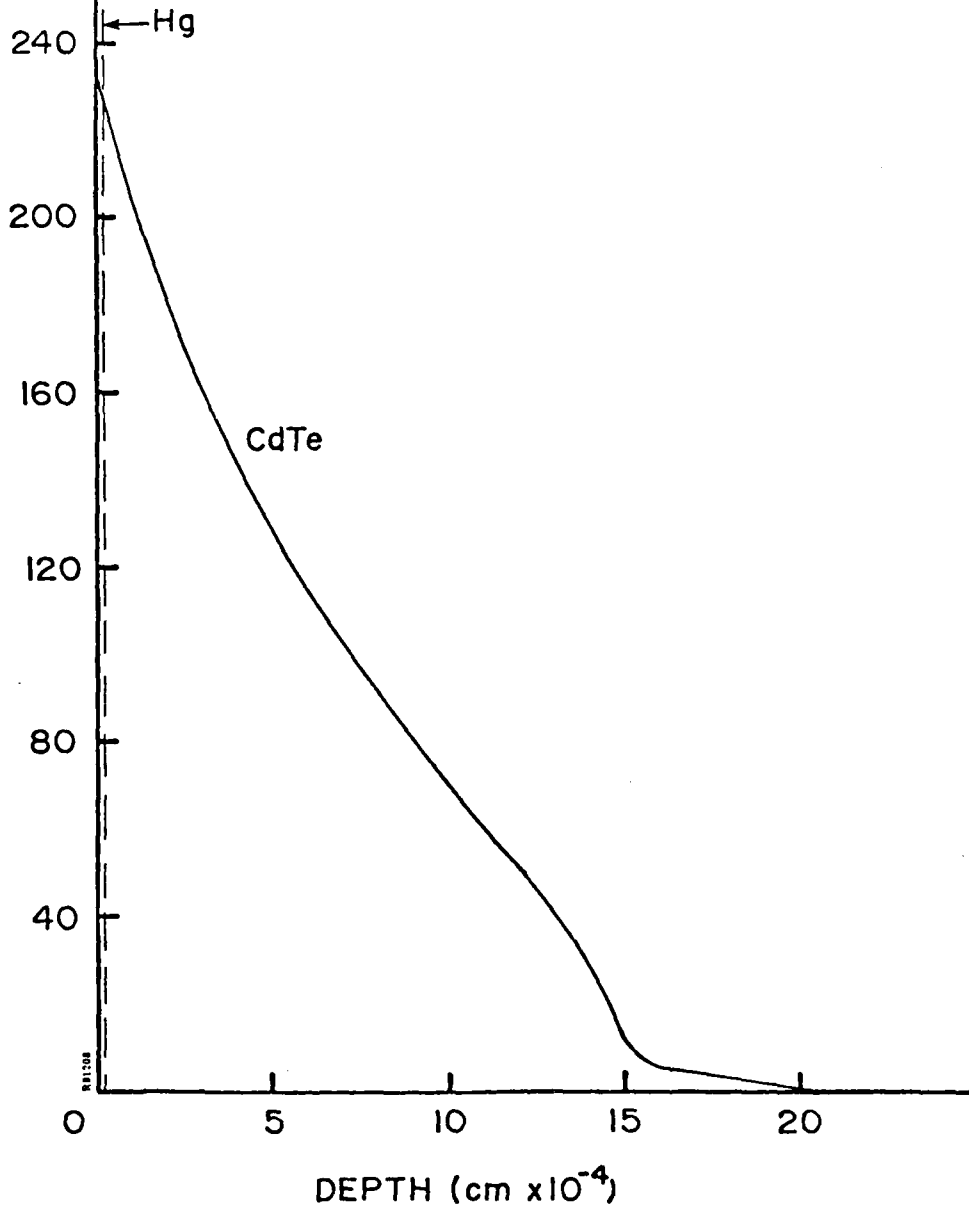
DOSE
E/Gm/E/cm²

DEPOSITION PROFILE
BEAM 1
.05 μ Hg, 19.95 μ CdTe



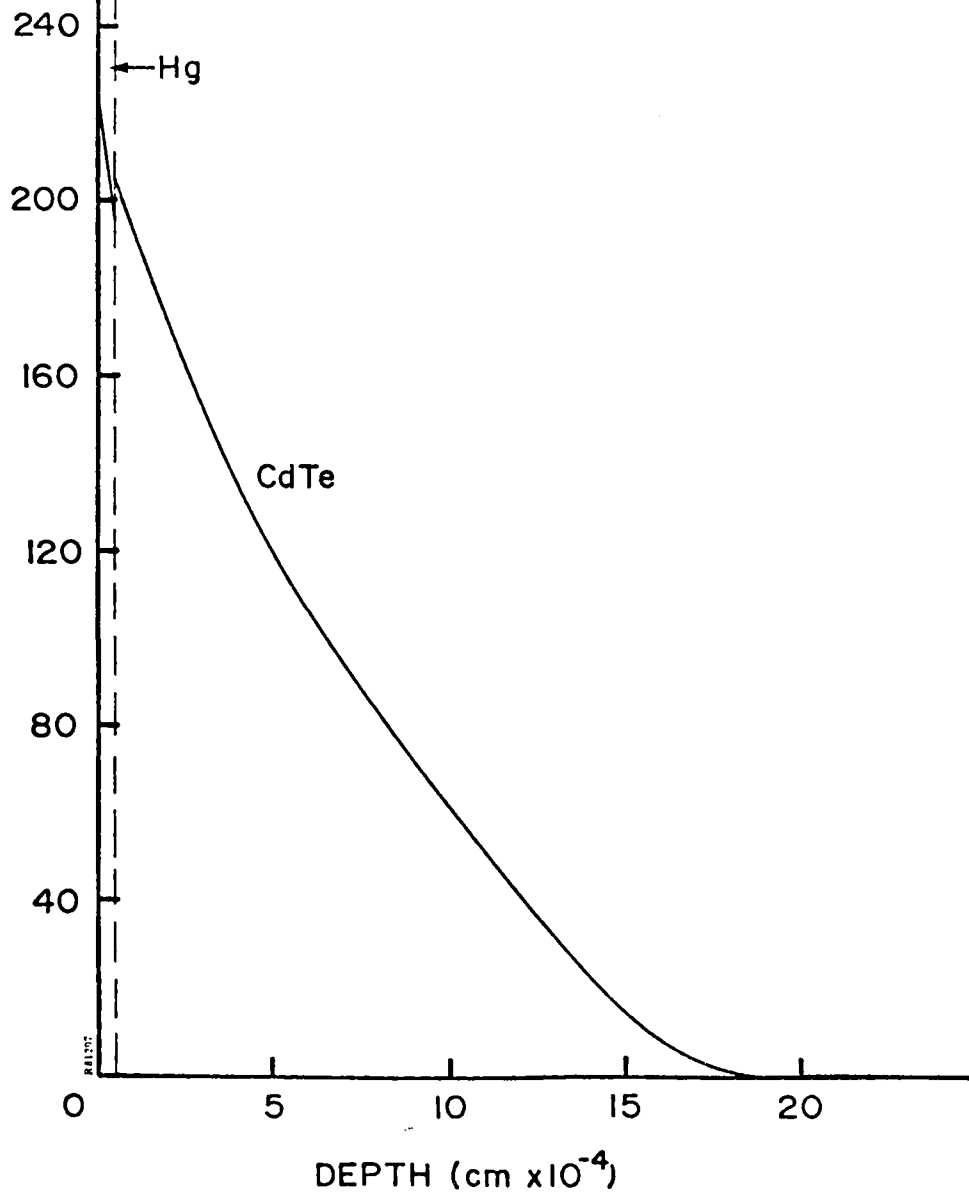
DOSE
E/Gm/E/cm²

DEPOSITION PROFILE
BEAM 1
.1 μHg on 19.9 μCdTe



DOSE
E/Gm/E/cm²

DEPOSITION PROFILE
BEAM 1
.5 μ Hg, 19.5 μ CdTe



DOSE
E/Gm/E/cm²

DEPOSITION PROFILE
BEAM 1
6.55 μ Hg, 21.44 μ CdTe

240

Hg

200

CdTe

160

120

80

40

0

5

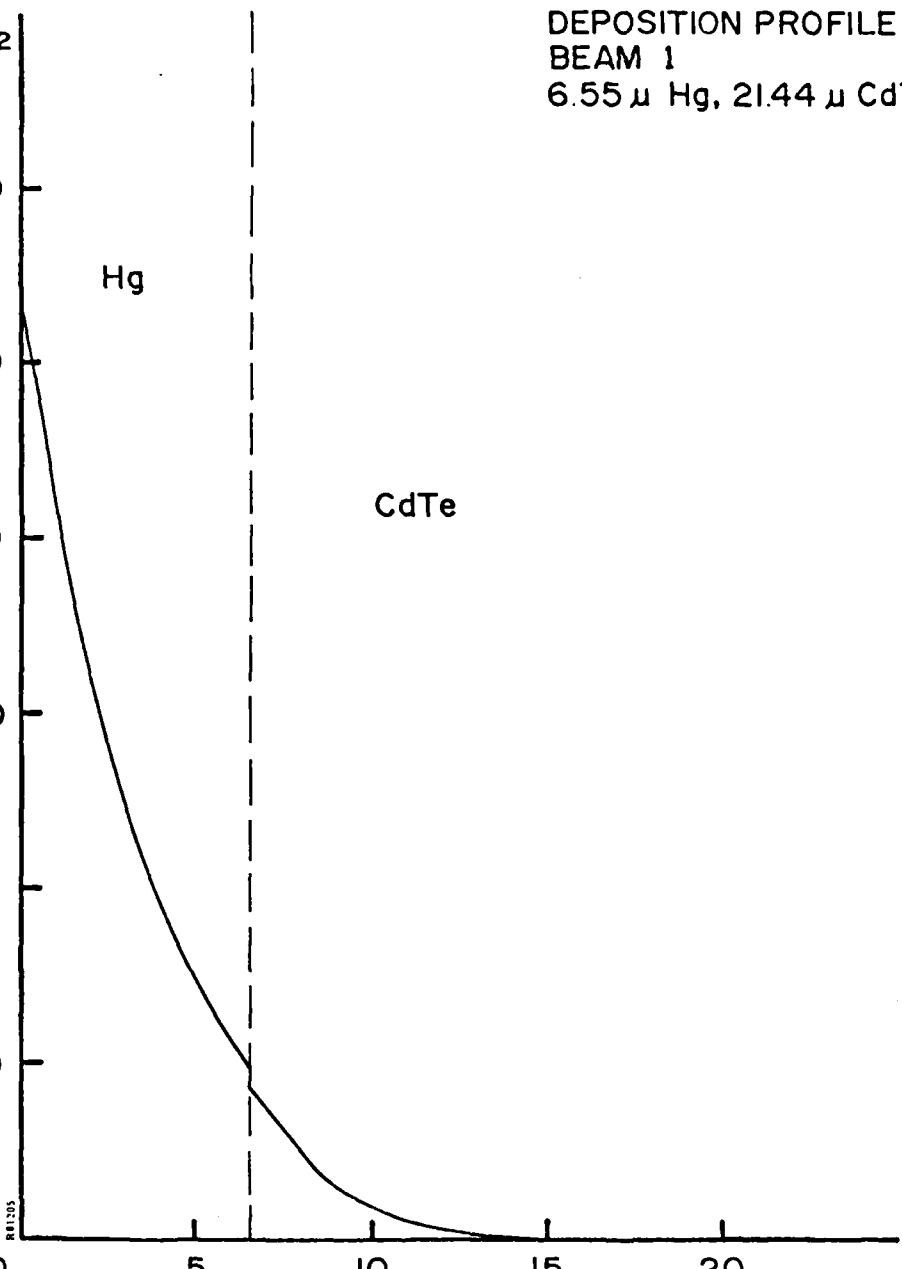
10

15

20

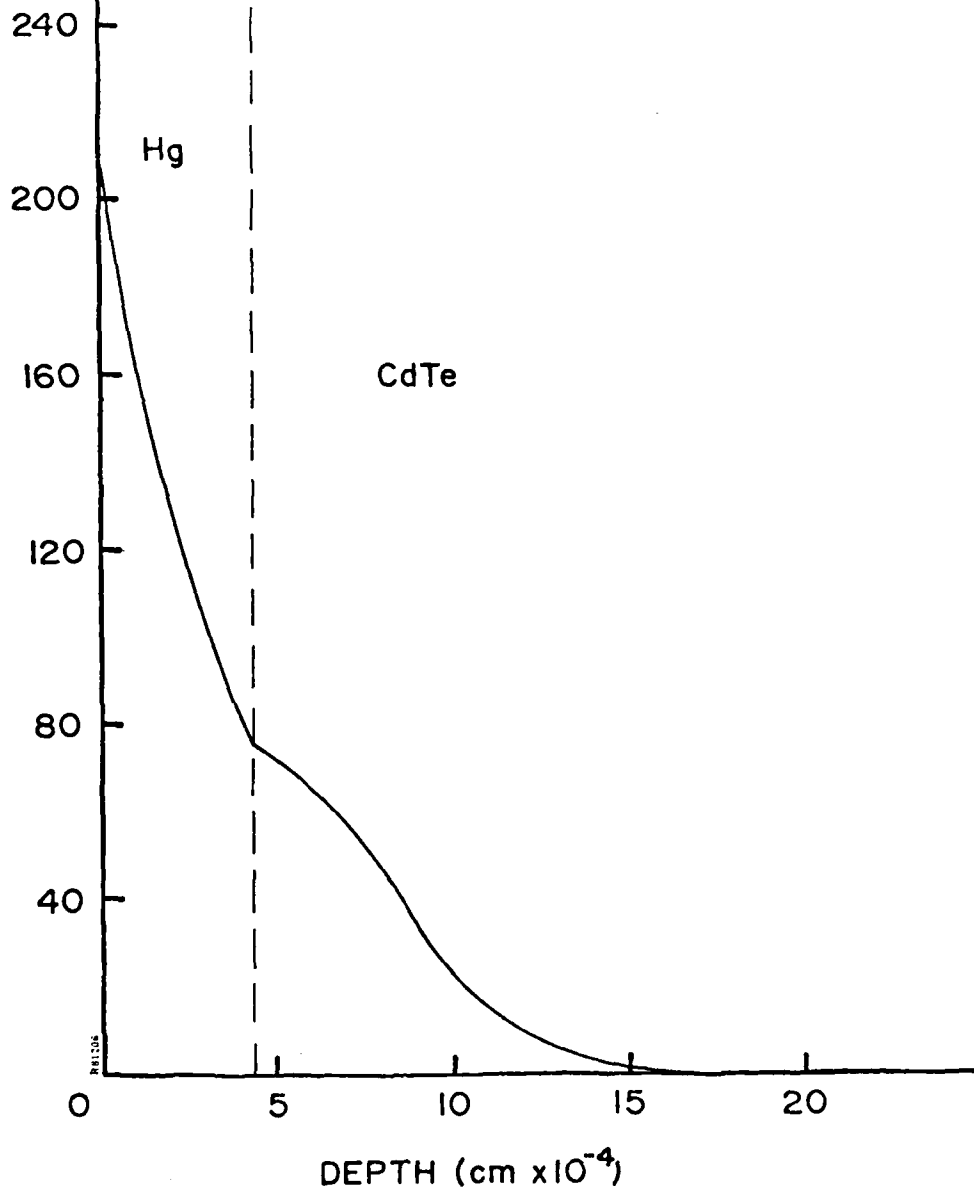
DEPTH (cm x 10⁻⁴)

REF 205



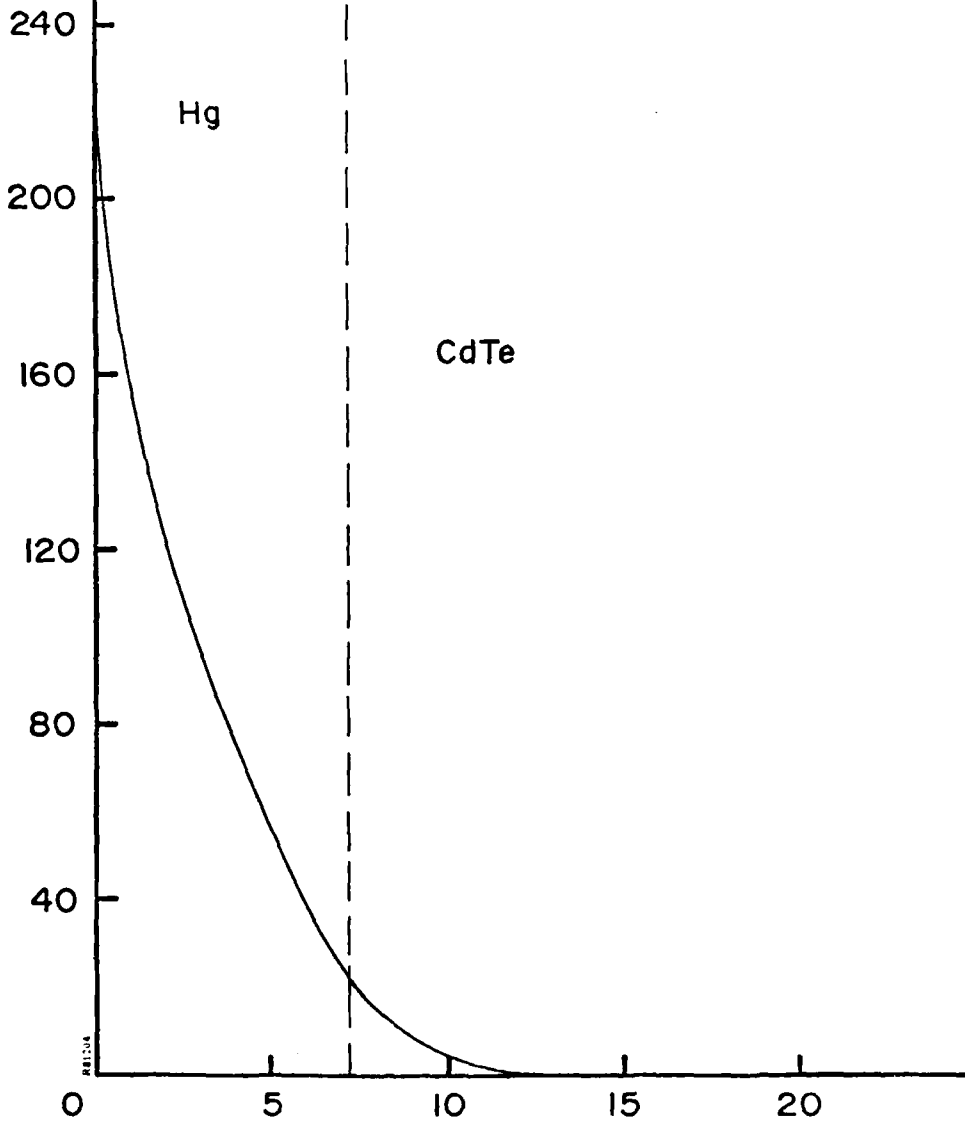
DOSE
E/Gm/E/cm²

DEPOSITION PROFILE
BEAM 1
4.24 μ Hg on 27.93 μ CdTe



DOSE
E/Gm/E/cm²

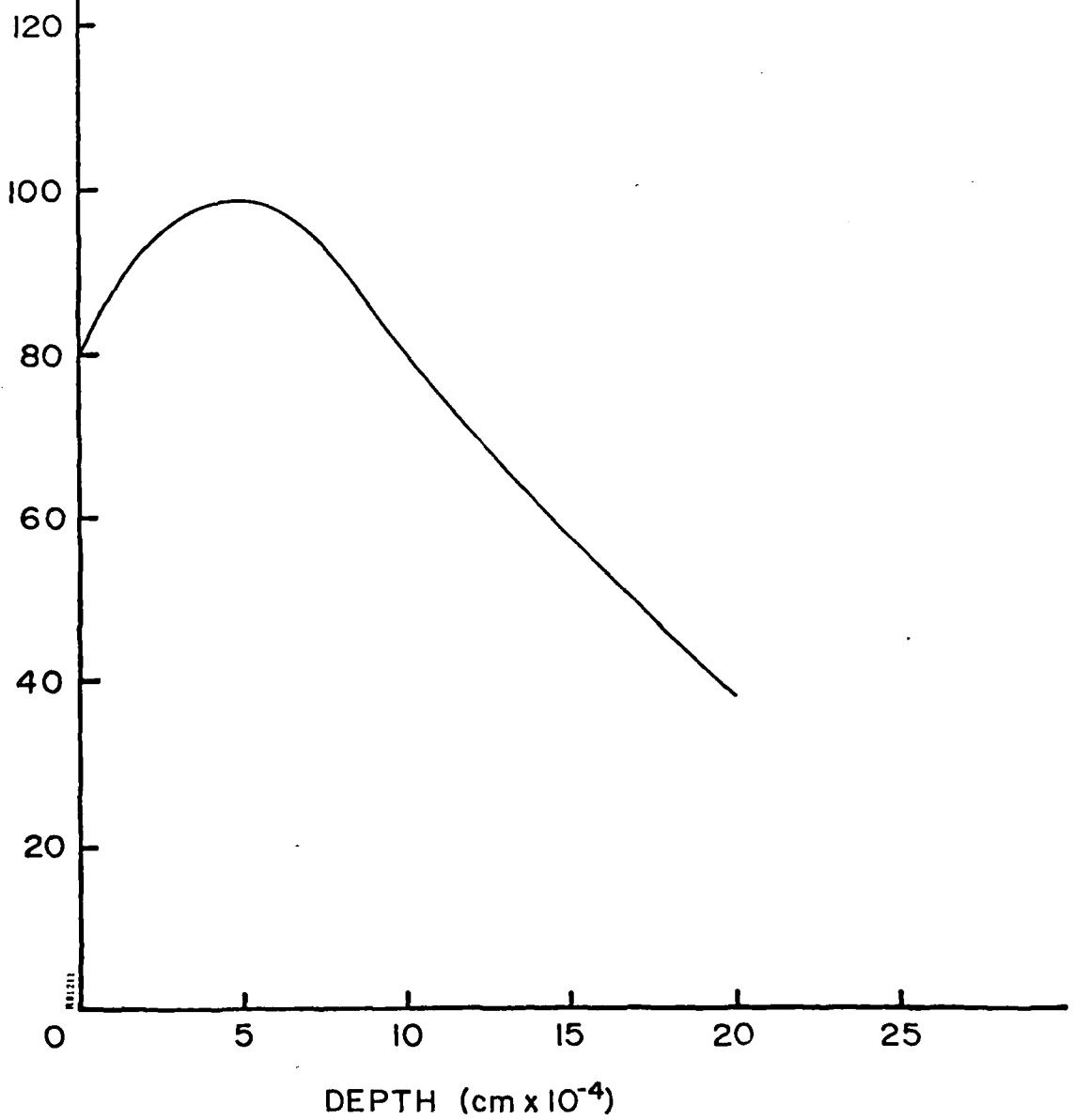
DEPOSITION PROFILE
BEAM 1
7.2 μ Hg, 12.8 μ CdTe



DEPTH (cm x 10⁻⁴)

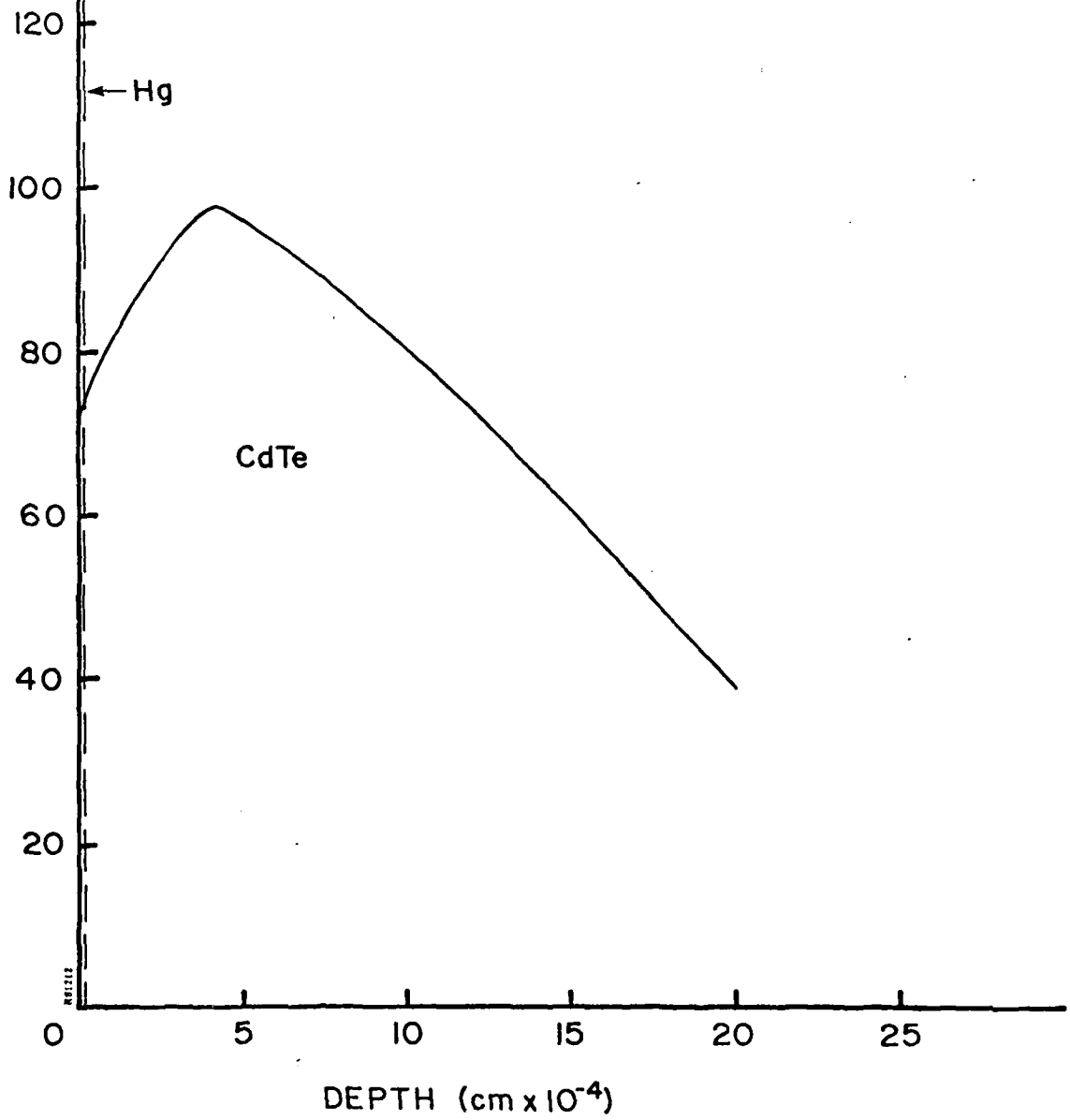
DOSE
E/Gm/E/cm²

DEPOSITION PROFILE
BEAM 4
.05 μ Hg, 19.95 μ CdTe



DOSE
E/Gm/E/cm²

DEPOSITION PROFILE
BEAM 4
.1 μ Hg over 19.9 μ CdTe



DOSE
E/Gm/E/cm²

DEPOSITION PROFILE
BEAM 4
.5 μ Hg over 19.5 μ CdTe

120 ← Hg

100

80

CdTe

60

40

20

0

5

10

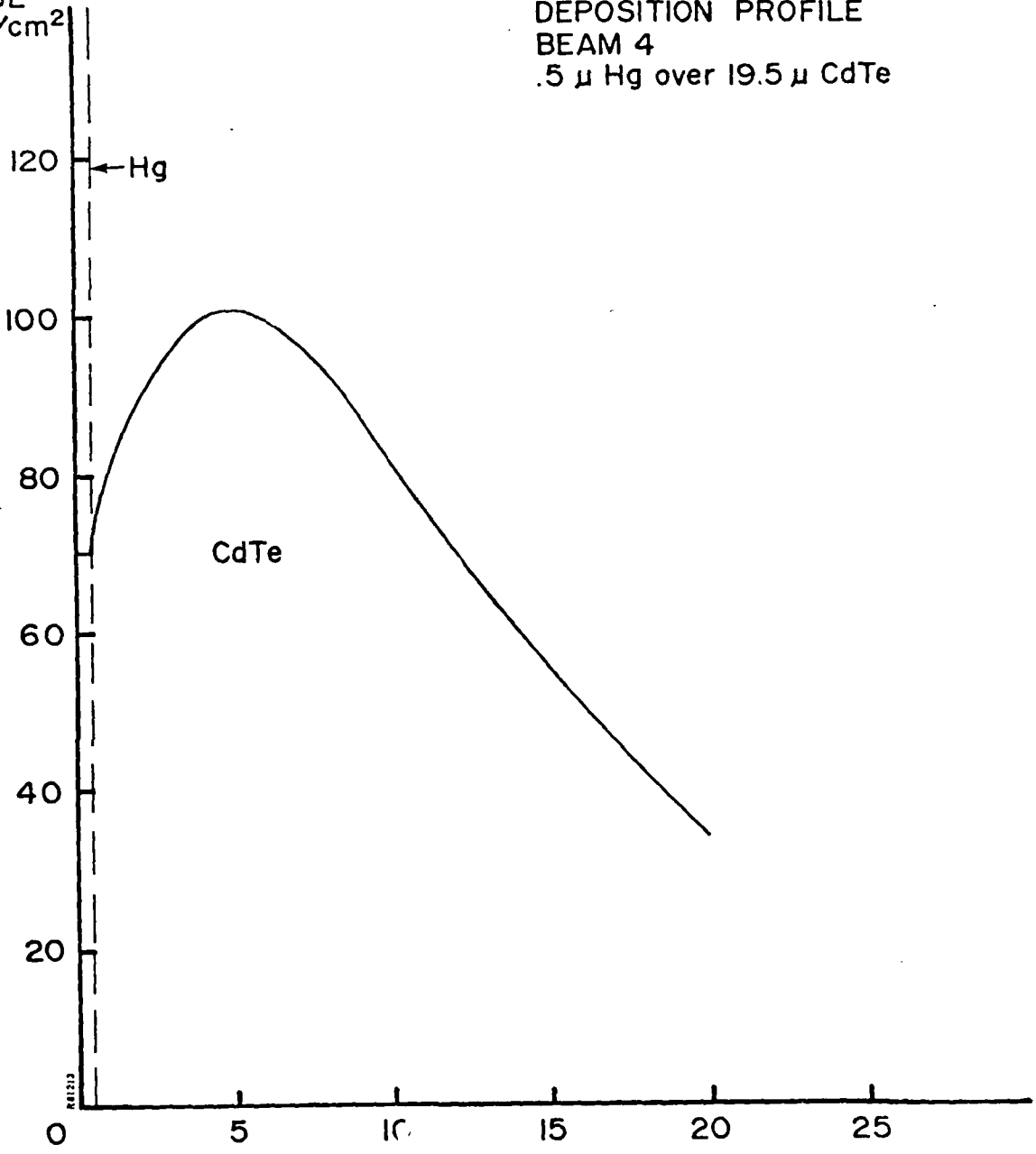
15

20

25

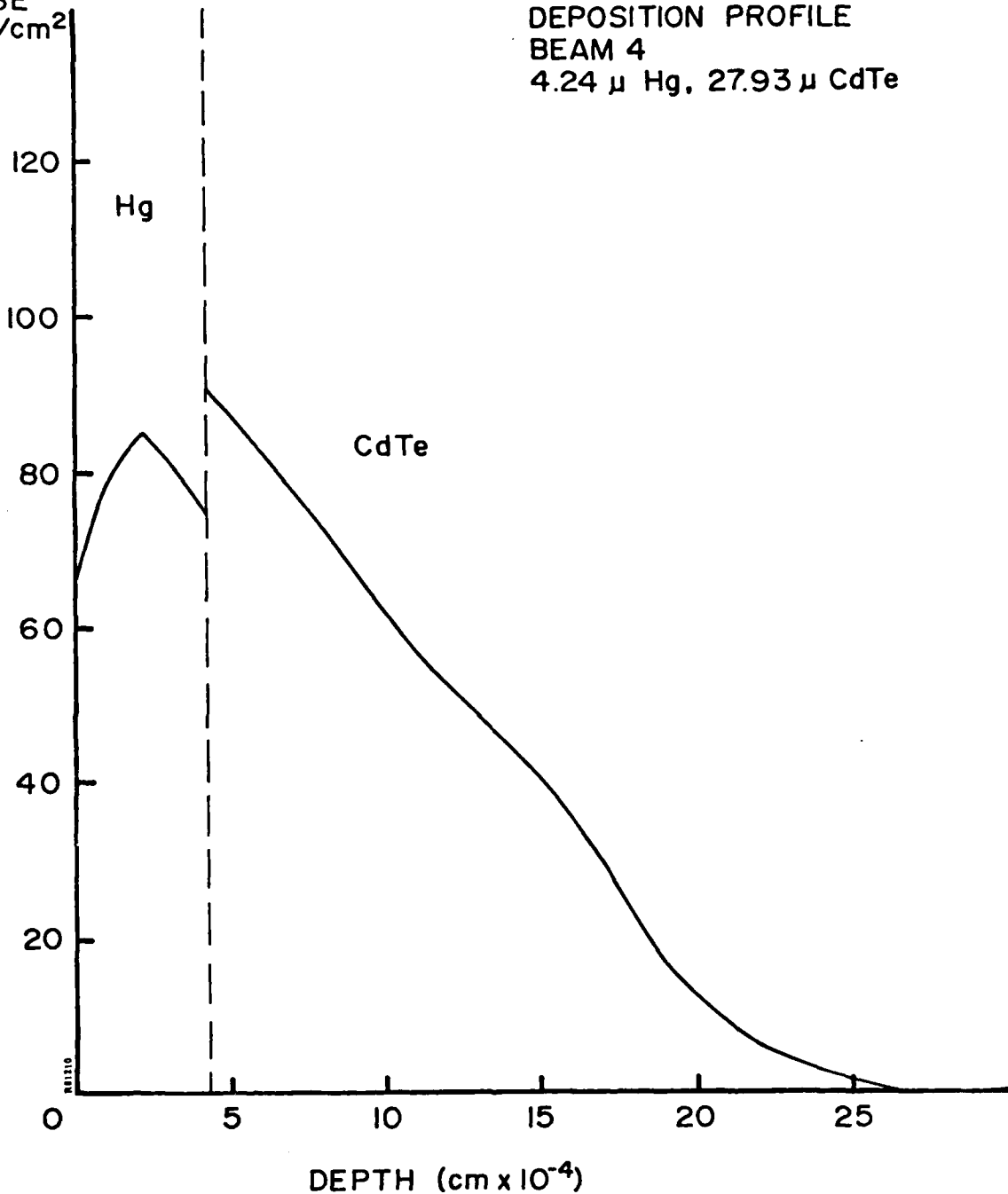
DEPTH (cm x 10⁻⁴)

APR 21 1964



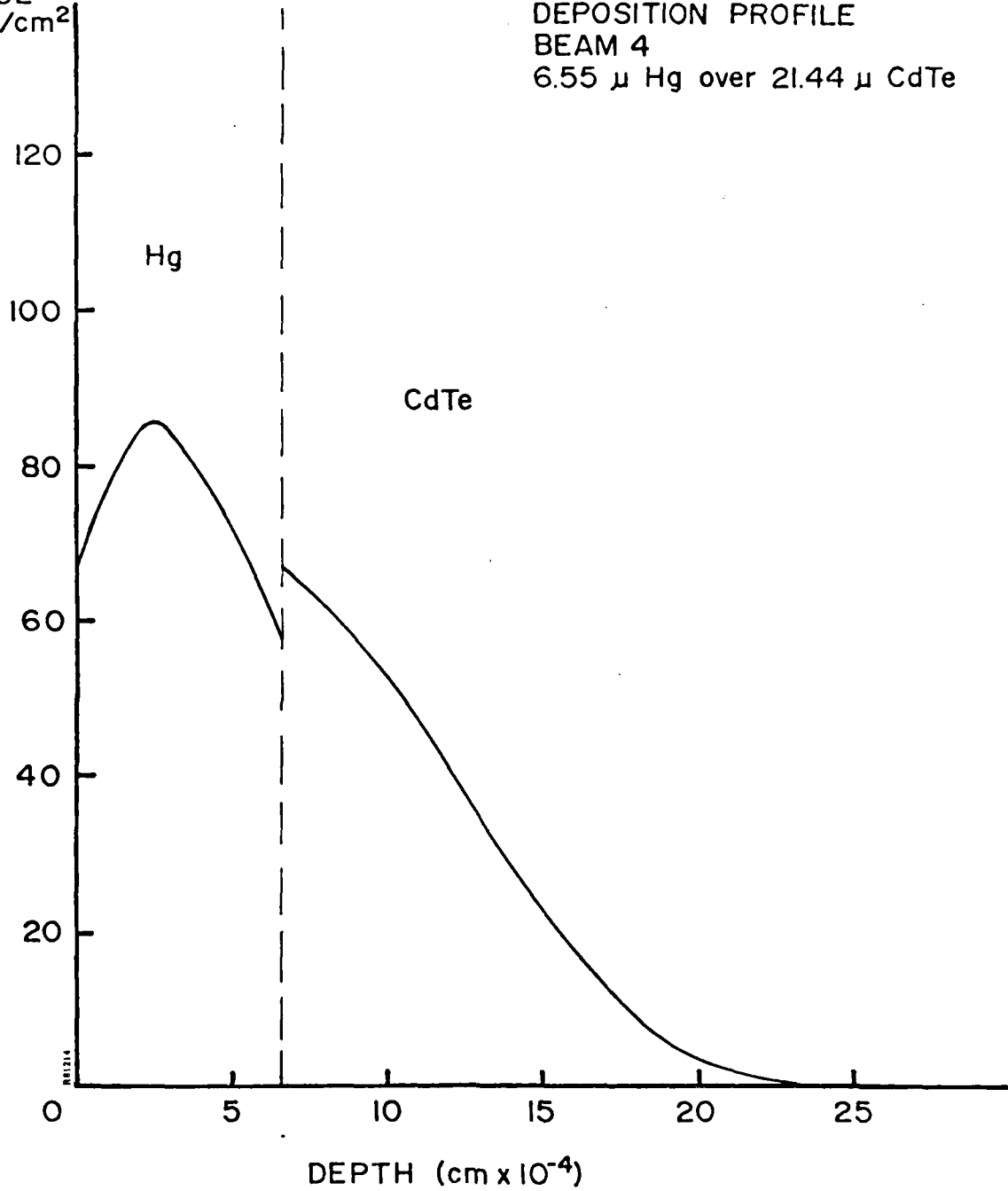
DOSE
E/Gm/E/cm²

DEPOSITION PROFILE
BEAM 4
4.24 μ Hg, 27.93 μ CdTe



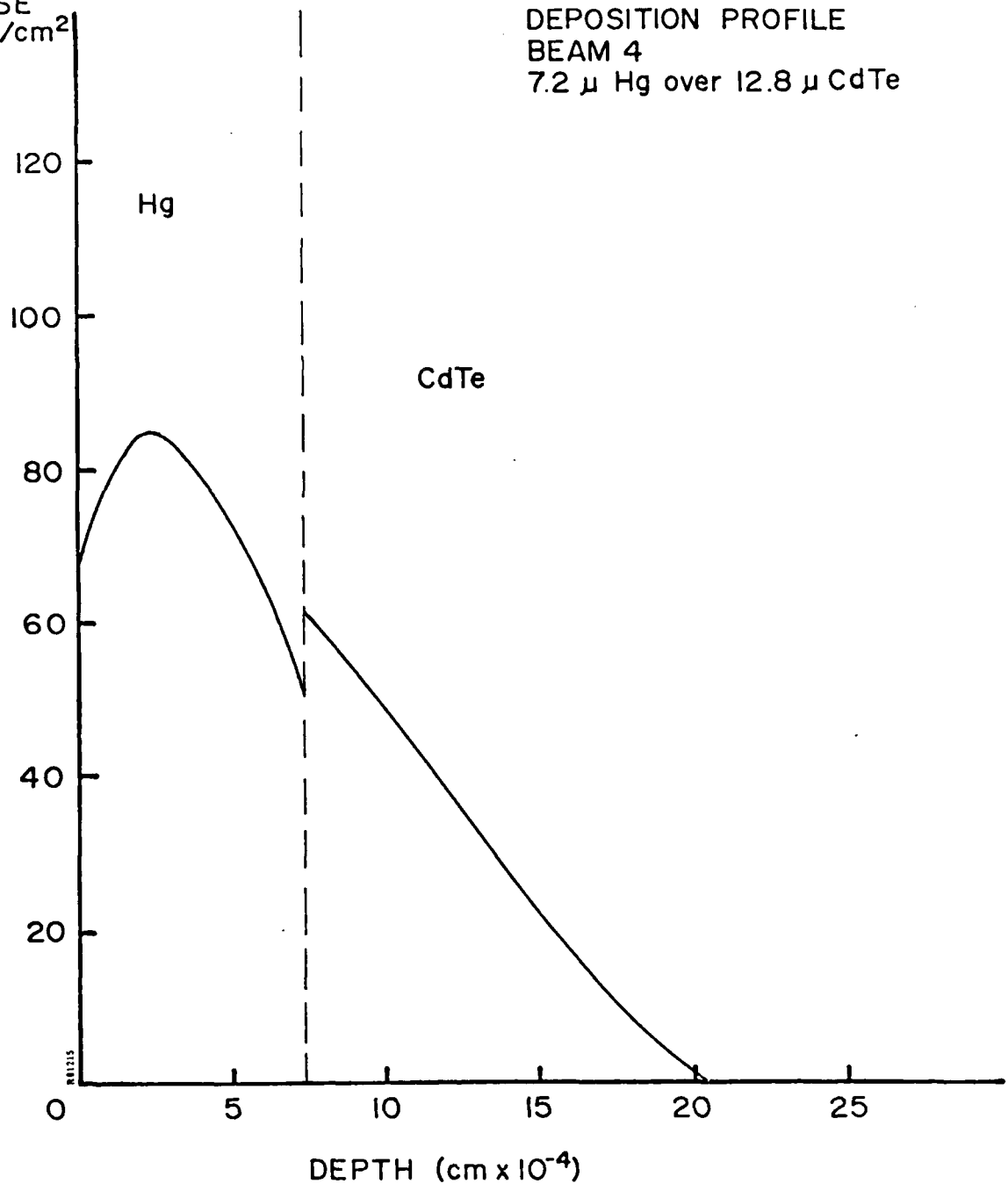
DOSE
E/Gm/E/cm²

DEPOSITION PROFILE
BEAM 4
6.55 μ Hg over 21.44 μ CdTe



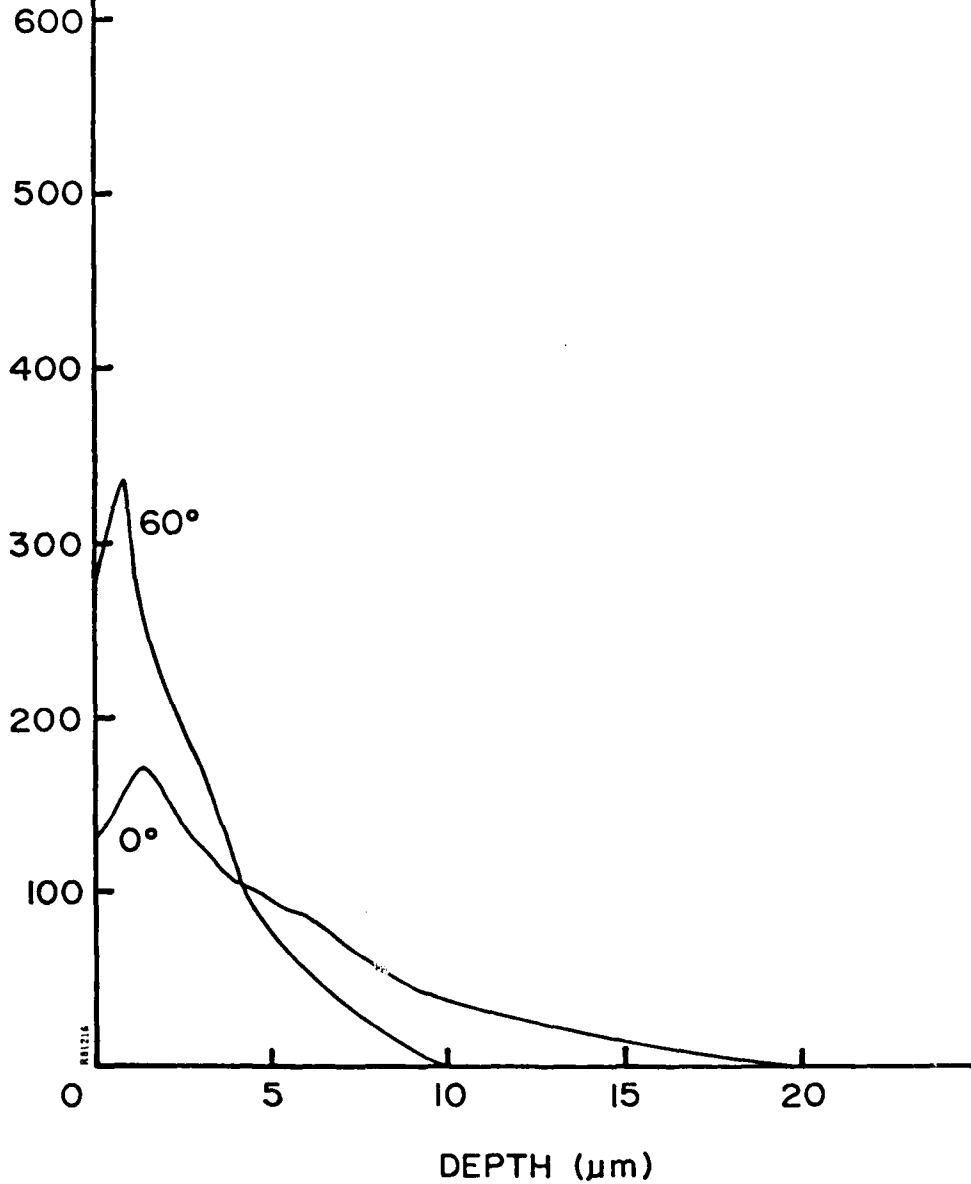
DOSE
E/Gm/E/cm²

DEPOSITION PROFILE
BEAM 4
7.2 μ Hg over 12.8 μ CdTe



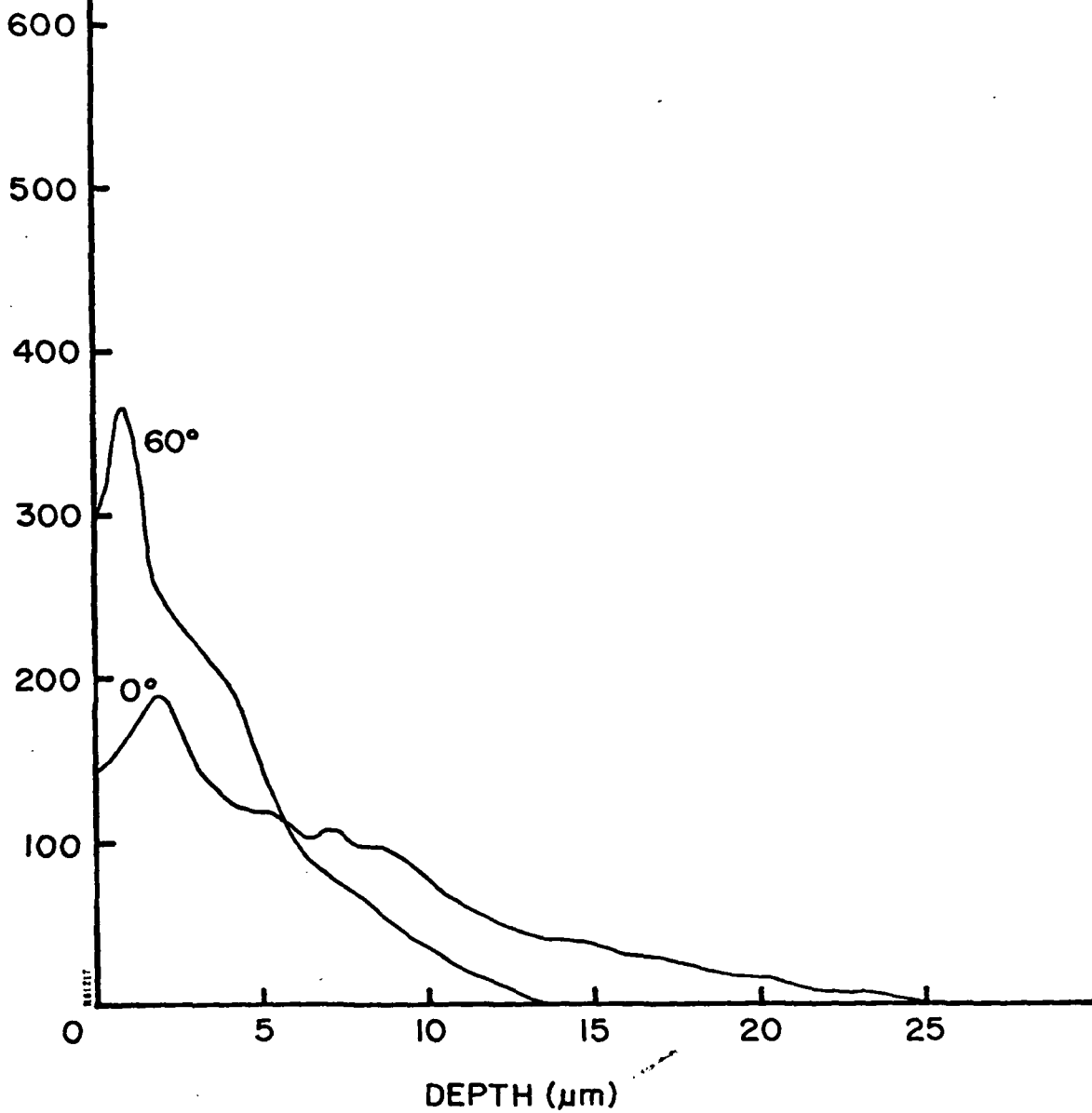
DOSE
E/Gm/E/cm²

DEPOSITION PROFILE
BEAM 3 - Hg₂Cd₂Te
0° and 60° Incidence Angle



DOSE
E/Gm/E/cm²

DEPOSITION PROFILE
BEAM 3 - CdTe
0° and 60° Incidence Angle



DOSE
E/Gm/E/cm²

DEPOSITION PROFILE
BEAM 1 - CdTe
0° and 60° Incidence Angle

